The enhancon mechanism in string theory

Järv, Laur

The Enhançon Mechanism in String Theory

Laur Järv

A Thesis presented for the degree of
Doctor of Philosophy

Centre for Particle Theory
Department of Mathematical Sciences
University of Durham
England

August 2002

Dedicated to my parents

The Enhançon Mechanism in String Theory

Laur Järv

Submitted for the degree of Doctor of Philosophy
August 2002

Abstract

The enhançon mechanism is a specific phenomenon in string theory which resolves a certain naked spacetime singularity arising in the supergravity description related to $\mathcal{N} = 2$ supersymmetric pure gauge theory. After reviewing the problem of singularities in general relativity as well as in string theory, and discussing the prototypical enhançon example constructed by wrapping D6-branes on a K3 surface, the thesis presents three generalisations to this static spherically symmetric case pertaining to large N $SU(N)$ gauge theory. First we will use orientifolds to show how the enhançon mechanism also works in similar situations related to $SO(2N+1)$, $USp(2N)$ and $SO(2N)$ gauge theories. Second we will wrap D-brane distributions on K3 to obtain the enhançon in oblate, toroidal and prolate shapes. Third we will study a rotating enhançon configuration and consider its implications for the black hole entropy and the second law of thermodynamics.

Declaration

The work in this thesis is based on research carried out at the Centre for Particle Theory, Department of Mathematical Sciences, University of Durham, England. No part of this thesis has been submitted elsewhere for any other degree or qualification. Chapter 3 of the thesis is based on a joint research with my supervisor Dr. C. V. Johnson, published in ref. [1]. Sections 4.1 – 4.5 of chapter 4 are based on a joint research with Dr. C. V. Johnson and L. M. Dyson, published in ref. [2], while section 4.6 of the same chapter contains the results of my independent additional work. Chapter 5 is based on a joint research with Dr. C. V. Johnson and L. M. Dyson, to be published soon in ref. [3]. References to other people's work are given as appropriate throughout the text.

Acknowledgements

I am especially grateful to my supervisor Dr. Clifford Johnson for his guidance and encouragement. It has been very stimulating and enjoyable to work with him. I am also deeply grateful to my first year supervisor Prof. Ed Corrigan for insightful conversations and for helping me to obtain a PhD position in Durham. Thanks to all staff members of the Maths Department.

Many thanks to Lisa Dyson for a fruitful collaboration. I have benefited a lot from discussions with Auttakit Chattaraputi, Mark Hale, and Jafar Sadeghi, but must also mention Daniel Bundzik, Apostolos Dimitriadis, Wajdi Gaddah, Mehrdad Ghominejad, William Gibbons, James Gregory, Ken Lovis, Cesar Maldonado-Mercado, Nuno Nunes, David Page, Giovanna Scataglini, Tom Weidig, and other postgraduates in the department. Thanks to Imran for the thesis template.

I would also like to thank Jüri, Kadri, and Riina, and the numerous friends and neighbours I had during the four years at Howlands Farm, it has been a nice time.

I am grateful to the Commitee of Vice-Chancellors and Principals of the Universities of the United Kingdom for offering me the Overseas Research Student Award, to the University of Durham for the Durham Postgraduate Research Award, and to the Graduate Society for the Accommodation Award. Thanks to the Estonian Science Foundation and Tartu University for additional financial support.

Last, but not least, the constant and many-sided support of my parents and relatives has been very important to me.

Contents

Abstract iii

Declaration iv

Acknowledgements v

1 Introduction 1

1.1 The problem of space-time singularities 2

1.1.1 Singularities in classical and quantum gravity 2

1.1.2 Singularities in string theory 3

1.1.3 The gravity/gauge theory correspondence and singularities . . 5

1.1.4 The enhançon mechanism 7

1.1.5 Outline of the thesis 9

1.2 Elements of string theory 10

1.3 Supergravity p–brane solutions 14

1.3.1 II A/B supergravity actions 14

1.3.2 Extremal p–brane solutions 15

1.4 D–brane dynamics 17

1.4.1 The Dirac-Born-Infeld action 17

1.4.2 The Wess-Zumino action 18

1.4.3 Curvature corrections 18

1.4.4 Gauge theory on the world-volume 19

1.4.5 Decoupling limit 21

1.5 D–branes as probes of geometry 22

1.6 Summary 24

2 The Enhançon Mechanism **26**

2.1 Wrapping branes on K3 27

2.1.1 The supergravity solution 29

2.2 The repulson geometry 29

2.3 Probing with branes 31

2.4 Enhanced gauge symmetry 32

2.4.1 Some dual situations 34

2.5 Consistency of excision in supergravity 35

2.5.1 Junction shell tension 37

2.6 Gauge theory moduli space 39

2.6.1 Including an extra modulus in the probe calculation 40

2.6.2 In the decoupling limit 42

2.6.3 Non-perturbative corrections 43

2.7 Adding D2–branes 45

2.8 Summary 47

3 Orientifolds, M-theory, and the ABCD's of the Enhançon **50**

3.1 Including orientifolds 51

3.1.1 Orientifold planes 51

3.1.2 Wrapping on K3 53

3.1.3 The *ABCD*'s of the enhançon 53

3.2 In eleven dimensions 54

3.2.1 Type IIA/M-theory duality 54

3.2.2 Uplifted enhançon 57

3.2.3 M-theory ancestor of an orientifold plane 59

3.3 Orientifolded enhançon 60

3.3.1 The supergravity solution 60

3.3.2 Probing the geometry 62

3.3.3 Gauge theory moduli space 63

3.4 Summary 64

4 Oblate, Toroidal, and Other Shapes for the Enhançon 66

4.1 D–Brane distributions . . . 67

4.1.1 Extremal limit of rotating p–branes . . . 67

4.1.2 Density of branes . . . 68

4.1.3 Dp–brane disc distributions . . . 71

4.1.4 The meaning of negative brane distributions . . . 72

4.1.5 Legendre polynomials . . . 74

4.1.6 Particle probes of the geometry . . . 75

4.2 Wrapping D6–brane distributions . . . 76

4.2.1 Shapes of the enhançon . . . 78

4.2.2 Particle probes of the geometry . . . 80

4.3 Excision in supergravity . . . 84

4.3.1 Toroidal enhançon . . . 85

4.3.2 Double and oblate enhançons . . . 87

4.4 Wrapping other D–brane distributions . . . 90

4.4.1 Unwrapped D5–brane distributions . . . 90

4.4.2 Wrapped D5–brane distributions . . . 91

4.5 Gauge theory results . . . 94

4.5.1 Metric on the moduli Space . . . 96

4.6 Prolate enhançon . . . 98

4.6.1 Unrapped prolate D6–brane distributions . . . 98

4.6.2 Wrapped prolate D6–brane distributions . . . 100

4.6.3 Discussion . . . 103

4.7 Summary . . . 105

5 Rotation, Black holes, and the Enhançon 107

5.1 Rotating enhançon . . . 108

5.2 Probing the geometry . . . 110

5.2.1 Static gauge . . . 112

5.2.2 "Spinning" gauge . . . 113

5.3 Excision . . . 115

5.3.1 Rotation of the space-time . . . 117

5.4 Constructing a black hole 118
5.4.1 Black holes in string theory 118
5.4.2 Five dimensional black hole from dimensional reduction 119
5.4.3 Bound on the angular momentum 120
5.4.4 Enhançon around the horizon 121
5.5 The black hole entropy and the second law 123
5.5.1 Entropy and the enhançon 123
5.5.2 Entropy and angular momentum 125
5.6 Summary 127

Conclusion **129**

Appendix **131**

A Supergravity Equations of Motion **131**

B Some Facts about the K3 Manifold **132**

C Magnetic Monopoles in SU(2) Gauge Theory **134**

D Extrinsic Curvature **139**

Bibliography **140**

List of Figures

1.1 A slice through the enhançon geometry before (left) and after (right) the excision. 8

2.1 Test particle effective potential in the gravitational background generated by wrapped D6–branes. 31

4.1 Disc density distributions of Dp–branes in a plane for $p = 0, \ldots, 5$, normalised to the same area. The case of D5–branes is a delta function on the edge, at $\rho = 1$. The pattern followed by these distributions is described in the text. 73

4.2 Gravitational features of the unwrapped D6–brane distribution as seen by a neutral test particle. The test particle effective potential (to) and its derivative (bottom) along the axis of symmetry ($\theta = 0$) corresponding to *(a)* $\ell = 0$, *(b)* $\ell > 0$. In the latter case the potential becomes repulsive at a distance ℓ from the origin. The effective potential for a particle moving on the equatorial plane ($\theta = \pi/2$) is always attractive, and is similar to case *(a)*. 76

4.3 A vertical slice through the non–spherical wrapped D6–brane geometry before excision. The origin $r = 0$ is placed in the centre of the figure, while the symmetry axis, $\theta = 0$, corresponds to the vertical direction and $\theta = \pm\pi/2$ to the horizontal. The full three-dimensional view emerges when the plots are revolved around the vertical axis. The region where the K3 volume $V(r,\theta) < 0$ is black. The region where $0 \leq V(r,\theta) < V_\star$ is dark grey (blue). The repulson radius $r_{\rm r}$ is marked by the border between these two regions. The physically acceptable region $V(r,\theta) \geq V_\star$, where the tension of the probe brane is positive, is in the light shade (different shades between yellow ($V(r,\theta)$ is close to $V_\star$) and white ($V(r,\theta)$ is close to V)). The enhançon radius $r_{\rm e}$ is the border between the dark grey (blue) and the light regions. Spherical enhançon is given by $\ell = 0$. For increasing values of ℓ, two disconnected shells appear forming a double enhançon. Once $\ell_{\rm e}^{\rm cr}$ is exceeded, the two shells join forming a single enhançon. This pattern can be seen explicitly in the figure for the following values of ℓ : $\ell = 0$ (top, left), $\ell = \frac{1}{2}\ell_{\rm r}^{\rm cr}$, $\ell = \ell_{\rm r}^{\rm cr}$, $\ell = \ell_{\rm e}^{\rm cr} - \frac{1}{2}(\ell_{\rm e}^{\rm cr} - \ell_{\rm r}^{\rm cr})$ (top, right), $\ell = \ell_{\rm e}^{\rm cr}$ (bottom, left), $\ell = \frac{9}{8}\ell_{\rm e}^{\rm cr}$, $\ell = 2\ell_{\rm e}^{\rm cr}$, $\ell = 8\ell_{\rm e}^{\rm cr}$ (bottom, right). Other parameters r_6, V, and $V_\star$ have been fixed to some typical values. 81

4.4 A slice through the untreated wrapped D6–brane geometry in "extended" coordinates. The colour coding is the same as in figure 4.3. The case $\ell = 0$ gives a spherical enhançon. For increasing values of ℓ, two disconnected enhançon shells appear forming coconut shape. Once $\ell_{\rm e}^{\rm cr}$ is exceeded, the two enhançon shells join to form a torus. This pattern can be seen for the following values of ℓ : $\ell = 0$ (top, left), $\ell = \frac{1}{2}\ell_{\rm r}^{\rm cr}$, $\ell = \ell_{\rm r}^{\rm cr}$, $\ell = \ell_{\rm e}^{\rm cr} - \frac{1}{2}(\ell_{\rm e}^{\rm cr} - \ell_{\rm r}^{\rm cr})$ (top, right), $\ell = \ell_{\rm e}^{\rm cr}$ (bottom, left), $\ell = \frac{9}{8}\ell_{\rm e}^{\rm cr}$, $\ell = 2\ell_{\rm e}^{\rm cr}$ (bottom, right). 82

4.5 Gravitational features of the D6–brane distribution wrapped on K3 as seen by a neutral test particle. Test particle effective potential V_{eff} and its derivative V'_{eff} along the axis of symmetry ($\theta = 0$) corresponding to different values of parameter ℓ: *(a)* $\ell = 0$, *(b)* $\ell = \ell_{\rm r}^{\rm cr}$, *(c)* $\ell = \ell_{\rm r}^{\rm cr} + \frac{1}{16}(\ell_{\rm e}^{\rm cr} - \ell_{\rm r}^{\rm cr})$, *(d)* $\ell = \ell_{\rm e}^{\rm cr}$. For $\ell > \ell_{\rm e}^{\rm cr}$ the effective potential becomes increasingly similar to that of the unwrapped case in figure 4.2*(b)*. The effective potential is singular (exhibiting infinite repulson) at the singularity radius $r_{\rm r}$. A test particle moving on the equatorial plane ($\theta = \pi/2$) has potential *(a)* for all values of ℓ. 83

4.6 A three dimensional depiction of the connected enhançon locus, at $\ell = \ell_{\rm e}^{\rm cr}$ giving an example of the "double shell" shape (left), and $\ell > \ell_{\rm e}^{\rm cr}$ giving an example of the toroidal shape (right). 86

4.7 Gravitational features of the distributed D5–brane solution as seen by a neutral test particle. Test particle effective potential (top) and its derivative (bottom) along the $\theta = 0$ ($\theta = \pi/2$) direction corresponding to *(a)* $\ell_1 = 0$ ($\ell_2 = 0$), *(b)* $\ell_1 > 0$ ($\ell_2 > 0$). The potential is always attractive for a particle moving in from the infinity. 92

4.8 Some two–dimensional slices through the non–spherical wrapped D5–brane geometry before excision. $\theta = 0$ corresponds to the vertical direction and $\theta = \pm\pi/2$ to the horizontal. The configuration is symmetric in ϕ_1 and ϕ_2 (not shown on the figure). The colour coding is as in figure 4.3. The shapes vary for different values of the parameters ℓ_1 and ℓ_2: $\ell_1 = \ell_2 = 0$ (top, left), $\ell_1 = \frac{7}{8}\ell_{\rm r}^{\rm cr}$, $\ell_2 = 0$ (top, second), $\ell_1 = 0$, $\ell_2 = \ell_{\rm r}^{\rm cr}$ (top, third), $\ell_1 = \ell_2 = \ell_{\rm r}^{\rm cr}$ (top, right), $\ell_1 = \ell_{\rm e}^{\rm cr}$, $\ell_2 = 0$ (bottom, left) $\ell_1 = 8\ell_{\rm e}^{\rm cr}$, $\ell_2 = 0$ (bottom, second) $\ell_1 = \ell_{\rm r}^{\rm cr}$, $\ell_2 = \ell_{\rm e}^{\rm cr}$ (bottom, third) $\ell_1 = \ell_2 = \ell_{\rm e}^{\rm cr} - \frac{1}{16}(\ell_{\rm e}^{\rm cr} - \ell_{\rm r}^{\rm cr})$ (bottom, right). 94

4.9 Gravitational features of the distributed D5–brane solution wrapped on K3 as seen by a neutral test particle. Test particle effective potential V_{eff} and its derivative V'_{eff} along the $\theta = 0$ ($\theta = \pi/2$) direction corresponding to *(a)* $\ell_1 = 0$ ($\ell_2 = 0$), *(b)* $\ell_1 = \ell_{\rm r}^{\rm cr}$ ($\ell_2 = \ell_{\rm r}^{\rm cr}$), *(c)* $\ell_1 = \ell_{\rm r}^{\rm cr} + \frac{1}{2}(\ell_{\rm e}^{\rm cr} - \ell_{\rm r}^{\rm cr})$, ($\ell_2 = \ell_{\rm r}^{\rm cr} + \frac{1}{2}(\ell_{\rm e}^{\rm cr} - \ell_{\rm r}^{\rm cr})$), *(d)* $\ell_1 = \ell_{\rm e}^{\rm cr}$ ($\ell_1 = \ell_{\rm e}^{\rm cr}$). Effective potential is singular (exhibiting infinite repulson) at $r_{\rm r}$ and has a minimum at $r_{\rm e}$. 95

4.10 A series of slices through the untreated wrapped D6–brane geometry. The singularity (inner solid line, red) is surrounded by the enhançon shell (outer solid line, blue). There is also a horizon present (denoted by the dotted black line), see discussion in the body of the text. The case $\tilde{\ell} = 0$ gives a spherical enhançon, and as $\tilde{\ell}$ increases, the enhançon shell takes an increasingly prolate shape. This pattern can be seen for the following values of $\tilde{\ell}$: $\tilde{\ell} = 0$ (left), $\tilde{\ell} = 2\ \tilde{\ell}_{\rm r}^{\rm cr}$, $\tilde{\ell} = 2\ \tilde{\ell}_{\rm e}^{\rm cr}$, $\tilde{\ell} = 2.5\ \tilde{\ell}_{\rm e}^{\rm cr}$ (right). 102

4.11 A slice through the untreated wrapped D6–brane geometry in "contracted" coordinates. The colour coding is the same as in our paper. The case $\tilde{\ell} = 0$ gives a spherical enhançon. As $\tilde{\ell}$ increases, the enhançon shell takes an increasingly prolate shape, until it gets disconnected into two pieces. This pattern can be seen for the following values of $\tilde{\ell}$: $\tilde{\ell} = 0$ (left), $\tilde{\ell} = 2\ \tilde{\ell}_{\rm r}^{\rm cr}$, $\tilde{\ell} = 2\ \tilde{\ell}_{\rm e}^{\rm cr}$, $\tilde{\ell} = 2.5\ \tilde{\ell}_{\rm e}^{\rm cr}$ (right). 104

List of Tables

2.1 A sketch of D6–branes wrapped on K3 and the induced negative D2–branes. The branes' world-volume directions are marked by "−", and transverse directions where the branes are point-like are denoted by "·", while "∼" indicates that the induced D2–branes are delocalised on K3. 28

3.1 A sketch of D6–branes wrapped on K3 in the presence of an O6–plane. The world-volume directions are marked by "−" and "∼" indicates that the induced effective D2–branes are delocalised on K3. In the transverse directions the branes are point-like which is denoted by "·", while the orientifold plane, sitting fixed at the origin ($r = 0$), puts a $\mathbb{Z}_2$ reflection on these directions, symbolised by "ıı". . . 52

3.2 M-theory origin of type IIA branes. "Vertical" dimensional reduction is denoted by "↓", "diagonal" dimensional reduction by "↙". 56

4.1 A sketch of a D6–brane distribution wrapped on K3 and the induced negative D2–branes. The branes' world-volume directions are marked by "−", while "∼" indicates that the induced D2–branes are delocalised on K3. In the transverse directions the branes are not coincident, but form a distribution, symbolised by "∗". 77

4.2 A sketch of a D5–brane distribution wrapped on K3 and the induced negative D1–branes. The branes' world-volume directions are marked by "−", while "∼" indicates that the induced D1–branes are delocalised on K3. In the transverse directions the branes form a distribution, symbolised by "∗". 93

5.1 A sketch of the D5–D1–pp configuration wrapped on K3. The world-volume directions are marked by "–" and transverse directions by "·", the symbol "∼" denotes that D1–branes are delocalised on K3, while "→" indicates the direction in which the wave is propagating. 109

C.1 Perturbative spectrum after "higgsing". 136

C.2 The full BPS spectrum. 138

Chapter 1

Introduction

The idea of this introductory chapter is to provide a context and motivation for the study of the enhançon mechanism. We begin by reviewing the problem of space-time singularities in classical and quantum gravity. Next we will discuss how singularities are understood and in some cases resolved from the point of view of string theory, which also provides a consistent quantum description of gravity. Recent years have seen remarkable progress in string theory, especially driven by the realisation of the important role played by certain non-perturbative objects in the theory known as "D–branes." The enhançon mechanism gives one particular example of how a class of naked space-time singularities is resolved using techniques related to the dynamics of D–branes. We will review the different circumstances where the enhançon mechanism has been studied and applied.

In the following sections of this chapter we introduce some basic notions and tools necessary in our study. We will provide a very brief overview of string theory and discuss how D–branes arise as hypersurfaces where open strings can end. At low energies the description of D–branes is twofold: on the one hand they are solitonic solutions of supergravity theories, on the other hand they are described by a gauge field theory on their world-volume. We will consider the world-volume action of D–brane dynamics and the various corrections it receives. Making use of this action allows us to introduce D–branes as probes of geometry in the end of the chapter.

1.1 The problem of space-time singularities

1.1.1 Singularities in classical and quantum gravity

Contemporary fundamental physics is based on two main theoretical pillars: the theory of general relativity and quantum theory (in the form of gauge field theory of Yang-Mills type). Phenomena at large scales are governed by gravitational interactions, and observations from cosmological distances to millimeter scales [4] are well described by general relativity. Phenomena at small scales are dominated by strong and electro-weak interactions, and observations at distances ranging from a fraction of a millimeter [5] down to 10^{-19} meters are well described by quantum mechanics and quantum field theory. All present experimental and observational tests are compatible with this two-part framework [6].

From the theoretical point of view, however, the state of affairs is not yet fully satisfactory. The foundations of general relativity – a dynamical space-time with no preferred reference frame or coordinate system – clash with the needs of quantum theory, which in its standard formulations requires a fixed background and a preferred splitting of space-time into space and time. General relativity is a classical, not quantum theory, and when considered in conjunction with quantum systems, several paradoxes tend to follow [7]. Unfortunately the usual perturbative approach to quantising general relativity fails, since the theory proves to be not renormalisable [8–10]. Also supergravities, the supersymmetric extensions of general relativity, do seem to have the same problem [11].

Even at the classical level general relativity can not be regarded as a complete theory, since it generally allows space-time singularities, as demonstrated by the well-known singularity theorems of Hawking and Penrose [12–14]. Classical space-time singularities defined via geodesic incompleteness tell us that in finite proper time, a test particle will reach regions of space-time beyond which its evolution is not defined. Infinite energy scales are invoked as the curvature invariants become infinite at the singularity and we cannot evolve the dynamical equations of the theory. The singularities essentially mark the breakdown of the classical theory, as predictability of the future or past is lost for world-lines which run into or out of the singularity.

Some of these singularities can be resolved by modifying the Einstein-Hilbert action of general relativity with new higher curvature interactions (and also higher derivative terms in the metric and any other matter fields). In the modified equations of motion, the contribution of these new terms will be negligible for modest gravitational fields, but in regions of large curvature, the higher curvature terms can greatly affect the nature of the solutions. In particular, the contributions from the higher curvature interactions spoil certain local energy conditions required to prove the singularity theorems, and one might hope to construct a singularity-free extension of general relativity in this manner [15]. There are also examples of singular solutions that become regular when embedded into higher dimensional theories [16].

Still, in the domain of Planck scale curvatures ($|R_{\mu\nu\rho\sigma}| \simeq \ell_{Planck}^{-2} \approx 3.9 \times 10^{65}\,\mathrm{cm}^{-2}$), the character of gravity is expected to change radically since its underlying quantum nature will become important. Therefore any prospective theory of quantum gravity faces a challenge for how to manage the space-time singularities arising in the classical description. One might expect that in the full quantum formulation these singularities get "smoothed out" into nonsingular states by quantum corrections.

Quantum gravity can not possibly "smooth out" all singularities, however. Some singular solutions, like the negative mass Schwarzschild, must rather be "disallowed", or "excised" *i.e.* forbidden from the start. A quantum theory that "smoothed out" the singularity of the negative mass Schwarzschild metric would then admit negative mass states (the mass can be deduced from from the long range fields of the solution), and there would be no stable vacuum state [17].

1.1.2 Singularities in string theory

String theory, although originally suggested for describing strong interactions, has emerged as a theory incorporating in a unified form both gauge theories and a consistent quantum theory of gravity.[1] In order for string theory to be consistent one

[1] We will briefly introduce some basic elements of string theory in the next section, for fuller treatment let us refer to the standard textbooks [18, 19]. Besides string theory another more

has to include supersymmetry, leading to five distinct superstring theories. In fact, all the five superstring theories together with 11-dimensional supergravity are related to each other by various dualities [27, 28], and can be understood as pertubative corners of an overarching "M-theory" [28, 29]. It has also been realised that string theory is not just a theory of strings, but "D–branes" [30] and other extended objects of various dimensions do play an important role in the theory.

String theory contains gravity in two ways: massless string excitations include gravitons – spin-2 states, and consistent propagation of the string requires the background space-time to satisfy Einstein's field equations at low energy, coupled to other massless fields in what is called supergravity (once we go the the full supersymmetric theory, as we will need to later for consistency). In fact, these two ways are connected. Consistency of the linearised approximation to the background fields (in which gravitons arise in field theory) requires that these two descriptions overlap. In this classical field theory picture string theory does not prohibit appearance of singularities. However there are various typically stringy mechanisms known by which these singularities can be resolved [31].

The first thing to note is that the definition of a space-time singularity is different in string theory than in general relativity, even classically. Instead of defining the singularity in terms of geodesic incompleteness based on the motion of test particles, we must use test strings. If the physics of strings on this background is not singular, the singularity in a metric does not matter since the space-time metric is only a low energy manifestation of stringy physics. The singularity can simply signal the omission of some of the degrees of freedom at a low energy approximation of the full string theory.

A simple example of this kind is provided by strings on orbifolds [32]. An orbifold is a quotient of space-time by a discrete group (often a subgroup of the rotation group). Consider an orbifold of flat space. Although it has vanishing curvature, the

widely pursued approach that aims at providing a quantum theory of gravity is loop quantum gravity or quantum geometry, reviewed in refs. [20–23]. For comparative reviews on the progress and issues in various approaches to quantum gravity see refs. [24, 25] and about experimental and phenomenological aspects ref. [26].

quotient is geodesically incomplete, there is a conical singularity at the origin. A field theory on such a background is generally problematic. But in string theory new light states (the so-called twisted sectors) are present, confined to the conical defect. Taking these extra states into account makes stringy physics perfectly consistent and free of singularities [32].

An example of curvature singularities that are harmless in string theory is encountered in string theory compactifications on a Calabi-Yau manifold. It is possible to construct solutions where the metric of the compact Calabi-Yau manifold slowly varies leading to a topology change and developing a curvature singularity in between. In many cases, this can be viewed as arising from a topologically nontrivial S^2 or S^3 being shrunk down to zero area. Again we see new degrees of freedom becoming massless as the surface shrinks to zero volume, and when these are included in the analysis the theory turns out to be non-singular. Two kinds of such topology change are known: flops [33,34] and conifold transitions [35,36].

Since string theory has had considerable success in providing physically sensible descriptions of certain time-like singularities in compactification geometries, one can hope that it will similarly provide insight into the space-like or null singularities which arise in various cosmologies, like the Big Bang and Big Crunch singularities. Proposals in this direction have appeared in the past [37–39] and more recently [40–49], motivated by interest in the string theory on time-dependent backgrounds.

While the cases mentioned above are examples of how string theory resolves space-time singularities by either "smoothing out" the geometry or by providing a well-defined physics, the enhançon mechanism gives a nice example how string theory manages to completely do away with a naked time-like singularity by excision.

1.1.3 The gravity/gauge theory correspondence and singularities

It is appropriate to discuss the enhançon in the context of gravity/gauge theory correspondences. Most of the best understood examples of such correspondences are motivated by the physics of D–branes, dynamical extended objects present in string theory. A Dp–brane is a p–dimensional object which sweeps out a $p+1$–dimensional

"world-volume" as it moves in time. The gravity/gauge theory correspondence has its origin in the fact that, on the one hand, D–branes are classical soliton solutions of the low-energy closed string effective action and, on the other hand, they have a description in terms of Dirichlet boundary conditions on the end-points of open strings. The latter description at low energy gives a gauge theory living on the branes' world-volume. This means the low energy dynamics of D–branes can be used to describe the properties of the gauge theory and *vice-versa.*

These two descriptions, one in terms of closed and another in terms of open strings, are complementary for all D–branes and in some cases there is a region of overlap between these two pictures leading to a gravity/gauge theory correspondence. A successful realization of this correspondence is the Maldacena conjecture [50–52], confirmed by subsequent studies [53], which grew out of the physics of D3–branes. In the open string description the low energy physics of a D3–brane is given by the four-dimensional $\mathcal{N} = 4$ supersymmetric $U(N)$ Yang-Mills gauge theory (which is conformally invariant) with gauge coupling g^2_{YM}. In the closed string description the space-time solution generated by the D3–brane is, in the appropriate limit,[2] $AdS_5 \times S^5$. The conjecture states these two descriptions are equivalent when the Yang-Mills theory is strongly coupled, or more precisely in the so-called 't Hooft limit ($N \to \infty$, $\lambda = Ng^2_{YM}$ fixed). One can use computations in the weakly coupled gravity theory to learn new information about the strongly coupled gauge theory and the other way round. This is a truly remarkable fact given how different from each other these theories seem at the outset.

There has been great interest in trying to extend this duality to other less supersymmetric and non-conformal gauge theories. Supergravity backgrounds have been found both as the deformation of the $AdS_5 \times S^5$ (which is dual to deforming the $\mathcal{N} = 4$ gauge theory by relevant perturbations) and from consideration of the near horizon limit of more complicated D-brane constructions. The supergravity solutions dual to non-conformal gauge theories with reduced supersymmetry are generically singular in the interior corresponding to the infrared (IR) regime of the

[2]This limit is called the "near-horizon" limit which focusses on the region of space-time near the brane. We will discuss to this notion in section 1.4.5.

gauge theory. Therefore it is important to understand, which of these singularities are physically acceptable [54] and one would expect some stringy mechanism to repair the singularities so as to match the true IR behaviour of the field theory. There are a several different examples, which seem to depend on the amount of supersymmetry present in the problem.

In the class of $\mathcal{N} = 1^*$ gauge theories obtained by mass deformation of parent $\mathcal{N} = 4$ gauge theories (the Polchinski-Strassler solution), the naked singularity of the gravitational dual is resolved by a Dp–brane polarization into a spherical D$(p+2)$-brane [55–60] via Myers' dielectric effect [61]. Another well known example pertaining to $\mathcal{N} = 1$ gauge theory is the Klebanov-Strassler solution of fractional D3–branes on a conifold, where the naked singularity is resolved by deforming the conifold [62, 63].

Supergravity duals of non-conformal $\mathcal{N} = 2$ gauge theories can be obtained as mass deformations of $\mathcal{N} = 4$ super Yang-Mills [64–67], using fractional branes at orbifold singularities [68–75], wrapping M5-branes on Riemann surfaces [76], five-branes on non-trivial two-cycles inside a Calabi-Yau two-fold [77, 78], or wrapping Dp–branes on the $K3$ manifold [79]. The naked time-like singularities which arise here seem to be resolved by the "enhançon" mechanism, which we describe next.

1.1.4 The enhançon mechanism

In studying brane configurations related to the $(p+1)$–dimensional $\mathcal{N} = 2$ supersymmetric large N $SU(N)$ pure gauge theories the authors of ref. [79] observed that the corresponding supergravity solution is apparently afflicted by a naked singularity known as a "repulson" [80–82], which is unphysical and incompatible with the physics of gauge theory. Upon closer examination, by probing the geometry with branes and considering how the configuration could be constructed out of large number of constituent BPS parts, the singularity appears not to be present. It is excised by the enhançon mechanism which corresponds to a locus where extra massless degrees of freedom in the parent type II string theory come into play enhancing the gauge symmetry in space-time. In the case of wrapping D$(p+4)$–branes on K3, the D–brane "building blocks" of the geometry cease to be sharply localised at the en-

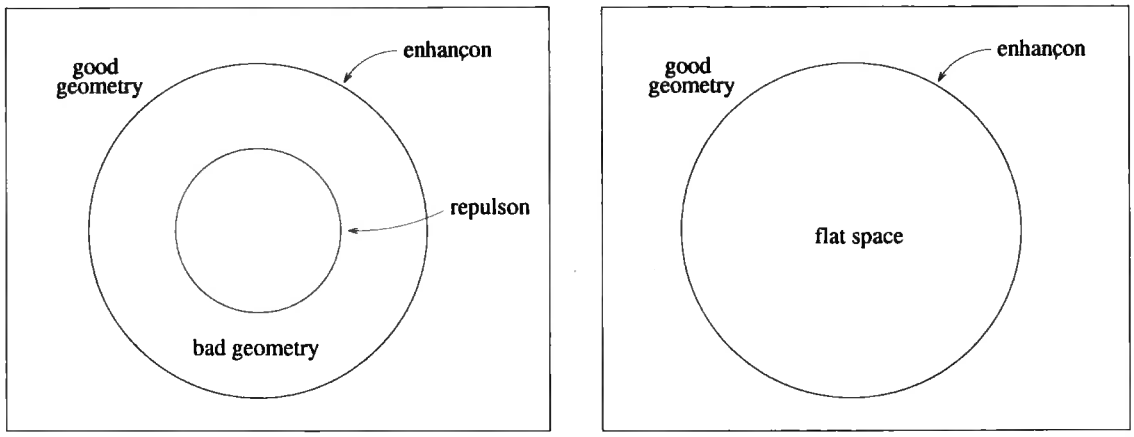

Figure 1.1: A slice through the enhançon geometry before (left) and after (right) the excision.

hançon locus and expand out into a $(4-p)$-sphere, S^{4-p}, surrounding the would-be singularity and effectively replacing the singular space-time region with flat space, see figure 1.1. (We will discuss many accompanying details and arguments to greater extent in chapter 2.)

The idea to excise the problematic geometry gets further support from a purely supergravity analysis. The source introduced at the excision surface between the interior and exterior geometries behaves exactly as a shell of wrapped branes, and in particular, the tension vanishes at precisely the enhançon radius [83]. Further investigations show that the shell is stable under perturbations [84, 85].

If $p = 2$ the physics of the brane configuration has an alternative description as the usual problem of monopoles in the $3+1$–dimensional $SU(2)$ gauge theory with adjoint Higgs [86, 87]. For example the smearing out of a D6–brane at the enhançon locus corresponds to a monopole merging with the other monopoles at the core. An attempt to derive the explicit supergravity lagrangian with enhanced gauge symmetry and the corresponding monopole physics manifest was made in ref. [88].

Adding an orientifold plane parallel to the wrapped D–brane configuration can make the large N gauge group on the branes to $SO(2N+1)$, $USp(2N)$ or $SO(2N)$ instead of $SU(N)$, therefore the enhançons may be broadly classified into types A, B, C and D [1]. The orientifold also puts an extra $\mathbb{Z}_2$ identification on the transverse directions, thus turning the enhançon locus from S^{4-p} into $\mathbb{RP}^{4-p} \equiv S^{4-p}/\mathbb{Z}_2$.

One can obtain enhançons of various non-spherical shapes, by wrapping distributions of D–branes on $K3$ [2], or by modifying the standard spherical solution by adding a term involving higher spherical harmonic functions [89]. Even a rotating enhançon configuration does exist [3]. (We will discuss the orientifolded, non-spherical, and rotating enhançons in chapters 3, 4, 5 of this thesis.)

The enhançon mechanism turns out to be crucial in maintaining the second law of black hole dynamics. When a black hole is constructed by wrapping certain brane configurations on K3, the enhançon mechanism will prevent the branes that would reduce the black hole entropy from entering the horizon [90, 91].

There are other instances of the enhançon mechanism studied in the literature following ref. [79]. The setup of wrapped branes on $K3$ is T-dual to the one with fractional D-branes [79, 92, 93] and the enhançon mechanism is also in action for the fractional brane configurations both on non-compact orbifolds like $\mathbb{C}^2/\Gamma$ [69–71, 74, 75, 95] and on the compact $T^4/\mathbb{Z}_2$ orbifold limit of $K3$ [94]. The enhançon mechanism on a conifold was analysed in ref. [96]. Ref. [97] studies the enhançon mechanism in heterotic string theory considering winding strings with momentum and the Kaluza-Klein dyons which are S-dual to the wrapped branes on $K3$ in type II string theory. Analogues to the enhançon mechanism have been also studied in the context of Calabi-Yau compactifications of 11-dimensional supergravity [98], and in a non-supersymmetric set-up, involving space-time varying string vacua [99, 100].

1.1.5 Outline of the thesis

The plan of the thesis is as follows. In the following sections of this chapter we will review some essential theoretical concepts and ingredients necessary in our study. Our key tool is provided by D–branes. On the one hand they emerge in the perturbative string theory as hypersurfaces where open strings can end, on the other hand they can be identified with solitonic p–brane solutions in supergravity. The dynamics of D–branes is captured by the Dirac-Born-Infeld – Wess-Zumino action, and we will discuss the various corrections it receives. In the end of the chapter we will use a Dp–brane to probe the geometry generated by N Dp–branes.

In chapter 2 we will discuss the enhançon mechanism in more detail using the

prototypical case of wrapped D6–branes on $K3$ as an example. This allows us to explain the salient features of the enhançon and go through the mathematical techniques and reasoning we will use later on in more complicated settings.

Chapter 3 presents a generalisation of the enhançon mechanism to situations pertaining to large N $SO(2N+1)$, $USp(2N)$ and $SO(2N)$ gauge theories using orientifolds. We will also comment on how the enhançon works in the context of the 11-dimensional M–theory.

In chapter 4 we are going to wrap distributions of D–branes on $K3$ to obtain enhançons of various shapes. These include a configuration of two enhançon shells one nested inside another and a toroidal enhançon. In the end, looking back to the various shapes obtained, we notice that varying the parameter which characterised the original distribution of D6–branes, yields a series of snapshots reminiscent of the scattering of two solitons.

In chapter 5 we study an example of a rotating enhançon. When compactified on $K3 \times S^1$ the configuration describes a five dimensional black hole. We will consider the implications an enhançon has on the black hole entropy and discover that the enhançon mechanism plays a crucial role to safeguard the second law of thermodynamics. Lastly, in chapter 6 we draw some conclusions of the whole study.

In this thesis we have tried to adopt the conventions and notation of ref. [101].

1.2 Elements of string theory

The motion of a string in a flat space-time is described by a two-dimensional sigma-model with an action[3]

$$S = -\frac{1}{4\pi\alpha'}\int_{\Sigma} d\tau d\sigma \sqrt{-\gamma}\gamma^{ab}\partial_a X^\mu \partial_b X^\nu \eta_{\mu\nu} \ , \tag{1.2.1}$$

where the coordinates τ, σ parametrise the string world-sheet Σ, the intrinsic world-sheet metric is $\gamma_{ab}(\tau,\sigma)$, and X^μ represent the D–dimensional space-time embedding coordinates of the string. The parameter α' of dimension $[L]^2$ (length-squared) is

[3]The following is just a brief review of string theory and D–branes. An extensive exposition of the subject is provided by *e.g.* refs. [18, 19, 101].

the only dimensionful parameter in string theory. It sets the "string length" ℓ_s by $\alpha' = \ell_s^2$ and is related to the string tension T by $T = \frac{1}{2\pi\alpha'}$.

Closed strings

Strings can be either open or closed. For closed strings one demands periodic boundary conditions. After quantisation the massless states in the closed string spectrum consist of the graviton $g_{\mu\nu}$, a scalar Φ called the dilaton, and an antisymmetric tensor $B_{\mu\nu}$ also known as the Kalb-Ramond field. The graviton $g_{\mu\nu}$ plays the role of the background space-time metric, while the exponent of the expectation value of the dilaton sets dimensionless sting coupling constant, $g_s = e^{<\Phi>}$, governing string splitting and joining interactions. The closed string spectrum also has a tachyon (a negative mass-squared state which fortunately will not survive in the superstring spectrum), and an infinite tower of massive states with masses inversely proportional to $\sqrt{\alpha'}$.

T-duality

If one of the space-time directions is compact with periodicity $2\pi R$, two types of states can appear in the uncompactified directions. First there are the so-called Kaluza-Klein states, as the centre-of-mass momentum in the compact direction takes discrete values n/R, with n integer, setting the mass of particles in lower dimensional theory. The other sector is a purely stringy phenomenon of winding states coming from strings wrapping w times around the compact direction. Since the string has tension $T = \frac{1}{2\pi\alpha'}$ such states have mass energy $2\pi RwT = \frac{wR}{\alpha'}$. As it turns out the compactified string spectrum is invariant under the exchange

$$R \leftrightarrow \frac{\alpha'}{R}, \qquad n \leftrightarrow w, \tag{1.2.2}$$

a symmetry known as T–duality. At the special radius $R = \sqrt{\alpha'}$ the theory becomes self-dual. In particular, additional string states become massless at this radius, enhancing the gauge symmetry of the Kaluza-Klein vector field (originating from the higher dimensional metric components which have one index in the compact dimension) from $U(1)$ to $SU(2)$.

Open strings

For open strings one may impose Neumann boundary conditions $\partial_\sigma X^\mu|_{\partial\Sigma} = 0$. The massless states in the open string spectrum are that of an $U(1)$ gauge boson A^μ. The full spectrum also includes the tachyon and an infinite tower of massive states as in the closed string case.

D–branes

Another choice for open string boundary conditions are the Dirichlet boundary conditions $\partial_\tau X^\mu|_{\partial\Sigma} = 0$, fixing open string endpoints to a surface. Since the momentum at the end of the string is not conserved, such boundary conditions require the string to couple to another dynamical object — a D–brane. If one imposes Neumann boundary conditions along the time[4] and p space directions, and Dirichlet boundary conditions along the remaining $D - p - 1$ directions, then the Neumann directions correspond to the $p+1$-dimensional world-volume of the Dp–brane, while the Dirichlet directions are transverse to the brane. In this configuration the massless string states are obtained from the case of pure Neumann boundary conditions by dimensional reduction: one gets a p–dimensional gauge boson A^a, $a = 0, 1, \ldots, p$ and $D - p - 1$ scalars Φ^i. In fact these scalars correspond to the transverse oscillations of the Dp–brane, and their vacuum expectation values are related to the position of the brane.

This fits well with T-duality, which interchanges Neumann and Dirichlet boundary conditions in the respective direction. If we T–dualise a direction orthogonal to the Dp–brane world-volume it turns into a D$(p+1)$–brane, and if we T–dualise in a parallel direction we get a D$(p-1)$–brane.

In the case of N parallel D–branes, the spectrum is augmented by additional states coming from strings stretching between different branes. As the branes approach each other some of these states get lighter, becoming massless when the branes finally coincide. These extra massless states enhance the original $U(1)^N$

[4]Imposing Dirichlet boundary conditions along the time direction leads to space-like S–branes [102–104].

gauge group of the individual D-branes to $U(N)$ in the adjoint representation. So for the system of N Dp-branes we have a $U(N)$ gauge theory with an adjoint Higgs mechanism. This has a nice geometrical interpretation: the Higgs expectation values correspond to the distances between branes, and the masses can be understood in terms of stretched strings between different branes.

Superstrings

We may generalise the bosonic string action (1.2.1) by including world-sheet fermions in a supersymmetric way. There are a few options how to construct a supersymmetric theory, of which only five give a consistent result: known as type IIA, type IIB, type I, and heterotic with either $SO(32)$ or $E_8 \times E_8$ gauge groups.

Here we are primarily interested in types IIA and IIB, which are endowed with $\mathcal{N} = 2$ supersymmetry in 10 space-time dimensions (32 supercharges). The massless bosonic states in these theories inhabit the so-called Neveu-Schwarz–Neveu-Schwarz (NS-NS) and Ramond–Ramond (R-R) sectors. The NS-NS sector is indentical for both IIA and IIB and in fact is the same we already encountered in the bosonic case: $g_{\mu\nu}$, Φ, $B_{\mu\nu}$. The R-R sector contains various n-form gauge potentials. In type IIA these are $C^{(1)}$, $C^{(3)}$ with $C^{(7)}$, $C^{(5)}$ as the respective magnetic duals. In type IIB these are $C^{(0)}$, $C^{(2)}$, $C^{(4)}$ with $C^{(8)}$, $C^{(6)}$ as magnetic duals, while the 4-form, $C^{(4)}$, is self-dual.

D–branes in superstring theories

It turns out the perturbative string states can not carry any charge with respect to the R-R gauge fields $C^{(p+1)}$. However, there is no need to look far for some objects to act as sources for these potentials, as the Dp–branes provide a natural candidate. Therefore one also has to include Dp–branes and the corresponding open string sectors to type II theories, p being even in IIA and odd in IIB.[5] The open string massless modes associated with a Dp–brane correspond to the dimensional

[5]Such cases preserve some supersymmetries, which can be subsequently used as a tool for controlling the dynamics. Even branes can appear in type IIB and odd in type IIA, but there can no longer be any preserved supersymmetry [105], see *e.g.* refs. [106, 107] for review.

reduction of a 10-dimensional vector multiplet down to $p+1$ dimensions. In the case of N parallel Dp–branes on top of each other the bosonic effective action (to leading order in α') is given by the dimensional reduction of $D = 10$, $\mathcal{N} = 1$ supersymmetric $U(N)$ gauge theory. Finally let us point out that under T–duality type IIA theory gets mapped onto IIB and *vice versa*.[6]

1.3 Supergravity p–brane solutions

1.3.1 II A/B supergravity actions

In the low energy limit (corresponding to massless states in the spectrum) and for the tree level interactions in perturbation theory the five superstring theories are effectively described by their respective supergravities. The bosonic part of IIA supergravity action in string frame is given by

$$\begin{aligned} S_{IIA} &= \frac{1}{2\kappa_0^2}\int d^{10}x\sqrt{-g}\, e^{-2\Phi}\Big\{R + 4\nabla_\mu\Phi\nabla^\mu\Phi - \frac{1}{12}H_{\mu\nu\rho}H^{\mu\nu\rho}\Big\} \\ &\quad -\frac{1}{4\kappa_0^2}\int G^{(2)}\wedge^\star G^{(2)} + \tilde{G}^{(4)}\wedge^\star \tilde{G}^{(4)} + B^{(2)}\wedge G^{(4)}\wedge G^{(4)} \end{aligned} \tag{1.3.1}$$

where $G^{(n)} = dC^{(n-1)}$ are the R-R field strengths whose kinetic term generalises Maxwell's action

$$-\frac{1}{2}\int G^{(n)}\wedge^\star G^{(n)} = -\frac{1}{2n!}\int d^Dx\sqrt{-g}\, G_{\mu_1\ldots\mu_n}G^{\mu_1\ldots\mu_n}\,. \tag{1.3.2}$$

The 3-form $H^{(3)} = dB^{(2)}$ is the field strength of the $B_{\mu\nu}$ tensor field, and we have also defined

$$\tilde{G}^{(4)} = G^{(4)} + H^{(3)}\wedge C^{(1)}\,. \tag{1.3.3}$$

[6] T–duality in the time direction takes IIA theory to its dual IIB* theory and IIB theory to its dual IIA* theory [108, 109]. The IIA* and IIB* theories are still formulated in 9+1 space-time dimensions, but their respective low energy supergravity limits differ from those of the IIA/B supergravities by having the signs of some of the kinetic terms reversed. The time-like T–duality takes the D–branes of type II theories, with Lorentzian world-volume signature, to the E–branes of type II* theories, which have Euclidean world-volume signatures.

The bosonic part of IIB supergravity action in string frame is given by

$$\begin{aligned} S_{IIB} &= \frac{1}{2\kappa_0^2}\int d^{10}x\sqrt{-g}\, e^{-2\Phi}\Big\{R + 4\nabla_\mu\Phi\nabla^\mu\Phi - \frac{1}{12}H_{\mu\nu\rho}H^{\mu\nu\rho}\Big\} \\ &\quad -\frac{1}{4\kappa_0^2}\int G^{(1)}\wedge^\star G^{(1)} + \tilde{G}^{(3)}\wedge^\star \tilde{G}^{(3)} + \frac{1}{2}\tilde{G}^{(5)}\wedge^\star \tilde{G}^{(5)} \\ &\qquad +C^{(4)}\wedge H^{(3)}\wedge G^{(3)} \end{aligned} \tag{1.3.4}$$

with the following definitions

$$\tilde{G}^{(3)} = G^{(3)} + H^{(3)}\wedge C^{(0)}\,, \tag{1.3.5}$$

$$\tilde{G}^{(5)} = G^{(5)} + \frac{1}{2}H^{(3)}\wedge C^{(2)} + \frac{1}{2}B^{(2)}\wedge G^{(3)}\,. \tag{1.3.6}$$

We also have to impose the self-duality condition $G^{(5)} =^\star G^{(5)}$ by hand in the equations of motion. In order to compute gravitational quantities like the ADM mass one has to convert actions (1.3.1, 1.3.4) into Einstein frame by rescaling the metric

$$G_{\mu\nu} = e^{(\Phi_0-\Phi)/2}g_{\mu\nu}\,. \tag{1.3.7}$$

Newton's constant G_N and gravitational coupling κ are set by

$$2\kappa^2 \equiv 2\kappa_0^2 g_s^2 = 16\pi G_N = (2\pi)^7\alpha'^4 g_s^2\,, \tag{1.3.8}$$

where the string coupling is given by the asymptotic value of the dilaton field at infinity $g_s \equiv e^{\Phi_0}$.

1.3.2 Extremal p–brane solutions

The actions (1.3.1, 1.3.4) admit a family of solutions charged under R-R fields and having p translational isometries — (black) p–branes [110]. We are mainly interested in the extremal "Bogomol'ny–Prasad–Sommerfield" or BPS limit (which preserves half of the original $\mathcal{N}=2$ ten dimensional supersymmetry) of these:[7]

$$\begin{aligned} ds^2 &= H_p^{-1/2}\eta_{ab}dx^a dx^b + H_p^{1/2}\delta_{ij}dx^i dx^j\,, \\ e^{2\Phi} &= g_s^2 H_p^{\frac{3-p}{2}}\,, \\ C^{(p+1)} &= (H_p^{-1}-1)g_s^{-1}dx^0\wedge\ldots\wedge dx^p\,, \end{aligned} \tag{1.3.9}$$

[7] See *e.g.* refs. [111,112] for a review.

where $a, b = 0, \ldots, p$ denote indices parallel and $i, j = p+1, \ldots, 9$ transverse to the brane ($0 \leq p \leq 6$). The function

$$H_p = 1 + \left(\frac{r_p}{r}\right)^{7-p} \tag{1.3.10}$$

is harmonic in transverse coordinates, and

$$r_p^{7-p} = d_p (2\pi)^{p-2} g_s N \alpha'^{(7-p)/2} , \qquad d_p = 2^{7-2p} \pi^{(9-3p)/2} \Gamma\left(\frac{7-p}{2}\right) . \tag{1.3.11}$$

The solution above carries N units of R-R charge

$$\mu_p = (2\pi)^{-p} (\alpha')^{-\frac{p+1}{2}} , \tag{1.3.12}$$

measuring the coupling of the $C^{(p+1)}$ potential to the p–brane source, and features N "units" of basic tension (mass per unit world volume)

$$\tau_p = g_s^{-1} \mu_p . \tag{1.3.13}$$

It is natural to interpret the configuration (1.3.9) as a geometry produced by N parallel p–branes, extended p-dimensional solitonic objects residing at the origin of transverse coordinates ($r = 0$). As BPS objects they enjoy static equilibrium — repulsive gauge forces cancel against the attractive gravitational and dilatonic forces. This property allows a multicenter generalisation of the solution with

$$H_p = 1 + \sum_{i=1}^{N} \frac{r_p^{7-p}}{|\vec{r} - \vec{r}_i|^{7-p}} , \tag{1.3.14}$$

representing N different branes located at arbitrary positions $\vec{r}_i$. We can combine the p–brane solutions in various ways to build more complicated supergravity solutions preserving less supersymmetries, *e.g.* by intersecting branes with each other, boosting them to finite momentum, or by wrapping / warping them on compact geometries.

It was an important realisation [30] that the supergravity p–branes can be identified with the Dp–branes of string perturbation theory. Able use of these two complementary descriptions provided a key for many significant discoveries since 1995, including the gravity/gauge theory correspondences, aspects of black hole quantum mechanics, *etc.*

1.4 D–brane dynamics

1.4.1 The Dirac-Born-Infeld action

As we hinted before, the leading order low-energy effective Dp-brane dynamics is given by the dimensional reduction of ten-dimensional $U(1)$ super-Yang-Mills (SYM) theory. The stringy higher order α'–corrections can be resummed for slowly varying field strengths and for arbitrary supergravity backgrounds to yield the Dirac-Born-Infeld (DBI) action [113]

$$S_{DBI} = -\tau_p \int_{\mathcal{M}_{p+1}} d^{p+1}\xi e^{-\Phi} \sqrt{-\det(g_{ab} + B_{ab} + 2\pi\alpha' F_{ab})}\, \mathcal{G}_{DBI} \,, \tag{1.4.1}$$

where ξ^a are independent coordinates on the $(p+1)$-dimensional brane world-volume and τ_p is the tension already familiar to us from equation (1.3.13). The quantity F_{ab} is the field strength of the brane world-volume gauge field A^a, and g_{ab} and B_{ab} are the pull-backs of space-time metric and Kalb-Ramond field

$$g_{ab} = \frac{\partial x^\mu}{\partial \xi^a}\frac{\partial x^\nu}{\partial \xi^b} g_{\mu\nu} \,, \qquad B_{ab} = \frac{\partial x^\mu}{\partial \xi^a}\frac{\partial x^\nu}{\partial \xi^b} B_{\mu\nu} \tag{1.4.2}$$

to the world-volume of the brane. So, the DBI action describes the Dp-brane coupling to the massless NS-NS fields of the bulk closed string theory. Integration over the determinant of the induced metric g_{ab} gives it also a geometric interpretation as a proper volume swept out by the Dp-brane, indicating that D-branes are really dynamical objects. Notice, this is just like the motion of a massive particle (with mass m) is described by the action

$$-m \int d\tau \sqrt{-\dot{X}^\mu(\tau)\dot{X}^\nu(\tau) g_{\mu\nu}} \tag{1.4.3}$$

which measures the length of the particle's "world-line" parameterised by τ. And similarly, the action for a string can be written as

$$-T \int d^2\xi \sqrt{-\det \partial_a X^\mu \partial_b X^\nu g_{\mu\nu}} \,, \tag{1.4.4}$$

where $\xi^{a,b}$ are the coordinates τ, σ on the string world-sheet and T the string tension. The action (1.4.4) above measures the area of the string world-sheet and is known as the Nambu-Goto action, it is (at least classically) equivalent to the Polyakov

action we introduced earlier as formula (1.2.1). As a matter of fact, we could have taken the world-volume term as a basic D–brane action and then by using T–duality arguments recovered the presence of other terms in action (1.4.1).

1.4.2 The Wess-Zumino action

D–brane interactions with the massless Ramond-Ramond (R-R) fields are incorporated in the generalised Wess–Zumino–like term [114, 115]

$$S_{WZ} = -\mu_p \int_{\mathcal{M}_{p+1}} \sum_p C^{(p+1)} \wedge e^{2\pi\alpha' F^{(2)} + B^{(2)}} \wedge \mathcal{G}_{WZ} \,, \tag{1.4.5}$$

where μ_p is the charge (1.3.12) and the pull-back of bulk space-time forms is understood. In the simplest case the interaction is just

$$\mu_p \int_{\mathcal{M}_{p+1}} d^{p+1}\xi \; \epsilon^{a_0 a_1 \cdots a_p} \, \partial_{a_0} x^{\mu_0} \, \partial_{a_1} x^{\mu_1} \ldots \partial_{a_p} x^{\mu_p} \, C_{\mu_0 \mu_1 \cdots \mu_p} \,, \tag{1.4.6}$$

showing that a Dp–brane acts as a source for the R-R $(p+1)$-form potential $C^{(p+1)}$. This is a higher dimensional generalisation of the way a particle with electric charge q couples to the electromagnetic potential A_μ *via* a term like

$$q \int d\tau \, \dot{X}^\mu(\tau) A_\mu \,, \tag{1.4.7}$$

and analogously a string couples to the 2–form form potential $B_{\mu\nu}$ as

$$T \int d^2\xi \, \epsilon^{ab} \partial_a X^\mu \partial_b X^\nu B_{\mu\nu} \,. \tag{1.4.8}$$

However, the formula (1.4.5) informs us that a Dp–brane can not only couple to the bulk $C^{(p+1)}$ potential, it can also couple to combinations of lower rank potentials.

1.4.3 Curvature corrections

It is important for us that both the DBI and WZ terms receive additional corrections from background curvature. The geometric part of the Wess-Zumino term reads [116, 117]

$$\mathcal{G}_{WZ} = \sqrt{\frac{\hat{\mathcal{A}}(4\pi^2\alpha' R_T)}{\hat{\mathcal{A}}(4\pi^2\alpha' R_N)}} = 1 - \frac{(4\pi^2\alpha')^2}{48} \left(p_1(R_T) - p_1(R_N)\right) + \mathcal{O}(\alpha'^4) \tag{1.4.9}$$

where $\hat{\mathcal{A}}$ is the "A-roof" or Dirac genus, p_1 is the first Pontryagin class

$$p_1 = -\frac{1}{8\pi^2}\mathrm{Tr}R \wedge R \,, \tag{1.4.10}$$

while R_T and R_N are the curvature 2-forms of the tangent and normal bundles of the brane.

The DBI term gets several corrections but the set of curvature-squared terms that will concern us soon is given by [118,119]

$$\mathcal{G}_{DBI} = 1 - \frac{(4\pi^2\alpha')^2}{768\,\pi^2}\left(R_{abcd}R^{abcd} - 2\hat{R}_{ab}\hat{R}^{ab} - R_{\alpha\beta ab}R^{\alpha\beta ab} + 2\hat{R}_{\alpha\beta}\hat{R}^{\alpha\beta}\right) + \mathcal{O}(\alpha'^4)\,, \tag{1.4.11}$$

where $a, \ldots, d$ are the tangent space indices running along the brane world-volume, while α, β are normal indices, running transverse to the world-volume. Also $\hat{R}_{ab}$, $\hat{R}_{\alpha\beta}$ are obtained by contraction of the pulled-back Riemann tensor.

1.4.4 Gauge theory on the world-volume

In the case of N coincident D–branes the gauge symmetry is enhanced to $U(N)$. The world-volume fields A^a and Φ^i become matrices valued in the adjoint and introduce host of related non-abelian modifications to the Dp–action [120], reviewed *e.g.* in ref. [121].

We may deduce the dimensionally reduced SYM theory which appears on the D–brane world-volume from the DBI action (1.4.1) above. First let us employ space-time diffeomorphims to position the world-volume on a fiducial surface $x^i = 0$, and the world-volume diffeomorphisms to match the world-volume coordinates with the remaining space-time coordinates on this surface, $\xi^a = x^a$, a setting known as "static gauge." Assuming the background is approximately flat and also the B_{ab} field vanishes,[8] then the expansion to second order in the gauge field yields

$$S_{YM} = -\frac{1}{4g_{YM,p}}\int d^{p+1}\xi e^{-\Phi}\mathrm{Tr}\Big\{F_{ab}F^{ab} + 2\mathcal{D}_a\Phi^i\mathcal{D}^a\Phi_i + [\Phi^i,\Phi^j]^2\Big\}\,, \tag{1.4.12}$$

where $\mathcal{D}^a$ is the (gauge) covariant derivative and the $(p+1)$-dimensional SYM coupling for the theory on the branes is

$$g^2_{YM,p} = \tau_p^{-1}(2\pi\alpha')^{-2}\,. \tag{1.4.13}$$

[8] Having a constant B-field in the background leads to noncommutative gauge theory [122,123].

The scalars Φ^i describe the transverse displacements of the D–brane through the identification

$$x^i(\xi^i) = 2\pi\alpha'\Phi^i(\xi^i)\,, \tag{1.4.14}$$

in the case of N branes these become $U(N)$ adjoint matrices encoding the collective transverse coordinates of the branes.

A classical vacuum of the action (1.4.12) corresponds to a static solution of the equations of motion whereby the potential energy of the system is minimized. It is given by the field configurations which simultaneously solve the equations

$$\begin{aligned} F_{ab} = \mathcal{D}_a\Phi^i &= 0 \\ V(\Phi) &= 0\,. \end{aligned} \tag{1.4.15}$$

Vanishing of the potential

$$V(\Phi) = \mathrm{Tr}[\Phi^i, \Phi^j]^2 \tag{1.4.16}$$

is equivalent to satisfying the conditions

$$[\Phi^i, \Phi^j] = 0 \tag{1.4.17}$$

for all i, j and at each point in the $(p+1)$-dimensional world-volume of the branes. This means the $N \times N$ matrix fields Φ^i must be simultaneously diagonalisable by a gauge transformation, and we may write

$$\Phi^i = \begin{pmatrix} x_1^i & 0 & \cdots & 0 \\ 0 & x_2^i & & \vdots \\ \vdots & & \ddots & 0 \\ 0 & \cdots & 0 & x_N^i \end{pmatrix}\,. \tag{1.4.18}$$

The simultaneous real eigenvalues x_A^i give the positions of the N distinct D–branes in the i-th transverse direction. It follows the "moduli space" of vacua for the $(p+1)$-dimensional field theory (1.4.12) arising from the dimensional reduction of the super-Yang-Mills in ten dimensions is the quotient space

$$\frac{(\mathbb{R}^{9-p})^N}{S_N}\,, \tag{1.4.19}$$

where the factors of $\mathbb{R}$ correspond to the positions of the N Dp–branes in the $(9-p)$-dimensional transverse space, and S_N is the symmetric group acting by permutations

of the N coordinates x_A. The group S_N corresponds to the residual Weyl symmetry of the $U(N)$, and it represents the permutation symmetry of a system of N indistinguishable D–branes.

1.4.5 Decoupling limit

The two descriptions of D–branes — the supergravity picture of section 1.3.2 (corresponding to the interactions mediated by massless closed strings) and the gauge field theory picture of section 1.4.4 (corresponding to the interactions of lightest open strings) — are good approximations in different domains. In order to reliably use supergravity as an effective low energy theory we are restricted to small curvature, measured in string units. This is equivalent to the condition $g_s N > 1$. On the other hand in the open string perturbation theory involving N D–branes a typical interaction diagram has a factor $g_s N$. So this picture is good as long $g_s N < 1$. (We also assume the string coupling constant g_s is small to suppress string loops.)

A very useful procedure in the game is to take the decoupling limit where the interactions between the open strings ending on branes and the closed strings in the bulk are turned off. This is achieved by

$$\alpha' \to 0, \qquad \text{holding fixed} \quad g_{YM,p} \quad \text{and} \quad U = r/\alpha' \,. \tag{1.4.20}$$

Asking α' to vanish relieves us from corrections due to massive (higher energy) string states both in the supergravity and the SYM description. From the supergravity point of view this procedure corresponds to taking the near-horizon limit, $r \to 0$, *i.e.* zooming in to the region close to the branes. In the gauge theory picture the scaled radial coordinate $U = r/\alpha'$ plays the role of energy scale, *e.g.* the mass of the W-boson. In the limit (1.4.20) the remaining supergravity quantities will have a physical meaning in the gauge theory on the brane, like the gauge coupling, *etc*, as we will explore shortly.

1.5 D–branes as probes of geometry

A fundamental string provides a probe which can probe the geometry only down to the string scale α', as increasing energy gets it smeared out. The characteristic size of D–branes, however, is much smaller than the string length when g_s is small [124]. This makes D–branes capable of exploring very short distances and they can serve as useful local test probes measuring the background metric and other fields at a point in space-time.

The basic idea behind D–brane probing techniques is that the brane world-volume theory must encode information about the background we are probing [125]. On the one hand, one can directly insert the background field configuration in the D–brane world-volume action. On the other hand the effects of the background fields on the probe must be precisely reproduced by the dynamics of the probe quantum field theory. In the latter description, space-time emerges as a derived concept, the low energy moduli space of a supersymmetric gauge theory [126].

Probing the geometry of N p–branes with a single Dp–brane

As an example let us probe the geometry generated by N p–branes with a single Dp–brane. We need to insert the supergravity solution (1.3.9) into the Dp–brane action (1.4.1 + 1.4.5). By the virtue of the static gauge

$$\begin{aligned} \xi^0 &= x^0 = t\,; \\ \xi^m &= x^m\,, \quad m = 1,\ldots,p\,; \\ x^i &= x^i(\xi^0)\,, \quad i = p+1,\ldots,9\,; \end{aligned} \tag{1.5.21}$$

the induced metric on the D–brane world-volume becomes

$$g_{ab} = \begin{pmatrix} g_{00} + g_{ij}v^iv^j & 0 & \cdots & 0 \\ 0 & g_{11} & & \vdots \\ \vdots & & \ddots & 0 \\ 0 & \cdots & 0 & g_{pp} \end{pmatrix}, \tag{1.5.22}$$

where $v^i \equiv dx^i/d\xi^0 = \dot{x}^i$ is the probe velocity in transverse directions. Inserting the p–brane metric here and taking the determinant gives

$$-\det g_{ab} = H_p^{-\frac{p+1}{2}} \left(1 - H_p v^2\right), \qquad v^2 = \sum_{i=p+1}^{9} (v^i)^2 . \tag{1.5.23}$$

Taking into account the dilaton factor we get

$$\begin{aligned} S_{DBI,p} &= -\frac{\mu_p}{g_s} \int d^{p+1}\xi H_p^{-1} \sqrt{1 - H_p v^2} \\ &\approx -\frac{\mu_p}{g_s} \int d^{p+1}\xi H_p^{-1} \left(1 - \frac{1}{2} H_p v^2\right) \end{aligned} \tag{1.5.24}$$

assuming the probe motion is slow enough that we can expand the square root and neglect higher than quadratic terms in v.

For the WZ term we need to pull back the $C^{(p+1)}$ R-R potential to the brane world-volume

$$C_{a_0 a_1 \ldots a_p} = \frac{\partial x^{\mu_0}}{\partial \xi^{a_0}} \frac{\partial x^{\mu_1}}{\partial \xi^{a_1}} \cdots \frac{\partial x^{\mu_p}}{\partial \xi^{a_p}} C_{\mu_0 \mu_1 \ldots \mu_p} , \tag{1.5.25}$$

thus yielding

$$S_{WZ,p} = \frac{\mu_p}{g_s} \int d^{p+1}\xi \left(H_p^{-1} - 1\right) . \tag{1.5.26}$$

So, putting (1.5.24) and (1.5.26) together the complete probe effective action is given by

$$S_{\text{probe}} = \frac{\mu_p V_p}{g_s} \int dt \left(-H_p^{-1} + \frac{1}{2} v^2 + H_p^{-1} - 1\right) , \tag{1.5.27}$$

where we have integrated over the spatial part of the brane world-volume, $\int d^p \xi = V_p$. As expected, the r-dependent potential terms do cancel, showing that there is no force between branes since the configuration is BPS. (This cancellation only happens in the slow motion approximation, if orders beyond v^2 need to be considered while expanding the square root, the BPS condition would not hold any more.) Therefore the probe dynamics in transverse directions is described by the lagrangian

$$\mathcal{L}_{\text{probe}} = \frac{1}{2} m_p v^2 - m_p \tag{1.5.28}$$

of a free particle of mass $m_p = \tau_p V_p$ moving in a constant potential.[9] The transverse

[9]The constant potential originated from the constant part of the $C^{(p+1)}$ field (1.3.9) and we will neglect this term from now on, since it is pure gauge.

metric seen by the probe can be read off from the coefficient of the v^2 term

$$ds^2 = \frac{m_p}{2}\,\delta_{ij}\,dx^i dx^j\,, \tag{1.5.29}$$

it is trivially flat.

Corresponding results can be also obtained from the world-volume field theory point of view. As we know already there is a $(p+1)$-dimensional $U(N)$ gauge theory with 16 supercharges on the world-volume of N Dp–branes, containing a A^a gauge field and $9-p$ scalars Φ^i in the adjoint of $U(N)$. Geometrically the latter where understood as collective coordinates for the transverse motions of branes. The components of Φ^i can take different vacuum expectation values, parameterising the moduli space of inequivalent vacua and corresponding to the data how the branes are distributed in the transverse space. The metric on this moduli space is equivalent to the space-time metric in directions transverse to the branes world-volume. For the case discussed in this section the moduli space is flat due to high amount of supersymmetry. But we will encounter a more interesting case in the next chapter.

1.6 Summary

In this chapter we have tried to lay out the context and to set the preliminaries for the enhançon mechanism in string theory. We began by outlining the problem of space-time singularities in the theories of gravity and noted that not all singularities could be possibly "smoothed out" to a small region of strong but finite curvature. Some singularities must rather be excised, *i.e.* prohibited as unphysical.

String theory does not rule out space-time singularities arising in the low energy field theory description, but there are several examples known how such singularities can be resolved in the sense of having a non-singular stringy physics on the background in question. Typically this involves new quantum degrees of freedom becoming massless and augmenting the initial field theory spectrum. We discuss some of these examples, before giving the first review of the enhançon, a mechanism in string theory which leads to the excision of a certain naked space-time singularity.

Much of the recent progress in string theory, including the enhançon mechanism, can be attributed to the study of D–branes, extended solitonic objects where open

strings can end. Therefore we have devoted the second half of the chapter to describe the main properties of D–branes. Most of it will be relevant and find direct applications later.

On the one hand D–branes are solutions of supergravity (section 1.3.2), on the other hand they are described by a gauge theory on their world-volume (section 1.4.4). To be precise, these two descriptions are valid in different regimes (section 1.4.5). The effective dynamics of D–branes, which can be used to link these two descriptions is given by the Dirac–Born–Infeld – Wess–Zumino action (sections 1.4.1 and 1.4.2), it receives corrections of various types, for example from the background curvature (section 1.4.3).

As the first application of these facts we used a single Dp–brane to probe the geometry generated by a large number of p–brane sources. As is expected from the BPS nature of the problem, the potential terms cancelled in the effective lagrangian of the probe, leaving only a kinetic term. The coefficient of this kinetic term, giving the tension (mass) of the probe, was related to the metric of the gauge theory moduli space.

Chapter 2

The Enhançon Mechanism

In this chapter we will use the configuration of D6–branes wrapped on $K3$ to review the salient features of the enhançon mechanism. This configuration provides a prototypical example we will generalise and modify in the chapters to follow, and studying it offers a good opportunity to explain the main calculational techniques we will apply many times later on.

We begin by considering how the procedure of wrapping D6–branes on a $K3$ manifold induces an extra amount of negative D2–brane charge, causing the corresponding naive supergravity solution to show a naked repulson singularity. However probing the geometry with constituent branes in section 2.3 reveals the actual situation to be different, as the branes expand into a sphere surrounding the would-be singularity leaving a flat geometry inside. This means the singularity gets excised, it was never really there. We will review the physical argument why this should be the case and mention some dual pictures of the system.

The analysis gets further support in section 2.5 from the supergravity junction conditions that are consistent with the excision of the singular region of the spacetime. Then we will turn to the gauge theory on the branes' world-volume and use parallels with a yet another dual description in terms of $SU(2)$ multi-monopoles. In the last section 2.7 we will generalise the situation by adding some real (and positive charge) D2–branes.

The material presented in this chapter is based mainly on refs. [79, 83, 86].

2.1 Wrapping branes on K3

We embark on our journey by wrapping N coincident D6–branes on a $K3$ manifold[1] of volume V_{K3}. Wrapping a brane on some compact manifold basically means that part of the brane's world-volume will reside on this manifold. The world-volume of a D6–brane is seven-dimensional (encompassing one time and six space directions), and $K3$ is a surface of four real dimensions. Thus wrapping a D6–brane on $K3$ results in four of the brane spatial world-volume directions wrapped on $K3$, while the remaining three world-volume directions stay unwrapped.

Since $K3$ is not flat, there are some curvature corrections to the brane dynamics we need to take into account. These happen to induce exactly $-N$ units of D2–brane charge on the unwrapped part of the D6–brane world-volume [116, 117]. The wrapped D6–brane is still coupling to the seven-form R-R potential $C^{(7)}$ as it was while unwrapped, but now it does also couple to $C^{(3)}$ *via* the $K3$ curvature. More precisely, this can be seen from the WZ part of the D6–brane action (1.4.5) which gets an additional term from (1.4.9)

$$\begin{aligned} -\mu_6 \frac{(4\pi^2\alpha')^2}{48} \int_{\mathcal{M}_3 \times K3} C^{(3)} \wedge p_1(K3) &= -\mu_6 (4\pi^2\alpha')^2 \int_{\mathcal{M}_3} C^{(3)} \\ &= -\mu_2 \int_{\mathcal{M}_3} C^{(3)} , \end{aligned} \tag{2.1.1}$$

where $\mathcal{M}_3$ stands for the unwrapped part of the world-volume and in the calculation we have used the fact that p_1 of K3 integrates to 48 (see Appendix B). The charges $\mu_6 = (2\pi)^{-6}(\alpha')^{-7/2}$, $\mu_2 = (2\pi)^{-2}(\alpha')^{-3/2}$ are as given in equation (1.3.12) previously.

The emergence of N units of negative D2–brane charge is a particular property of K3, had we wrapped the branes on a four-torus for instance, nothing of this sort would have happened since T^4 is flat. We may think of the result as an effective D2–brane bound within the unwrapped part of the D6–brane world-volume but "delocalised" in K3 directions. However, it is important not to confuse these induced effective D2–branes with true D2–branes which we will introduce to the system later in section 2.7. Also, although the induced object carries negative amount of D2–brane charge it is not an anti–D2–brane, since it preserves the same supersymmetries

[1] Some relevant facts about $K3$ manifolds are mentioned in Appendix B.

	$\mathbb{R}^{5,1}$						K3			
	x_0	x_1	x_2	x_3	x_4	x_5	x_6	x_7	x_8	x_9
D6	–	–	–	·	·	·	–	–	–	–
D2	–	–	–	·	·	·	∼	∼	∼	∼

Table 2.1: A sketch of D6–branes wrapped on K3 and the induced negative D2–branes. The branes' world-volume directions are marked by "–", and transverse directions where the branes are point-like are denoted by "·", while "∼" indicates that the induced D2–branes are delocalised on K3.

as a correct sign D2–brane with the same orientation. To sum up the story so far we have sketched the resulting configuration in table 2.1.

As we already mentioned, wrapped D6–branes still couple to the seven-form potential $C^{(7)}$ as usual. We may integrate the latter term over $K3$, gaining a factor of the volume V_{K3}. So the total charge of the resulting $(2+1)$-dimensional object is N units of

$$\mu = \mu_6 V_{K3} - \mu_2 \ . \tag{2.1.2}$$

Since the charge and tension are related, $\tau = g_s^{-1}\mu$, equation (1.3.13), this object also has a corresponding effective tension

$$\tau = \tau_6 V_{K3} - \tau_2 \ . \tag{2.1.3}$$

In fact the shift from the original D6–brane tension is fully expected because the DBI part (1.4.1) of the D–brane action does also receive curvature corrections. The result above comes from integrating over the $R_{abcd}R^{abcd}$ term in equation (1.4.11), while other terms in (1.4.11) vanish, since $K3$ is Ricci-flat.

Before writing down the supergravity solution let us remark that the configuration we are talking about preserves 1/4 of the original supersymmetry (8 supercharges out of 32). Half of the supersymmetry was broken by considering a D–brane, and yet another half was broken by wrapping it on $K3$.

2.1.1 The supergravity solution

The supergravity solution corresponding to our configuration can be obtained by superimposing solutions of the constituent D6- and (effective) D2–branes from equation (1.3.9), but taking into account that the D2–branes are really delocalised on $K3$. So we get (in string frame)

$$\begin{aligned} ds^2 &= H_2^{-1/2}H_6^{-1/2}(-dt^2+dx_1^2+dx_2^2)+H_2^{1/2}H_6^{1/2}\left(dr^2+r^2\,d\theta^2+r^2\sin^2\theta\,d\phi^2\right) \\ &\quad +V^{1/2}H_2^{1/2}H_6^{-1/2}ds_{K3}^2\,, \\ e^{2\Phi} &= g_s^2H_2^{1/2}H_6^{-3/2}, \\ C^{(3)} &= g_s^{-1}H_2^{-1}dt\wedge dx_1\wedge dx_2\,, \\ C^{(7)} &= g_s^{-1}H_6^{-1}dt\wedge dx_1\wedge dx_2\wedge ds_{K3}\,, \end{aligned} \tag{2.1.4}$$

where the harmonic functions and charges are given by

$$H_2 = 1+\frac{r_2}{r}\,, \qquad r_2 = -\frac{(2\pi)^4 g_s N\alpha'^{5/2}}{2V}\,, \tag{2.1.5}$$

$$H_6 = 1+\frac{r_6}{r}\,, \qquad r_6 = \frac{g_s N\alpha'^{1/2}}{2}\,. \tag{2.1.6}$$

The spherical coordinates r,θ,ϕ parametrise transverse directions x^i with $i=3,4,5$, and x^μ, $\mu=0,1,2$, correspond to the unwrapped world-volume directions. Also, ds_{K3} is the metric of unit volume $K3$, while the solution adjusts itself such that

$$V(r) = \frac{VH_2(r)}{H_6(r)} \tag{2.1.7}$$

is the measured volume of $K3$ at radius r, V being the volume at infinity. A special value of the $K3$ volume

$$V_\star = (2\pi)^4\alpha'^2 \tag{2.1.8}$$

will become significant later.

2.2 The repulson geometry

Upon closer examination the classical solution (2.1.4) exhibits an unsettling feature, it has a naked singularity at the radius

$$r_{\rm r} = |r_2| = \frac{V_\star}{V}r_6\,. \tag{2.2.1}$$

This is where curvature invariants like R, $R_{\mu\nu}R^{\mu\nu}$, $R_{\mu\nu\rho\sigma}R^{\mu\nu\rho\sigma}$ blow up, and the K3 volume $V(r)$ shrinks down to zero. Inside this radius the metric is imaginary. In fact, massive particles get repelled if they approach the singularity, hence it is known as "repulson" [80–82].

To see the repulson let us probe the geometry transverse to the branes with a test particle of unit mass moving with four-velocity $\mathbf{u}$. The Killing vectors $\zeta = \frac{\partial}{\partial t}$ and $\eta = \frac{\partial}{\partial \phi}$, associated with the symmetries of the geometry, provide conserved quantities

$$e = -\xi \cdot \mathbf{u} \,, \qquad L = \eta \cdot \mathbf{u} \,, \tag{2.2.2}$$

the total energy and angular momentum per unit mass of the particle. The velocity of a massive particle is time-like, *i.e.* obeys

$$g_{\mu\nu}u^{\mu}u^{\nu} = -1 \,. \tag{2.2.3}$$

Assuming $u^{\theta} = 0$ so that the motion lies on the equatorial plane, and substituting the constants of motion (2.2.2) into (2.2.3) gives

$$E = \frac{1}{2}\left(\frac{dr}{d\tau}\right)^2 + V_{eff}(r) \,, \tag{2.2.4}$$

where we redefined $E = \frac{e^2-1}{2}$. Thus the motion of the probe particle is governed by the effective potential

$$V_{eff}(r) = \frac{1}{2}\left(-g_{tt}\left(1 + \frac{L^2}{g_{\phi\phi}}\right) - 1\right) \,. \tag{2.2.5}$$

For our purposes it is sufficient to consider only radial motion and we can set $L = 0$. Now figure 2.2. depicts the how this potential looks like when we substitute in our solution (2.1.4) as the background. As the probing particle moves in from infinity it feels an attractive gravitational force, but at certain radius the force becomes repulsive. The potential diverges at $r = r_{\rm r}$, exhibiting an infinite repulsive force at the singularity. The turning point of the potential occurs when

$$V'_{eff} = 0 \tag{2.2.6}$$

which for our metric is equivalent to the condition

$$\left(\frac{H'_2}{H_2} + \frac{H'_6}{H_6}\right) = 0 \,. \tag{2.2.7}$$

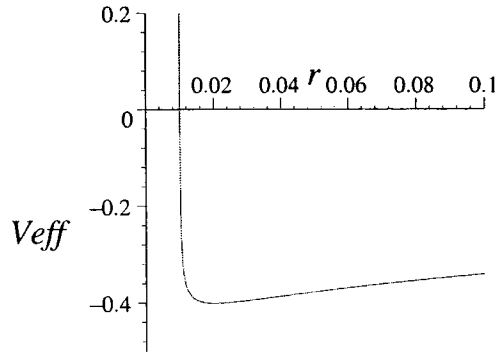

Figure 2.1: Test particle effective potential in the gravitational background generated by wrapped D6–branes.

Solving the equation above gives

$$r_e = \frac{2V_\star}{V - V_\star} r_6 \tag{2.2.8}$$

as the radius where the geometry becomes repulsive.

2.3 Probing with branes

Now it is time to apply the techniques introduced in section 1.5 of the previous chapter and probe the geometry with a single wrapped D6–brane. Taking into account the new induced WZ term (2.1.1) and the tension (2.1.3) the effective world-volume action for the probe is

$$S = -\int_{\mathcal{M}_3} d^3\xi\, e^{-\Phi}\,(\mu_6 V(r) - \mu_2)\,(-\det g_{ab})^{1/2} + \mu_6 \int_{\mathcal{M}_3\times K3} C^{(7)} - \mu_2 \int_{\mathcal{M}_3} C^{(3)}\,, \tag{2.3.1}$$

here ξ^a $(a, b = 0, 1, 2)$ are the coordinates on the unwrapped part of the world-volume, and g_{ab} is the induced metric. Adopting the static gauge $\xi^a = x^a$, $x^i = x^i(t)$ as before and assuming the probe velocity

$$v^2 = \dot{r}^2 + r^2\,\dot{\theta}^2 + r^2 \sin^2\theta\,\dot{\phi}^2 \tag{2.3.2}$$

is small, we carry out computations similar to what we did in section 1.5 to obtain the effective Lagrangian

$$\begin{aligned}\mathcal{L} &= -\frac{\mu_6 V H_2 - \mu_2 H_6}{g_s H_2 H_6} + \frac{1}{2g_s}\,(\mu_6 V H_2 - \mu_2 H_6)\,v^2 + \frac{\mu_6 V}{g_s H_6} - \frac{\mu_2}{g_s H_2} \\ &= \frac{1}{2g_s}\,(\mu_6 V H_2 - \mu_2 H_6)\,v^2\,.\end{aligned} \tag{2.3.3}$$

Here again the potential terms do exactly cancel, as we still have a BPS configuration, and what is left in the effective lagrangian is just the kinetic term. The coefficient of v^2 gives the effective tension of the probe

$$\tau_{\text{eff}} = \frac{1}{g_s}\left(\mu_6 V H_2 - \mu_2 H_6\right) = \frac{\mu_6}{g_s}\left(V H_2 - V_\star H_6\right) = \frac{\mu_6}{g_s} H_6 \left(V(r) - V_\star\right) . \qquad (2.3.4)$$

Notice there is a marked difference between this result and the effective lagrangian (1.5.28) we had when probing the geometry of N Dp–branes with a Dp–brane. Now the tension is changing as the probe moves in the transverse space, meaning also that the moduli space metric it sees is not flat any more. We assume the probe tension (and the metric) is positive at spatial infinity, implying the asymptotic $K3$ volume $V > V_\star$. As the probe approaches the origin, its tension becomes less and less until inside the radius

$$r_{\text{e}} = \frac{2V_\star}{V - V_\star} r_6$$

the tension τ_{eff} threatens to become negative. Correspondingly, at this radius the running $K3$ volume takes the special value $V(r_{\text{e}}) = V_\star$, and from equation (2.2.8) we see it is actually the limit beyond which the geometry becomes repulsive. It is easy to see all this happens above the singularity since $r_{\text{e}} > r_{\text{r}}$.

Having a negative tension brane here is hardly a physical affair and rather indicates that we are missing some vital understanding. The interpretation of the situation, due to ref. [79], is the following: as the tension vanishes the probe ceases to be point-like in transverse dimensions and it smears around over the sphere of radius r_{e}. The brane can not move further in to the region where its tension would be negative. Let us look more closely why this is the case.

2.4 Enhanced gauge symmetry

Our $(2+1)$-dimensional membranes in six dimensions are BPS objects, and we already noticed how the forces between them cancel in equation (2.3.3). They are really a higher dimensional generalisation of magnetic monopoles,[2] carrying a mag-

[2]In D dimensions a p-dimensional fundamental electric object has a $(D-p-4)$-dimensional magnetic partner. It is a coincidence in four dimensions that the fundamental electric particle and

netic charge of a certain $U(1)$ 1-form potential. Compactification of type IIA string theory on $K3$ produces a host of 24 1-form fields in six dimensions, as we briefly review in appendix B. But only two of these concern us here: the direct descendant of the ten dimensional $C^{(1)}$ R-R potential and the $C^{(5)}$ potential wrapped on the volume 4-cycle of $K3$. In ten dimensions the D6–brane already couples magnetically to $C^{(1)}$, while the D2–brane has a similar relation to $C^{(5)}$. Now as seen in six dimensions our monopole is charged under a diagonal combination of the two 1-forms mentioned above.

As a matter of fact, we do not just have monopoles, there are W–bosons and a Higgs field too. The former are the D4–branes and anti–D4–branes wrapped on $K3$ (point particles in six dimensions), while the latter is related to the running $K3$ volume. Therefore we have all the ingredients of the well-known setup of $SU(2)$ magnetic monopoles.[3] In view of this fact the situation becomes more understandable.

The ratios $\mu_0/\mu_4 = \mu_2/\mu_6 = V_\star$ are equal, so the wrapped D4–brane becomes massless at the same radius where the wrapped D6–branes have a vanishing tension. But a massless D4–brane is a massless W–boson indicating that the broken $SU(2)$ symmetry is restored at this radius. D4–brane and anti–D4–brane together with the $U(1)$ R-R field combine together into an $SU(2)$ gauge field. Therefore we have an occurrence of enhanced gauge symmetry (from $U(1)$ to $SU(2)$) and the locus of points where this happens, *i.e.* a sphere of radius r_e, can be justly called an "enhançon".

The mass of the $SU(2)$ monopole is proportional to the mass of the corresponding W–boson, while its characteristic size is inversely proportional to the mass. In the region where W–bosons are massless and $SU(2)$ is restored, the monopole becomes massless and grows in size, ceasing to be sharply localised. As we identify our wrapped D6–brane probe with a magnetic monopole, the behaviour of brane tension (2.3.4) starts to make sense. The probe begins to expand as it approaches the

its dual magnetic monopole are both 0-dimensional, *i.e.* point-like. In fact, from the three transverse dimensions point of view our wrapped branes also look like point-like magnetic monopoles.

[3]For the benefit of the reader we review the story of $SU(2)$ monopoles in appendix C.

enhançon locus, and spreads around the sphere when its tension vanishes.

It is instructive to think we can build the configuration by bringing slowly in single wrapped D6–branes one by one from infinity. Each of them will essentially behave like the probe described above. None of them can move further inside from the enhançon radius, but will melt smoothly into the shell made of the branes already residing at r_e. Only the shell grows in size as more branes come in, since r_e depends on the number N of the branes in the configuration. In this sense we really have a big multi-monopole constructed by having N individual monopoles merged at the core.

What about the repulson singularity we were so worried about before? Since there can be no brane sources inside of the enhançon radius but all of them are smeared on a surrounding sphere, the internal geometry must be flat to a first approximation (forming a smooth junction with the outside geometry at $r = r_e$, as we will discuss in section 2.5). The metric inside is modified and therefore the singularity gets excised — in quantum string theory it was never really there!

The phenomenon of gauge symmetry enhancement means we can take our supergravity solution (2.1.4) at its face value only down to the enhançon radius. Beyond this radius new massless degrees of freedom, coming from the the full string theory, must be taken into account. The solution (2.1.4) was an attempt from supergravity to represent the geometry given the asymptotic charges. The attempt was not successful in the internal region because it was not aware of the new degrees of freedom coming to play there. The putative repulson singularity was simply an artefact of supergravity falling short of an accurate description of the stringy physics.

2.4.1 Some dual situations

The argument for Dp–branes of different p runs along similar lines as above. Wrapping N Dp–branes on $K3$ induces $-N$ units of D$(p-4)$–brane charge on the $(p-3)$-dimensional world-volume and suggests a supergravity solution with an apparent repulson singularity. The wrapped branes become tensionless on a sphere S^{8-p} (in $9-p$ transverse dimensions), where the running $K3$ volume reaches its special value $V_\star$, and the physics goes beyond the naive supergravity description. For even p we

see the $SU(2)$ gauge symmetry restored, for odd p there is the A_1 two-form gauge theory [79].

The system has many other dual realisations as outlined in ref. [79]. For instance under S–duality between type IIA strings on $K3$ and heterotic strings on T^4 [27,28] the wrapped D6–brane maps [127] to a bound state of a Kaluza-Klein monopole [128,129] and an H–monopole [130–132] made by wrapping the heterotic NS5–brane [79,133]. Also the IIA wrapped D4–brane is dual to a winding heterotic string on T^4, and vanishing of the brane tension corresponds to the vanishing of the winding string mass at the self-dual radius and enhanced gauge symmetry.

Another interesting dual realisation of the wrapped Dp–brane system is given by N D$(p-3)$–branes stretched between two parallel NS5–branes [79,134]. For example wrapped D6–branes correspond to stretching D3–branes, which from the NS5–branes' world-volume gauge theory point of view are $SU(2)$ magnetic monopoles, $SU(2)$ being spontaneously broken to $U(1)$ by the separation of NS5–branes.

2.5 Consistency of excision in supergravity

We mentioned before that the singular internal geometry should be replaced by a flat space. But can we be sure the geometry constructed in this manner is actually consistent? This kind of problem can be tackled with the Darmois'–Israel formalism [135,136] (see also [137]) for matching space-times across some surface Σ. We demand the metric of these two space-times glued together to be continuous on the junction surface Σ. There may be a discontinuity in the extrinsic curvature at the surface, which gives this boundary an interpretation as a thin shell acting as a δ-function source of stress-energy located at the surface. In the computation below (first performed in ref. [83]) we see the resulting stress-energy is in agreement with our understanding that there is a shell of wrapped D6–branes surrounding the part of the original supergravity geometry we needed to replace.

In order to be able to interpret the discontinuity in the extrinsic curvature as a stress-energy, we need to transform our string frame solution (2.1.4) into Einstein

frame by using (1.3.7). The rescaled Einstein frame metric $G_{\mu\nu}$ is

$$ds^2_{(E)} = H_2^{-5/8} H_6^{-1/8} \eta_{\mu\nu} + H_2^{3/8} H_6^{7/8} (dr^2 + r^2 d\theta^2 + r^2 \sin^2\theta d\phi^2) + V^{1/2} H_2^{3/8} H_6^{-1/8} ds^2_{K3} \tag{2.5.1}$$

where the harmonic functions H_2 and H_6 are the same as in equation (2.1.5). We need to match this metric to a flat metric at some incision radius r_i, which for the moment may not coincide with the enhançon radius r_e. To ensure the metric is continuous over the junction surface, let us assume the internal metric has the same form as the external metric (2.5.1), but the harmonic functions H_2 and H_6 are replaced by constants

$$h_2 = 1 + \frac{r_2}{r_i} , \qquad h_6 = 1 + \frac{r_6}{r_i} . \tag{2.5.2}$$

Now we can compute the discontinuity in the extrinsic curvature.[4] The boundary between the two geometries is a sphere with radius r_i (in the three dimensions transverse to the branes). More precisely, the complete junction surface Σ is 9-dimensional, extending in all directions except r, where it is fixed by the equation $r - r_i = 0$. We may identify the coordinates ξ^A on Σ with the space-time coordinates: $\xi^{\mu,\nu} = x^{\mu,\nu}$, $\mu, \nu = 0, 1, 2$ are the directions filled by the unwrapped part of branes' world-volume, $\xi^{a,b} = x^{a,b}$ the four $K3$ directions, and finally $\xi^{i,j} = \theta, \phi$. The unit normal vectors of the radial boundary are

$$n^A_{\pm} = \mp \frac{1}{\sqrt{G_{rr}}} \left(\frac{\partial}{\partial r}\right)^A , \tag{2.5.3}$$

where n_+ (n_-) is the outward pointing normal for the space-time region $r > r_i$ ($r < r_i$). The general formula for the extrinsic curvature (D.2) simplifies considerably due to the spherical symmetry of the problem and yields

$$K^{\pm}_{AB} = \frac{1}{2} n^C_{\pm} \partial_C G_{AB} = \mp \frac{1}{2\sqrt{G_{rr}}} \frac{\partial G_{AB}}{\partial r} . \tag{2.5.4}$$

The discontinuity in the extrinsic curvature across the junction is defined as

$$\gamma_{AB} = K^+_{AB} + K^-_{AB} . \tag{2.5.5}$$

[4] See appendix D.

The stress-energy tensor supported at the junction surface is given by the Lanczos equation [138]

$$S_{AB} = \frac{1}{\kappa^2}\left(\gamma_{AB} - G_{AB}\gamma^C{}_C\right) , \tag{2.5.6}$$

where κ is the gravitational coupling defined previously in equation (1.3.8).

After inserting our metric into the formulas above a straightforward computation shows the discontinuity tensor is

$$\gamma_{\mu\nu} = \frac{1}{16}\frac{1}{\sqrt{G_{rr}}}\left(5\frac{H_2'}{H_2} + \frac{H_6'}{H_6}\right) G_{\mu\nu} , \tag{2.5.7a}$$

$$\gamma_{ij} = -\frac{1}{16}\frac{1}{\sqrt{G_{rr}}}\left(3\frac{H_2'}{H_2} + 7\frac{H_6'}{H_6}\right) G_{ij} , \tag{2.5.7b}$$

$$\gamma_{ab} = -\frac{1}{16}\frac{1}{\sqrt{G_{rr}}}\left(3\frac{H_2'}{H_2} - \frac{H_6'}{H_6}\right) G_{ab} , \tag{2.5.7c}$$

where a prime denotes ∂_r and all the quantities are evaluated at the incision surface $r = r_i$. The trace is

$$\gamma^C{}_C = -\frac{1}{16}\frac{1}{\sqrt{G_{rr}}}\left(3\frac{H_2'}{H_2} + 7\frac{H_6'}{H_6}\right) . \tag{2.5.8}$$

So, finally we have found the stress-energy tensor of the junction shell to be

$$S_{\mu\nu} = \frac{1}{2\kappa^2\sqrt{G_{rr}}}\left(\frac{H_2'}{H_2} + \frac{H_6'}{H_6}\right) G_{\mu\nu} , \tag{2.5.9a}$$

$$S_{ij} = 0 , \tag{2.5.9b}$$

$$S_{ab} = \frac{1}{2\kappa^2\sqrt{G_{rr}}}\left(\frac{H_6'}{H_6}\right) G_{ab} . \tag{2.5.9c}$$

2.5.1 Junction shell tension

Already the first glance reveals this result is consistent with our ideas of having a junction shell made of wrapped D6–branes. Vanishing S_{ij} (in the transverse directions) at a generic radius r_i is related to the fact that the constituent branes are BPS objects and no force is needed between them to support the shell. Next, the S_{ab} components (in the $K3$ directions) involve only H_6, which is appropriate since only the D6–branes were wrapped on $K3$ (while the effective D2–branes were delocalised in these directions).

Up to an overall sign, the coefficient of the metric components in the stress-energy formula gives an effective tension in the corresponding directions. As a check

for our interpretation that the boundary surface is made of branes, we may expand the effective tension in (2.5.9a) and (2.5.9c) for large r_i:

$$\begin{aligned} \tau_{mem}(r_i) &= \frac{1}{\kappa^2}\frac{r_6}{r_i^2}\left(1-\frac{V_\star}{V}\right) = \frac{N}{(2\pi)^6(\alpha')^{7/2}g_s}(V-V_\star)\frac{1}{4\pi r_i^2 V} \\ &= N(\tau_6 V-\tau_2)\left(\frac{1}{4\pi r_i^2 V}\right), \qquad (2.5.10a) \\ \tau_{K3}(r_i) &= \frac{1}{\kappa^2}\frac{r_6}{r_i^2} = \frac{N}{(2\pi)^6(\alpha')^{7/2}g_s}\frac{1}{4\pi r_i^2} \\ &= N\tau_6\left(\frac{1}{4\pi r_i^2}\right), \qquad (2.5.10b) \end{aligned}$$

to find a good agreement with our expectations. In the $K3$ directions the effective tension matches that of N D6–branes, with an additional averaging factor coming from smearing the branes over the transverse sphere. In the unwrapped world-volume directions the tension is again related to that of N D6–branes minus N units of D2–brane tension arising as a result of wrapping on $K3$, compare with equation (2.1.3).

Furthermore, notice the effective tension of the shell in the unwrapped part is proportional to $H_2'/H_2 + H_6'/H_6$. But this expression, as we observed after equation (2.2.7), vanishes precisely at the enhançon radius r_e. So the supergravity matching computation here and the probe calculation of section 2.3 both tell the same thing, the shell of branes at the enhançon radius has a vanishing tension.

For $r < r_e$ the tension in (2.5.9a) becomes negative, which is problematic also in supergravity. On the other hand, the computation shows we can put a shell of branes with positive tension at any radius $r \geq r_e$, and make an incision from there. This is in accordance with the fact that for brane probes the forces cancel and they can stay motionless at an arbitrary position outside the enhançon. The enhançon radius is special in the sense it sets a limit where we can place the branes and perform incision.

One can go on and show that the stress-energy of the shell is in general (not just for large r_i) precisely the same as the stress-energy of N wrapped D6–branes distributed uniformly on the sphere [83]. Also the behaviour of the dilaton field at $r = r_i$ is correctly accounted by the source shell of wrapped D6–branes.

2.6 Gauge theory moduli space

In the preceding sections of this chapter we studied the system of N D6–branes wrapped on $K3$ mainly from the supergravity point of view. But as introduced in the discussions of chapter 1, all this has a corresponding meaning from the point of view of the gauge theory on the branes' world-volume.

So, there is an $SU(N)$ gauge theory with eight supercharges on the (2+1)-dimensional unwrapped world-volume of the N D–branes we have. The gauge multiplet consists of a gauge field A^μ and three scalars Φ^i $(i = 3, 4, 5)$, transforming in the adjoint representation of $SU(N)$. As we already know, these scalars encode information about the positions of the D6–branes in the transverse directions x^i. The gauge theory has a scalar potential of the form $\mathrm{Tr}[\Phi^i, \Phi^j]^2$, and the moduli space of supersymmetric vacua is parameterised by the vacuum expectation values ("vevs") of the scalars. To make the potential vanish the "vevs" live in the Cartan subalgebra of $SU(N)$, breaking the gauge symmetry from $SU(N)$ to $U(1)^{N-1}$. This is known as the "Coulomb branch" of the moduli space since there are generically $U(1)$'s unbroken.[5]

The moduli space parameterised by the three scalars Φ^i is $3(N-1)$ dimensional, but in 2+1 dimensions we can dualise the abelian gauge fields A^μ to give $N-1$ more scalars. Therefore the classical moduli space[6] of the theory is $4(N-1)$-dimensional

$$\mathcal{M}_{cl}^N = \frac{(\mathbb{R}^3 \times S^1)^{N-1}}{S_{N-1}}, \tag{2.6.1}$$

where the S^1 factors represent the periodic scalars resulting from dualising the gauge fields, and S_{N-1} is the Weyl group of $SU(N)$ permuting the $N-1$ eigenvalues of the Φ^i. (Remember the discussions after formula (1.4.18) in chapter 1.) The $U(1)^{N-1}$ is the gauge symmetry of N wrapped D6–branes at arbitrary positions in the transverse dimensions. The extra $U(1)$ we might expect corresponds to the overall centre of

[5] Another typical branch of the moduli space, called the "Higgs branch," is not available in the theory since there are no hypermultiplets. We can get the hypermultiplets by introducing extra (unwrapped) D2–branes in addition to the wrapped D6–branes.

[6] This classical moduli space will receive quantum corrections which make it a smooth hyper-Kähler manifold, as we will argue soon.

mass of the system.

Now we take all the wrapped D6–branes to be coincident (meaning all the "vevs" of adjoint scalars are given the same value in the gauge theory), except for a single brane (which has a complete multiplet of four scalars giving its location in the background of all the others). We can use this single wrapped D6–brane to probe the resulting subspace of the moduli space. Notice, now we have less supersymmetry than in the first chapter example of probing N Dp–branes with a Dp–brane. As a consequence the moduli space metric will not be trivially flat any more.

In fact, we have already done the probing. Because probing the moduli space in gauge theory corresponds to probing the geometry in the supergravity picture.

2.6.1 Including an extra modulus in the probe calculation

Looking our previous probe calculation results (2.3.3) there seems to be one important bit of data missing. Our supergravity probe was moving in three transverse directions r, θ, ϕ, but as we have established just before, the gauge theory relative moduli space (*i.e.* the moduli space corresponding to the motion of a single brane in the background of others) must be four dimensional.

In general a $(2+1)$-dimensional theory with eight supercharges has a moduli space metric which is hyper-Kähler [139], requiring a dimension multiple of four. Anticipating what we will see soon, let us note that a four dimensional hyper-Kähler metric can be written in the form [140]:

$$ds^2_{hK} = F(\vec{R})d\vec{R}^2 + F^{-1}(\vec{R})\left(dX_4 + \vec{A}d\vec{R}\right)^2, \tag{2.6.2}$$

where $\vec{R} = (X_1, X_2, X_3)$, and $\vec{A}$ satisfies $\vec{\nabla} \times \vec{A} = \vec{\nabla}F$.

It is not hard to guess the extra modulus we were missing is related to the $(2+1)$–dimensional gauge field which can be dualised to a periodic scalar. Indeed if we think about it and remember the generic formulae (1.4.1), (1.4.5), it becomes apparent the probe action (2.3.1) should get an extra contribution both to the DBI and WZ parts. This comes from the gauge field A^μ, living on unwrapped world-volume of the brane. So the full probe effective action should read (with an understanding

that the bulk space-time forms need to be pulled back to the world-volume)

$$\begin{aligned} S &= -\int_{\mathcal{M}_3} d^3\xi\, e^{-\Phi}\,(\mu_6 V(r)-\mu_2)\,\sqrt{-\det g_{\mu\nu}+2\pi\alpha' F_{\mu\nu}} \\ &\quad +\mu_6\int_{\mathcal{M}_3\times K3} C^{(7)} - \mu_2\int_{\mathcal{M}_3} C^{(3)} - 2\pi\alpha'\mu_2\int_{\mathcal{M}_3} C^{(1)}\wedge F^{(2)}\,, \end{aligned} \tag{2.6.3}$$

where $F^{(2)}=dA^{(1)}$ is the field strength of the gauge field A^μ, and $C^{(1)}$ is the magnetic dual of $C^{(7)}$, which given the solution (2.1.4) we have, is

$$C^{(1)} = -\frac{r_6}{g_s}\cos\theta d\phi\,. \tag{2.6.4}$$

Instead of operating with a A^μ we would like to exchange it with a scalar s, Hodge-dual to a vector potential in three dimensions. The trick [141, 142] is to introduce an auxiliary vector field v_μ and write the first and the last term of the action (2.6.3) above as

$$\begin{aligned} S &= -\int_{\mathcal{M}_3} d^3\xi\, e^{-\Phi}\,(\mu_6 V(r)-\mu_2)\,\sqrt{-\det g_{\mu\nu}+e^{2\Phi}\,(\mu_6 V(r)-\mu_2)^{-2}\,v_\mu v_\nu} \\ &\quad -2\pi\alpha'\int_{\mathcal{M}_3}(\mu_2 C^{(1)}-v)\wedge F^{(2)}\,, \end{aligned} \tag{2.6.5}$$

Integrating out v gives us back the action (2.6.3) we started with. Instead, we treat the gauge field A^μ as a Lagrange multiplier and integrate it out. The only term in (2.6.5) involving A^μ is

$$-\int_{\mathcal{M}_3}(\mu_2 C^{(1)}-v)\wedge dA^{(1)} = \int_{\partial\mathcal{M}_3}(\mu_2 C^{(1)}-v)\wedge A^{(1)} - \int_{\mathcal{M}_3} d(\mu_2 C^{(1)}-v)\wedge A^{(1)}. \tag{2.6.6}$$

The boundary term at infinity should vanish, while the last term enforces a constraint

$$d(\mu_2 C^{(1)}-v)=0\,, \tag{2.6.7}$$

which can be solved by

$$\mu_2 C_\mu - v_\mu = -\partial_\mu s\,. \tag{2.6.8}$$

Here s is the extra scalar modulus we were after. By equation (2.6.8) it is possible to replace v_μ in the action (2.6.5). Using a static gauge we can work out (potentials cancel *etc.*) the effective lagrangian of the probe:

$$\mathcal{L} = F(r)\left(\dot r^2 + r^2\dot\Omega^2\right) + F(r)^{-1}\left(\dot s/2 - \mu_2 C_\phi\dot\phi/2\right)^2, \tag{2.6.9}$$

where

$$F(r) = \frac{H_6}{2g_s}(\mu_6 V(r) - \mu_2) \tag{2.6.10}$$

and $\dot{\Omega}^2 = \dot{\theta}^2 + \sin^2\theta\dot{\phi}^2$. Despite adding an extra coordinate s, this effective lagrangian still informs us that the brane tension vanishes at radius r_e.

2.6.2 In the decoupling limit

To decouple the gauge theory from the rest of the bulk physics we should go to the decoupling limit as described in section 1.4.5. So, take $\alpha' \to 0$ while holding the gauge theory coupling

$$g^2_{YM} = g^2_{YM,6} V^{-1} = (2\pi)^4 g_s \alpha'^{3/2} V^{-1} \tag{2.6.11}$$

and the scale $U = r/\alpha'$ fixed. In this limit we can extract from the kinetic lagrangian (2.6.9) the following metric:

$$ds^2 = f(U)\left(\dot{U}^2 + U^2 d\Omega^2\right) + f(U)^{-1}\left(d\sigma - \frac{N}{8\pi^2}A_\phi d\phi\right)^2 \tag{2.6.12}$$

where

$$f(U) = \frac{1}{4\pi^2 g^2_{YM}}\left(1 - \frac{g^2_{YM}N}{U}\right), \tag{2.6.13}$$

while $A_\phi = \pm 1 - \cos\theta$ is a $U(1)$ monopole potential, and $\sigma = s\alpha'$ is periodic with period 4π. The metric is hyper-Kähler, as can be established by comparison with equation (2.6.2) and noting $\nabla f = \nabla \times A$, where $A = (N/8\pi^2)A_\phi d\phi$.

The moduli space metric (2.6.12) is the same as the one which can be derived from field theory, where it has an interpretation as the tree-level plus one loop result [79]. This metric is singular at $U_e = g^2_{YM}N$, a scale which corresponds to the enhançon radius in the supergravity picture. In the gauge theory this divergence can be understood as the Landau pole, representing a place where the one-loop correction makes the gauge coupling diverge. The singularity warns the moduli space metric is still incomplete. However, it does not receive any more perturbative corrections (from higher loops), but gets fixed non-perturbatively by instanton corrections.

2.6.3 Non-perturbative corrections

The last statement can be justified for instance by invoking connection with monopole physics. Our discussions in section 2.4 may already hint the metric (2.6.12) should be related to the moduli space metric of $SU(2)$ magnetic monopoles. Indeed, this is the case. The Coulomb branch of the $(2+1)$-dimensional $\mathcal{N}=4$ supersymmetric (8 supercharges) $SU(N)$ Yang-Mills theory moduli space is isomorphic [134, 143, 144] as a hyper-Kähler manifold to the "strongly-centred" moduli space of charge N $SU(2)$ BPS monopoles in four dimensions [145, 146]. Here by "strongly-centred" we mean the $(4N-4)$-dimensional relative moduli space where the overall centre of mass and overall phase of the monopoles is not included. Our metric (2.6.12) describes a four dimensional subspace of this full (relative) monopole moduli space.

For $N=2$, *i.e.* the case of two monopoles of charge 1, the moduli space manifold [147] is the Atiyah-Hitchin manifold [148]:

$$ds^2_{AH} = f^2 d\rho^2 + a^2\sigma_1^2 + b^2\sigma_2^2 + c^2\sigma_3^2 \,, \tag{2.6.14}$$

with

$$\begin{aligned} \sigma_1 &= -\sin\psi d\theta + \cos\psi \sin\theta d\phi \,, \\ \sigma_2 &= \cos\psi d\theta + \sin\psi \sin\theta d\phi \,, \\ \sigma_3 &= d\psi + \cos\theta d\phi \,, \end{aligned} \tag{2.6.15}$$

where $0 \le \theta < \pi$, $0 \le \phi < 2\pi$, $0 \le \psi < 4\pi$. The functions a, b, c must satisfy cyclic permutations of

$$\frac{2bc}{f}\frac{da}{d\rho} = (b-c)^2 - a^2, \tag{2.6.16}$$

while $\rho = 2K(k)$, where $K(k)$ is the elliptic integral of the first kind

$$K(k) = \int_0^{\frac{\pi}{2}} (1 - k^2 \sin^2\tau)^{\frac{1}{2}}. \tag{2.6.17}$$

Also, $0 \le k \le 1$ and $\pi \le \rho \le \infty$.

To see how our metric (2.6.12) could be related to the Atiyah-Hitchin metric (2.6.14), let us rescale the variables, defining $\rho = U/g^2_{YM}$, $\psi = 4\pi^2\sigma$, and gauge

transform $A_\phi = -\cos\theta$ [86]. Then the metric (2.6.12) becomes

$$\begin{aligned} ds^2 &= \frac{g_{YM}^2}{8\pi^2} ds^2_{TN-} \\ ds^2_{TN-} &= \left(1-\frac{2}{\rho}\right)(d\rho^2+\rho^2 d\Omega_2^2) + 4\left(1-\frac{2}{\rho}\right)^{-1}(d\psi+\cos\theta d\phi)^2. \end{aligned} \quad (2.6.18)$$

This can be recognized as the Euclidean Taub-NUT metric [149] with a negative mass parameter. The latter is precisely in the form one gets from the large ρ expansion [150] of the Atiyah-Hitchin metric (2.6.14). The difference between (2.6.14) and (2.6.18) is given by a family of exponential $e^{-\rho}$ corrections. For large ρ the negative mass Taub-NUT metric is exponentially close to the Atiyah-Hitchin, but towards smaller ρ the exponential corrections become important. At $\rho = 2$ the metric (2.6.18) is actually singular, but by then the corrections are strong enough to resolve the singularity. The Taub-NUT is just an approximation to the true moduli space which is described by the smooth Atiyah-Hitchin metric.

Well, the Atiyah-Hitchin metric actually has a singularity at $\rho = \pi$, but this is just a harmless "bolt" coordinate singularity [150]. It has a physical meaning too in the picture of two magnetic monopoles, where the coordinate ρ describes the relative separation of the monopoles. As the monopoles move closer, their positions get blurred until they completely merge together forming a charge 2 monopole at $\rho = \pi$. Smaller values of ρ have no meaning in this description. Notice this "bolt" singularity occurs at slightly larger radius than the singularity in the Taub-NUT metric.

In the gauge theory variables these exponential corrections go as e^{-U/g_{YM}^2}. Happily, this is the right form for instanton corrections [151] suggesting the singularity of gauge theory moduli space (2.6.12) is resolved in this manner.

The considerations above stem from the $N = 2$ case, but we are more interested in what happens when N is large and the supergravity description of the enhançon is valid. Rescaling $\rho = 2U/g_{YM}^2 N$, $\psi = 8\pi^2\sigma/N$ gives [86]

$$ds^2 = \frac{g_{YM}^2 N^2}{32\pi^2} ds^2_{TN-}, \quad (2.6.19)$$

and one is tempted to think the manifold controlling non-perturbative corrections for large N is still Atiyah-Hitchin. However, the candidate manifold can not be true

Atiyah-Hitchin, but its close relative [86]. For example the instanton corrections in the gauge theory are still typically of order e^{-U/g_{YM}^2}, which translates to $e^{-N\rho/2}$ for corrections to the Taub-NUT metric (not $e^{-\rho}$ it has with the original Atiyah-Hitchin metric). There is also a question in the period of variable ψ and the isometry group of the geometry, but we will not stop at these details.

So, the Atiyah-Hitchin manifold was the relative moduli space of two unit charge magnetic monopoles, moving in relation to each other. The problem related to the enhançon deals with a huge monopole of charge N at the centre, which is probed with a single monopole of charge one. In the latter case the relative moduli space of the problem can be linked to the geometry of the space-time, since now the centre of mass is fixed to a good approximation at the center of the N-monopole core.

The "bolt" singularity of the two monopole case was the point of closest possible approach of the two monopoles. In the large N case a generalisation of this "bolt" represents the closest possible approach of the single monopole probe to the N monopole. At this point the probe merges completely with its big brother, and this marks the smoothed non-perturbative enhançon locus. Again, we expect it to occur at a slightly larger radius than the singularity in the Taub-NUT metric, which corresponded to the perturbative enhançon. However, the corrections are exponentially small, suppressed by factor N in the exponent.

2.7 Adding D2–branes

Let us stress once again that the induced negative amount of D2–brane charge does not mean there are true anti–D2–branes present, it is just an effect due to D6–brane interaction with K3 curvature. In fact, we may consider adding extra real D2–branes to the wrapped D6–brane configuration with the same orientation as the unwrapped part of the D6–branes. This does not break any further supersymmetry.

So, let there be N_6 D6–branes and N_2 (positive charge) D2–branes. As a result the corresponding harmonic function (2.1.5) in the supergravity solution changes to

$$H_2 = 1 + \frac{r_2}{r}\,, \qquad r_2 = \frac{(2\pi)^4 g_s \alpha'^{5/2}}{2V}(N_2 - N_6)\,. \tag{2.7.1}$$

Obviously this modifies the enhançon radius

$$r_{\rm e} = \frac{2r_6 V_\star}{V - V_\star}\left(1 - \frac{N_2}{2N_6}\right) . \tag{2.7.2}$$

The shell is shrinking when we add extra D2–branes, if $N_2 \geq 2N_6$ there is no enhançon shell at all and the geometry is fine down to $r = 0$.

We may use both D6–branes or D2–branes to probe the geometry, but there is also a possibility to probe with a D6–D2–bound configuration, *i.e.* having instantonic D2–branes smeared over the world-volume of D6–branes. Say, we have a composite probe consisting of n_6 D6–branes and n_2 D2–branes. The effective action is

$$\begin{aligned} S &= -\int_{\mathcal{M}_3} d^3\xi e^{-\Phi}(n_6\tau_6 V(r) + (n_2 - n_6)\tau_2)(-\det g_{ab})^{1/2} \\ &\quad + n_6\tau_6 \int_{\mathcal{M}_3\times K3} C^{(7)} + (n_2 - n_6)\tau_1 \int_{\mathcal{M}_3} C^{(3)} , \end{aligned} \tag{2.7.3}$$

which in the static gauge gives the following lagrangian

$$\mathcal{L} = \frac{1}{2}(n_6\tau_6 H_2 V + (n_2 - n_6)\tau_2 H_6)v^2 . \tag{2.7.4}$$

If there are no D2–branes ($n_2 = 0$) we recover the familiar result of equation (2.3.3), showing that the probe tension vanishes at the enhançon radius. If we remove all D6–branes instead ($n_6 = 0$), then it becomes apparent that the probing pure D2–branes can float past the enhançon radius without any problem since their tension is positive everywhere. Interestingly enough, this construction also provides a way how to send wrapped D6–branes to the enhançon interior. What we have to do is to dress them appropriately with D2–branes so that the tension of the compound object does not become negative. But in general whenever there are more D6–branes than D2–branes making up the probe ($n_6 > n_2$), there will be a generalisation of the enhançon radius, where the composite probe will become tensionless and must stop.

So, bringing extra D2–branes into the game allows all the D2–branes and a certain number of D6–branes to be inside the enhançon radius. This is going modify the interior supergravity solution and therefore also the matching computation. Consider a situation where all N_2 D2–branes and some number N_6' of D6–branes are

placed at the origin $r = 0$, while $N_6 - N_6'$ D6–branes remain on the enhançon shell. Now the interior geometry is not flat any more. The metric is still of the form (2.1.4) but the harmonic functions are modified:

$$\begin{aligned} h_2 &= 1 + \frac{r_2 - r_2'}{r_i} - \frac{r_2'}{r}\,, \qquad r_2' = r_6 \frac{V_\star}{V} \frac{N_6' - N_2}{N_6}\,, \\ h_6 &= 1 + \frac{r_6 - r_6'}{r_i} + \frac{r_6'}{r}\,, \qquad r_6' = r_6 \frac{N_6'}{N_6} = \frac{g_s N_6' \alpha'^{1/2}}{2}\,. \end{aligned} \tag{2.7.5}$$

These harmonic functions are chosen to mimic the ones in exterior, equation (2.1.5), while the constant terms guarantee that the interior and exterior solutions match exactly at the incision radius r_i. Computations analogous to those of section 2.5 give the stress tensor

$$S_{\mu\nu} = \frac{1}{2\kappa^2\sqrt{G_{rr}}}\left(\frac{H_2'}{H_2} + \frac{H_6'}{H_6} - \frac{h_2'}{h_2} - \frac{h_6'}{h_6}\right) G_{\mu\nu} \tag{2.7.6a}$$

$$S_{ij} = 0 \tag{2.7.6b}$$

$$S_{ab} = \frac{1}{2\kappa^2\sqrt{G_{rr}}}\left(\frac{H_6'}{H_6} - \frac{h_6'}{h_6}\right) G_{ab}\,. \tag{2.7.6c}$$

We see once again that the pressure in the shell directions vanishes, in agreement with the fact that the system is still BPS. Furthermore the effective tension in the $x^{0,1,2}$ directions vanishes precisely at the enhançon radius, and more generally one can show the discontinuities at the shell agree with the source terms in the world-volume action of $N_6 - N_6'$ wrapped D6–branes.

2.8 Summary

In this chapter we have provided an overview of the enhançon mechanism, taking the configuration N D6–branes wrapped on a $K3$ manifold as an example. This has also allowed us to explain in detail the various calculations and interpretations which we will use (and generalise) frequently in the chapters to follow.

First by considering curvature corrections to the brane world-volume action, we observed how wrapping D6–branes on $K3$ induces units of negative D2-brane charge on the unwrapped part of their world-volume. We used this data to write down the corresponding supergravity solution which has a naked singularity at radius $r_{\rm r}$.

Probing the geometry with a massive test particle showed how the particle gets repelled from the singularity, illustrating the name "repulson" of the singularity.

Next, in section 2.3, we turned to the technique of using a single constituent brane to probe the background geometry generated by all others. As a result we found the effective tension varies with the radius (in the transverse directions), vanishing completely at $r_e > r_r$. The physical interpretation of the situation was that the probe ceases to be a point-like object but is smeared around a sphere of radius r_e. We backed up this interpretation by making connection with $SU(2)$ monopoles, arguing the probe is actually a magnetic monopole while the radius r_e corresponds to the locus where the gauge symmetry is restored from $U(1)$ to $SU(2)$. Hence the name "enhançon".

At this locus new degrees of freedom become massless, which render the original supergravity description inadequate. As there are no D–brane sources inside the enhançon radius r_e, the geometry inside must be flat to the first approximation. Therefore the repulson singularity gets excised, it was just an artefact of the supergravity description blind to the new degrees of freedom. To determine the true geometry we have to take into account stringy physics in all its glory.

This state of affairs got further support from considering supergravity junction conditions which revealed it is consistent to replace the internal geometry with a flat space. The stress-energy at the junction surface agrees with the understanding that there are wrapped D6–branes smeared around the junction shell.

In section 2.6 we focussed upon the pure $SU(N)$ gauge theory on the branes' world-volume, wanting to retrieve information about its moduli space. General considerations suggested the moduli space must be four dimensional (not just the three transverse coordinates we had previously). This made us to reconsider the probe calculation, now taking into account the gauge field A^μ, which lives on the probe brane world-volume. The latter could be dualised to a scalar, giving the fourth (periodic) modulus.

In the decoupling limit the moduli space metric, extracted from the effective kinetic lagrangian of the probe, turned out to be the Taub-NUT metric with a negative mass. At large radii this is known to be an approximation to the Atiyah-

Hitchin metric. Invoking again a connection with the $SU(2)$ monopoles, we argued the complete non-perturbative metric for large N should be a generalisation of the Atiyah-Hitchin metric, which is smooth and relevant to the case $N = 2$. The Taub-NUT metric is understood as the perturbative tree-level plus one loop result, receiving exponential corrections from instantons. In this picture the enhançon (corresponding to the singularity in the negative mass Taub-NUT metric) is the point where instanton effects become important.

At last, in section 2.7, we added extra parallel D2–branes to the wrapped D6–branes configuration. These D2–branes we free to move inside the enhançon radius and make the geometry of the internal region curved (but not singular). It was also possible to bind a wrapped D6–brane with a D2–brane to let it pass through the enhançon shell. Keeping these features in mind we reconsidered the supergravity junction computation accordingly.

Chapter 3

Orientifolds, M-theory, and the ABCD's of the Enhançon

The enhançon configuration studied in detail in the previous chapter involved a configuration of N D–branes, which had an $SU(N)$ gauge theory on their world-volume. In this chapter we show how the enhançon arises naturally in configurations pertaining to $SO(2N+1)$, $USp(2N)$, and $SO(2N)$ gauge groups. Thus the enhançons may be broadly classified into types A, B, C, and D.

The construction involves orientifold planes, and we will briefly describe their characteristic features. Combining orientifolds with D–branes has an effect of changing the $SU(N)$ gauge group on the D–branes' world-volume to the groups mentioned above. So the main problem in what follows is how to construct the corresponding supergravity solutions.

We solve this problem by using the duality between type IIA strings and M–theory (eleven dimensional supergravity in the low energy limit). Namely the D6–brane solution uplifted to eleven dimensions becomes the Taub-NUT metric, while one of the so-called orientifold six–planes has an eleven-dimensional realisation as the Atiyah-Hitchin manifold. This fact allows us to combine the supergravity solutions together and bring down to ten dimensions. We see how the "orientifolded" enhançons differ from the usual configuration by factors of order $1/N$, and having a global $\mathbb{Z}_2$ reflection on the transverse geometry. Meanwhile we also use an opportunity to consider the enhançon in eleven dimensional terms.

3.1 Including orientifolds

3.1.1 Orientifold planes

Orientifold planes are another class of extended objects in string theory. From the point of view of perturbative string theory orientifolds appear when one considers the T-duality properties of unoriented strings which carry only states invariant under world-sheet parity. Enforcing T–duality mixes world-sheet parity with space-time parity that puts a $\mathbb{Z}_2$ reflection on the T–dual coordinate. Thus due to the orientifold fixed planes, called O–planes for short, the physics of a string at some point x^i is related to the string at the image point $-x^i$.

In contrast with D–branes, orientifold planes are not dynamical, they do not have a gauge theory on their world-volume nor moduli describing their positions in the transverse directions. Still, they act as sources for R-R and NS-NS fields and are loci of singular curvature. The Op–plane charge μ_p' and tension τ_p' are related to the Dp–brane charge (1.3.12) and tension (1.3.13) by

$$\mu_p' = \mp 2^{p-5}\mu_p \ , \qquad \tau_p' = \mp 2^{p-5}\tau_p \ . \tag{3.1.1}$$

When N Dp–branes coincide with an Op–plane, strings stretching between branes and their image branes do also become massless. This contributes additional states to the branes' world-volume gauge theory to change the gauge group from $U(N)$ to $SO(2N)$ or $USp(2N)$ depending whether the Op–plane charge is negative or positive respectively. There is also a third possibility when a "half" Dp–brane is put on a negative charge Op–plane. Here "half" means the Dp–brane lacks a mirror partner to make its reflection on the other side and thus it must remain trapped on the Op–plane. In this case the world-volume theory has $SO(2N+1)$ gauge group.

Considerations for the enhançon

Our strategy is rather simple: we would like to insert an orientifold six–plane (O6–plane) parallel to the D6–branes and wrap the configuration on K3, to see how the enhançon story gets modified. On general grounds, we may expect a similar picture to emerge as for the un-orientifolded case with $SU(N)$ gauge theory on the

	$\mathbb{R}^{5,1}$						K3			
	x_0	x_1	x_2	x_3	x_4	x_5	x_6	x_7	x_8	x_9
D6	–	–	–	·	·	·	–	–	–	–
D2	–	–	–	·	·	·	∼	∼	∼	∼
O6	–	–	–	ıı	ıı	ıı	–	–	–	–

Table 3.1: A sketch of D6–branes wrapped on K3 in the presence of an O6–plane. The world-volume directions are marked by "–" and "∼" indicates that the induced effective D2–branes are delocalised on K3. In the transverse directions the branes are point-like which is denoted by "·", while the orientifold plane, sitting fixed at the origin ($r = 0$), puts a $\mathbb{Z}_2$ reflection on these directions, symbolised by "ıı".

world-volume, since all of the constituent features which are required to make the enhançon mechanism to work are still present. The details of precisely where the enhançon is located (corresponding to where in the transverse directions the $K3$ volume reaches the value $V_\star$) will be modified, but only at subleading order in N. Globally, the orientifold will also place a $\mathbb{Z}_2$ identification on the transverse $\mathbb{R}^3$ ($\mathbb{Z}_2$ acts by multiplying each of the transverse coordinates x^3, x^4, x^5 by -1), turning the S^2 of the enhançon into $\mathbb{RP}^2 \equiv S^2/\mathbb{Z}_2$. The configuration is sketched as a diagram in table 3.1.1.

The main problem we face is how to write down the supergravity solution in the presence of the orientifold. But first, let us understand the physics of the perturbative string theory description, containing the weakly coupled gauge theory. For small g_sN, we have N D6–branes, and an O6–plane parallel to them. This construction allows three possibilities for the gauge group on the branes world-volume:

- $SO(2N+1)$ by trapping a half D6–brane on the negative charge O6–plane: this combination is often referred to as an $\widetilde{\text{O6}}$–plane, with charge $-3\mu_6/2$,
- $USp(2N)$ when the O6–plane has positive charge, equal to $+2\mu_6$, and may be denoted by O6^+,
- $SO(2N)$ when the O6–plane has negative charge $-2\mu_6$ and is called O6^-.

To be concise, we will use the symbol α to denote these O6–charges, measured in

D6–brane units. It takes the values

$$\alpha = -3/2, +2, -2, \tag{3.1.2}$$

for the cases of $\widetilde{\mathrm{O6}}$, $\mathrm{O6}^+$, and $\mathrm{O6}^-$ respectively.

3.1.2 Wrapping on K3

We proceed by wrapping the whole system on $K3$. This results in the induced negative charge D2–branes as described before, but with an additional contribution. This is due to a curvature coupling, now on the world–volume of the O6–plane [118, 152–156] similar to equation (2.1.1). The couplings induce some $C^{(3)}$ charge are different in each case $\widetilde{\mathrm{O6}}$, $\mathrm{O6}^+$, $\mathrm{O6}^-$:

$$\begin{aligned}
-\mu_6 \frac{(4\pi^2\alpha')^2}{32} \int_{\mathcal{M}_3\times K3} C^{(3)} \wedge p_1(K3) &= -\frac{3}{2}\mu_2 \int_{\mathcal{M}_3} C^{(3)}\,, \\
-\mu_6 \frac{5(4\pi^2\alpha')^2}{48} \int_{\mathcal{M}_3\times K3} C^{(3)} \wedge p_1(K3) &= -5\mu_2 \int_{\mathcal{M}_3} C^{(3)}\,, \\
-\mu_6 \frac{(4\pi^2\alpha')^2}{48} \int_{\mathcal{M}_3\times K3} C^{(3)} \wedge p_1(K3) &= -\mu_2 \int_{\mathcal{M}_3} C^{(3)}\,.
\end{aligned} \tag{3.1.3}$$

Let us define β, the induced charge in D2–brane units, which for the three cases is

$$\beta = -3/2, -5, -1, \tag{3.1.4}$$

respectively. This will modify the contribution to the induced D2–brane charge from $-N$ (for the $SU(N)$ case) to $-N-3/2$, $-N-5$ and $-N-1$, respectively. These extra charges do not mean we have induced wrong sign O2–planes on the unwrapped part of the world-volume. Otherwise the resulting charges would be hard to interpret given the existing types of O2–branes already known. Also this would put a $\mathbb{Z}_2$ identification on the $K3$ part of the space-time, which is hard to justify as the result of a smooth wrapping process. The changes are to be thought of as $1/N$ corrections to the original case.

3.1.3 The $ABCD$'s of the enhançon

We can now consider taking g_sN large to enter the regime where the supergravity description of the system is valid. We expect the phenomena which occurred for

$SU(N)$ to happen again, giving an enhançon for each case. Let us name the types of enhançon which can occur in each situation as the A–type (for $SU(N)$), B–type (for $SO(2N+1)$), C–type (for $USp(2N)$) and D–type (for $SO(2N)$).

There is no natural definition of an E–type, for (at least) two reasons: There is no known perturbative way to make $E_{6,7,8}$ gauge symmetry with D–branes, and furthermore, the enhançon as a smooth geometric object is a large N phenomenon, which is incompatible with the fact that the maximum rank of the exceptional groups is eight.

The next step in our story will be to write down the geometry corresponding to the large g_sN physics of the wrapped system of D–branes in the presence of an orientifold. We will achieve this by making a detour into eleven dimensions where the ancestor of the O6$^-$ geometry is known to live.

3.2 In eleven dimensions

3.2.1 Type IIA/M-theory duality

String theory is entangled in a profound web of dualities. In the introduction we discussed T–duality and mentioned this provides a mapping between type IIA and IIB theories. In section 2.4.1, we noted that type IIA theory on $K3$ is S–dual to heterotic theory on T^4, and the enhançon in the IIA picture corresponded to the heterotic string winding on circles of self-dual radius. The argument in this chapter relies on yet another duality relating type IIA strings in ten dimensions to an eleven dimensional theory called "M–theory."

We already know type IIA string theory accommodates a series of D–branes, among them point-like D0–branes charged under the R-R $C^{(1)}$ field. A bound state of n D0–branes has a mass

$$n\tau_0 = \frac{n}{g_s\alpha'^{1/2}}. \tag{3.2.1}$$

Curiously, this reminds (from page 11 discussions on T–duality) us of a spectrum of Kaluza-Klein states for a periodic dimension of radius $R = g_s\alpha'^{1/2}$. Going to the

strong coupling limit[1] has a similar effect to making R large, and it seems an extra (eleventh) dimension is opening up. This leads to a conjecture: in the strong coupling limit type IIA string theory approaches an eleven dimensional Lorentz invariant theory (the so-called "M–theory"), whose low energy limit is eleven dimensional supergravity [28,29].

It was known long before that IIA supergravity can be obtained from the eleven dimensional supergravity by dimensional reduction on S^1. The novel point of the duality conjecture was about the existence of a complete quantum theory in eleven dimensions corresponding to the quantum IIA string theory in ten dimensions. However, a perturbative definition of M–theory is still lacking, the main difficulty being there no dimensionless parameter to use for a perturbation expansion (the ten dimensional dilaton which gives the string coupling constant g_s is related to the radius of the eleventh dimension and part of the eleven dimensional metric).

The eleven dimensional supergravity is given by the action

$$S_{11\mathrm{d}} = \frac{1}{2\kappa_{(11)}^2}\int d^{11}x\sqrt{-g^{(11)}}R - \frac{1}{4\kappa_{(11)}^2}\int F^{(4)}\wedge{}^\star F^{(4)} - \frac{1}{3}A^{(3)}\wedge F^{(4)}\wedge F^{(4)}, \quad (3.2.2)$$

where $F^{(4)} = dA^{(3)}$ is the field strength of (eleven dimensional) 3-form potential, and the gravitational coupling is defined as

$$2\kappa_{(11)}^2 = 16\pi G_N^{(11)} = (2\pi)^8\alpha'^{9/2}g_s^3\,. \quad (3.2.3)$$

Under compactification, *i.e.* making the eleventh dimension $x^\natural$ periodic of a very small radius, the relation between the eleven and ten dimensional (bosonic) fields is the following:

$$\begin{aligned} ds_{11}^2 &= e^{-2\Phi/3}g_{\mu\nu}dx^\mu dx^\nu + e^{4\Phi/3}(dx^\natural + C_\mu dx^\mu)^2, \\ A^{(3)} &= \frac{1}{6}C_{\mu\nu\rho}\,dx^\mu\wedge dx^\nu\wedge dx^\rho + \frac{1}{2}B_{\mu\nu}\,dx^\mu\wedge dx^\nu\wedge dx^\natural, \end{aligned} \quad (3.2.4)$$

where $g_{\mu\nu}$, Φ, $B_{\mu\nu}$, $C^{(1)}$, $C^{(3)}$ are the familiar ten dimensional fields of IIA supergravity ($\mu = 0,\ldots,9$). Using the ansatz (3.2.4) we may "uplift" the solutions of IIA supergravity into eleven dimensions, or the other way round, compactify eleven dimensional solutions down to ten dimensions.

[1] D–brane masses, although originally computed in the perturbative string theory with g_s small, can be trusted for all regimes of g_s, since D–branes are BPS states.

M-theory	W		M2		M5		KK	
	↙	↓	↙	↓	↙	↓	↙	↓
Type IIA	D0	W	F1	D2	D4	NS5	KK	D6

Table 3.2: M-theory origin of type IIA branes. "Vertical" dimensional reduction is denoted by "↓", "diagonal" dimensional reduction by "↙".

M-theory origin of type IIA branes

Given the D-branes have a description as p–brane solutions in supergravity, it is not surprising that the origin of branes in type IIA theory can be traced back to M–theory in eleven dimensions [29, 141].

M–theory has two brane solutions, the eleven dimensional membrane (M2–brane) which is electrically charged under the $A^{(3)}$ potential, and the five–brane (M5–brane) which is magnetically charged under the same $A^{(3)}$. The compactification ansatz (3.2.4) allows us two options: either we choose to compactify one of the transverse directions to the M–branes world-volume, or alternatively, we may wrap one of the world-volume dimensions on the periodic $x^\natural$ we will shrink into oblivion. The first option, a "vertical" dimensional reduction, takes an M2–brane into a D2–brane, and an M5–brane into a NS5–brane. The second option, a "diagonal" (or double) dimensional reduction, strips away one of the extended world-volume dimensions, taking an M2–brane into a fundamental string F1, and an M5–brane into a D4–brane.

The eleven dimensional supergravity has two more solutions, which are relevant in this game: a gravitational wave (W), and Kaluza-Klein monopole (KK). A vertical dimensional reduction takes the eleven dimensional gravitational wave into a ten dimensional gravitational wave, while diagonal dimensional reduction gives a D0–brane. A diagonal dimensional reduction of the Kaluza-Klein monopole solution gives a Klauza-Klein monopole in ten dimensions, while vertical dimensional reduction gives a D6–brane. (These facts are summarized in table 3.2.1.)

The last of the aforementioned relations deserves our special attention. This is because our A–type enhançon was built of D6–branes and we would like to uplift the

solution it into eleven dimensions. The eleven dimensional Kaluza-Klein monopole, given by the Taub–NUT space times seven dimensional flat space is (defining the eleventh direction $\psi = x^\natural/16m$):

$$\begin{aligned} ds_{11}^2 &= -dt^2 + dx_1^2 + dx_2^2 + dx_6^2 + dx_7^2 + dx_8^2 + dx_9^2 \\ &\quad + F(r)(dr^2 + r^2 d\Omega_2^2) + F^{-1}(r)\left(d\psi + C_\phi d\phi\right)^2 , \end{aligned} \tag{3.2.5}$$

where, with $0 \leq \psi < 4\pi$,

$$d\Omega_2^2 = d\theta^2 + \sin^2\theta d\phi^2 , \quad F = 1 + \frac{4mN}{r} , \quad C_\phi = 4mN\cos\theta . \tag{3.2.6}$$

Reducing the solution (3.2.5) along the ψ–circle, *i.e* making use of the ansatz (3.2.4), we recover a familiar ten dimensional solution:

$$\begin{aligned} ds_{10}^2 &= H_6^{-1/2}(-dt^2 + dx_1^2 + dx_2^2 + dx_6^2 + dx_7^2 + dx_8^2 + dx_9^2) \\ &\quad + H_6^{1/2}(dr^2 + r^2 d\Omega_2^2) \\ H_6 &= F(r) ; \qquad e^{2\Phi} = H_6^{-3/2}(r) , \qquad C_\phi = 4mN\cos\theta , \end{aligned} \tag{3.2.7}$$

which is precisely the D6–brane solution, if we identify $4mN = r_6$ (and set the asymptotic value of the dilaton to $\log g_s$.) The one–form potential $C^{(1)} = C_\phi d\phi$ can be Hodge–dualised in ten dimensions to give an electric source for $C^{(7)}$ of the form given in equation (2.1.4).

3.2.2 Uplifted enhançon

Let us now turn to the A-type enhançon solution, given previously in equation (2.1.4), and apply the prescription of (3.2.4). The components of the ten dimensional $C^{(7)}$ potential are Hodge-dualised into $C^{(1)}$ and join the eleven dimensional metric, while the components of the three–form potential $C^{(3)}$ give the components of the eleven dimensional three–form $A^{(3)}$. It is easy to write an eleven dimensional solution for the uplifted D6–D2 system:

$$\begin{aligned} ds_{11}^2 &= \widetilde{H}_2^{-2/3}(-dt^2 + dx_1^2 + dx_2^2) + \widetilde{H}_2^{1/3}\widetilde{V}^{1/2} ds_{\mathrm{K3}}^2 \\ &\quad + \widetilde{H}_2^{1/3}\left[\widetilde{H}_6(dr^2 + r^2 d\Omega_2^2) + \widetilde{H}_6^{-1}\left(d\psi + C_\phi d\phi\right)^2\right] , \\ A^{(3)} &= \widetilde{H}_2^{-1} dx^0 \wedge dx^1 \wedge dx^2 , \end{aligned} \tag{3.2.8}$$

with

$$\widetilde{H}_2 = g_s H_2 \ , \quad \widetilde{H}_6 = g_s^{-1} H_6 \ , \quad \widetilde{V} = g_s^2 V \ . \tag{3.2.9}$$

It is interesting to contrast the interpretation of this solution with the ten dimensional discussion. Recall that from the point of view of ten dimensions, there is the geometry of $K3$, accompanied by D6–branes wrapped on it. The wrapping induced some negative charge D2–branes, completely delocalised in the $K3$. We were able to probe the geometry of the supergravity solution (2.1.4) with one of its basic constituents, a single D6–D2 BPS object.

From the point of view of the eleven dimensional supergravity solution (3.2.8), everything is geometry: there are no branes here. The Taub–NUT part lies in the $x^{3,4,5,\natural}$ directions, while $K3$ lies in the $x^{6,7,8,9}$ directions. Together, they act as a source for the three–form potential $A^{(3)}$, due to the supergravity term [158, 159]:

$$\int A^{(3)} \wedge X^{(8)} \ , \qquad X^{(8)} = \frac{1}{24}\left(p_2 - \frac{1}{4} p_1 \wedge p_1\right) \ . \tag{3.2.10}$$

For Taub–NUT of charge N, $p_1 = 2N$ and, as stated before, for $K3$ we know that $p_1 = 48$. Thus we get $-N$ units of $A^{(3)}$ charge, as the solution shows. This fits, as (3.2.10) is the M–theory origin of the brane world–volume term (2.1.1).

There is no natural extended dynamical object which we can use as a candidate for the basic constituent of the geometry. Thus, we cannot perform a world–volume probe computation to deduce the true geometry. We might consider reading the $\widetilde{H}_2$ part of the geometry as representing a "wrong sign" M2–brane which is otherwise dynamical, but this cannot work. The putative negative charge M2–brane necessarily would have negative tension at all locations in $x^{3,4,5}$, and since there is no larger wrapped brane with positive tension to combine it with to make a positive tension object, we cannot write a sensible world-volume action. Of course, a probe computation with a correct sign M2–brane (which preserves the same amount of supersymmetry) gives a sensible result: simply the pure (with mass parameter of $+4mN = r_6$) Taub–NUT metric, as it should, with no sign of either enhançon or repulson. This is in accord with our expectation that the repulson (still present at $r = |r_2|$) is an artefact, while the enhançon should be invisible to an M2–brane because its world–volume theory does not relate to the $SU(N)$ gauge theory.

If all is just geometry and we are unable to point out dynamical objects, which can be interpreted as building blocks of the supergravity solution, how to understand the mechanism by which the troublesome repulson singularity at $r = |r_2|$ is resolved? In the string theory situation, we saw that the $K3$ reached the natural value $V_\star = (2\pi\ell_s)^4$, before it reached its singular value (zero), and the physics of the enhanced gauge symmetry took over. Is there a special value for the volume of $K3$ in this case? In eleven dimensions the natural length scale is set by the Planck length, $\ell_{11} = g_s^{1/3}\ell_s$, which the system again reaches before the singular value of zero. Once $K3$ has shrunk to that size, we should search for a better description than eleven dimensional supergravity.

The alternative to using the full (unknown) M–theory is to search for a dual description. Happily, eleven dimensional supergravity on such a small $K3$ is well described by the heterotic string on T^3 [28]. The distinguished ψ–circle which is fibred to make the Taub–NUT joins the rest to become a T^4, and the Taub–NUT structure becomes a "warped" [127] (not "wrapped") NS–fivebrane/Kaluza–Klein monopole structure giving rise to a monopole membrane whose mass goes to zero at an $SU(2)$ enhanced point of the torus [79, 133] (see also [162, 163]). So we see that again, stringy physics (now heterotic) takes over before we get to the repulson radius, and repairs the geometry with the same $SU(2)$ physics that we saw in type IIA string theory.

3.2.3 M-theory ancestor of an orientifold plane

Just as the D6–brane has an interpretation as the Taub–NUT space-time upon going to low energy M–theory (eleven dimensional supergravity), in a similar fashion, the O6$^-$–plane becomes [164, 165] the Atiyah–Hitchin manifold, described by a metric already familiar to us:

$$\begin{aligned} ds_{11}^2 &= -dt^2 + dx_1^2 + dx_2^2 + dx_6^2 + dx_7^2 + dx_8^2 + dx_9^2 \\ &\quad + f(\rho)d\rho^2 + 8m^2\left(a^2(\rho)\sigma_1^2 + b^2(\rho)\sigma_2^2 + c^2(\rho)\sigma_3^2\right) , \end{aligned} \tag{3.2.11}$$

where

$$\rho = \frac{r}{8m} , \qquad \psi = \frac{x^\natural}{16m} , \tag{3.2.12}$$

and the rest of the definitions can be found after equation (2.6.14) on page 43. There is also an identification by:

$$(r, \theta, \phi, \psi) \to (r, \pi - \theta, \pi + \phi, -\psi) \ , \tag{3.2.13}$$

which, in terms of the coordinates (x^3, x^4, x^5) and the M–direction $x^\natural$, is simply a multiplication by a minus sign on all directions. The displayed metric (3.2.11) has a conical singularity at $r = 8\pi m$. The space made by imposing the $\mathbb{Z}_2$ identification (3.2.13) is the Atiyah–Hitchin space, and it is free of conical singularities.

We already know that for large r the metric becomes a negative mass Taub-NUT:

$$\begin{aligned} ds_{11}^2 &= -dt^2 + dx_1^2 + dx_2^2 + dx_6^2 + dx_7^2 + dx_8^2 + dx_9^2 \\ &\quad + G(r)(dr^2 + r^2 d\Omega_2^2) + G^{-1}(r)\left(d\psi + C_\phi d\phi\right)^2 \ , \end{aligned} \tag{3.2.14}$$

where

$$G = 1 - \frac{16m}{r} \ , \qquad C_\phi = 16m\cos\theta \ , \tag{3.2.15}$$

When reduced down to ten dimensions this solution features -2 units of D6–brane charge [164], which is in accord with our knowledge of the charge of an O6$^-$–plane from perturbative string theory. (The actual appearance of $-16m$ in the metric instead of $-8m$ follows from the fact that the displayed metric is the double cover of the actual solution: recall that we must divide by the $\mathbb{Z}_2$ action.)

3.3 Orientifolded enhançon

3.3.1 The supergravity solution

Now we have prepared the ingredients necessary for constructing the eleven-dimensional geometry which gives rise to the D–type enhançon under compactification. We simply combine the geometry of the Atiyah–Hitchin manifold (representing O6$^-$–plane) with that of N coincident–centred Taub–NUT (representing N wrapped D6–branes). The exact smooth metric certainly exists, but we need not be able to write it down exactly to get at the physics we require. The radius at which the enhançon appears, can be tuned to be arbitrarily large by making N as large

as we like, so that we can reliably use the large r approximation (3.2.14) for the Atiyah–Hitchin manifold and capture the essential physics for large N.

Once we relax the condition of exactness, and focus on the large r part of the solution, we can also include the cases of the B– and C–type enhançons. While a precise relation to a cousin of the smooth Atiyah–Hitchin+Taub–NUT geometry is not known, at large r, the difference is immaterial, as only the leading behaviour is needed to characterise the enhançon at large enough N. We can simply use the same supergravity solution as before, but with different numbers inserted into the $1/N$ corrections to the harmonic functions.

It is clear therefore, that for all cases our solution can be written (for large enough r) in the covering space in the precise form of equation (3.2.8), but with the replacement of $\widetilde{H}_2$ and $\widetilde{H}_6$ by (respectively):

$$\widetilde{H}_2' = g_s\left(1 - \frac{2|r_2|(1-\beta/N)}{r}\right), \qquad \widetilde{H}_6' = \frac{1}{g_s}\left(1 + \frac{2r_6(1+\alpha/N)}{r}\right). \tag{3.3.1}$$

Here[2] $\beta = -3/2, -5, -1$, and $\alpha = -3/2, +2, -2$ for types B, C, D, respectively. Remember α was the orientifold plane charge measured in D6-brane units, equation (3.1.2), and β was the shift in the effective D2–brane charge induced by curvature corrections from the orinetifold plane, equation (3.1.4). Also notice that the contribution to the harmonic functions of (what will become) the orientifolds is simply a $1/N$ correction to the geometry, since in ten dimensions there is only one orientifold plane present in the solution in comparison with N D–branes. This will turn into part of the family of $1/N$ corrections to the location and shape of the enhançon locus, once we return to string theory.

While we know (in the D–type case) precisely how the harmonic function $\widetilde{H}_6'$ gets corrected into the smooth Atiyah–Hitchin+Taub–NUT solution, we do not know how $\widetilde{H}_2'$, which owes its presence to the $K3$ part of the eleven dimensional geometry, gets corrected. We have deduced the asymptotic form of $\widetilde{H}_2'$ from the fact that it

[2]It is interesting to note that the sum $\alpha + \beta$ is the same in each case. We do not know if this has any physical significance. Later, in equation (3.3.5), we shall see that it is $\alpha - \beta$ which controls the leading $1/N$ correction to the enhançon in each case. Were it the sum which appeared, we would have had a remarkably universal result.

must give the correct induced D2–brane mass and charge at large r in the string theory limit. Details for the small r remain unknown to us.

The metric (3.3.1) should be taken to mean the metric on the covering space of our solution, and we must divide by the $\mathbb{Z}_2$ action in order to reconstruct the correct solution, as before. This also accounts for the factors of two we have inserted into the harmonic functions.

The final step is straightforward. We return to type IIA string theory by reducing on the ψ–circle, recovering a supergravity solution representing the large g_sN geometry of a system of wrapped D6–branes and an O6–plane. The solution is simply the geometry (2.1.4) with H_2 and H_6 replaced by their $1/N$ corrected counterparts in (3.3.1) with the factors of g_s and $1/g_s$ removed. Crucially, there is a $\mathbb{Z}_2$ identification on the (x^3, x^4, x^5) directions, making it globally distinct from the A–type case, in addition to the different structure of the subleading behaviour in N.

3.3.2 Probing the geometry

Back in string theory, the natural object to construct this geometry out of is the D6–D2 at large g_sN, now in the presence of an orientifold. We may examine the nature of the geometry as seen by the probe by a computation precisely along the lines of section 2.3. A crucial difference is that we are working on the covering space of the actual geometry, and so we should insert a mirror image of the probe at the image position obtained by reflecting through the orientifold fixed point. The result is structurally identical to equation (2.6.9):

$$\mathcal{L} = F'(r)\left(\dot{r}^2 + r^2\dot{\Omega}_2^2\right) + F'(r)^{-1}\left(\dot{s}/2 - \mu_2 C_\phi \dot{\phi}/2\right)^2 , \tag{3.3.2}$$

where now

$$F'(r) = \frac{1}{2g_s}(\mu_6 V H_2' - \mu_2 H_6') , \tag{3.3.3}$$

with

$$\begin{aligned} H_2' &= \left(1 - \frac{2|r_2|(1-(\beta+1)/N)}{r}\right) \\ H_6' &= \left(1 + \frac{2r_6(1+(\alpha-1)/N)}{r}\right) . \end{aligned} \tag{3.3.4}$$

There is a minor but important difference in that we have shifted N to $N-1$ to represent separating off the probe. This is because strictly speaking, there are $N-1$ D6–D2–brane units being probed by one separated unit, giving N in total. The difference is a $1/N$ effect, we did not consider before, but should be included here since we are discussing a family of corrections at that order.

The location $r'_{\rm e}$ of the "orientifolded" type enhançon can be read off as the place in r where the mass of the probe becomes zero (equivalent to $V(r'_{\rm e}) = V_\star$):

$$r'_{\rm e} = \frac{2V}{V - V_\star}|r_2|\left(1 - \frac{\gamma}{N}\right) , \tag{3.3.5}$$

with

$$\gamma = -\left(\frac{\alpha - \beta - 2}{2}\right) = 1 , -\frac{5}{2} , \frac{3}{2} \tag{3.3.6}$$

in each case B, C, D. The analogous expression for the A case — with the $1/N$ correction from separating off the probe, *c.f.* equation (2.3.5), has $\gamma = 1$. (Note that for case B the effect of the O6–plane is precisely cancelled by the effect of the D2–brane contribution which is produces from wrapping, giving the same leading $1/N$ contribution as for type A.)

3.3.3 Gauge theory moduli space

Correspondingly, when we take the limit where we decouple the gauge theory with $\alpha' \to 0$ holding $g^2_{\rm YM}$ fixed, we recover the prediction for the metric on the moduli space of the gauge theory at large N (in the coincident limit):

$$\mathcal{L} = f'(U)\left(\dot{U}^2 + U^2\dot{\Omega}_2^2\right) + f'(U)^{-1}\left(\dot{\sigma} - \frac{N(1-\gamma/N)}{8\pi^2}A_\phi\dot{\phi}\right)^2 , \tag{3.3.7}$$

where

$$f'(U) = \frac{1}{8\pi^2 g^2_{\rm YM}}\left(1 - \frac{g^2_{\rm YM}N}{U}\left(1 - \frac{\gamma}{N}\right)\right) . \tag{3.3.8}$$

Remembering discussions in section 2.6.2, we recognize this as the one-loop expression for the metric on moduli space for the $SO(2N+1)$, $USp(2N)$ or $SO(2N)$ 2+1 dimensional gauge theory. On general grounds, the classical moduli space has the geometry

$$\mathcal{M}_{\rm cl} = \frac{\left(\mathbb{R}^3 \times S^1\right)^N}{S_N \times \mathbb{Z}} \tag{3.3.9}$$

where there is a natural $\mathbb{Z}_2$ action reflecting the N eigenvalues into (minus) themselves, to be contrasted with equation (2.6.1). In the subspace where we set all the vev's (but four) to be equal, we are reduced to

$$\mathcal{M}_{\rm cl} = \frac{\mathbb{R}^3 \times S^1}{\mathbb{Z}_2} \tag{3.3.10}$$

for the classical moduli space. Our metric (3.3.7) above, with the $\mathbb{Z}_2$ action (imposed, recall, for smoothness of the Atiyah–Hitchin manifold representing the O6$^-$–plane), is the one–loop expression for the metric on the full moduli space. Like we discussed in section 2.6.3 these results have a dual interpretation as an approximate result for the metric on moduli space of N monopoles. This time, they are monopoles of a spontaneously broken $SU(2)$ theory which has an identification by $\mathbb{Z}_2$.

3.4 Summary

We have shown in this chapter how to generalise the enhançon configuration pertaining to large N $SU(N)$ gauge theory on the branes' world-volume to that of gauge groups $SO(2N+1)$, $USp(2N)$, and $SO(2N)$.

We have done this using orientifold planes. Orientifolds in string theory are not dynamical objects themselves, although in conjunction with D–branes they change the gauge group on the branes' world-volume. The construction involved N D6–branes wrapped on $K3$, as before, and as a new ingredient also the presence of an orientifold plane (three different types possible). This brought about an order $1/N$ corrections to the overall D6–brane charge, while the wrapping process on $K3$ induced another set of $1/N$ corrections to the effective D2–brane charge.

To find the respective supergravity solutions, we relied upon our knowledge of how the various type IIA solutions are related to the corresponding solutions in eleven dimensions *via* the type IIA/M–theory duality. Namely, a D6–brane has an eleven dimensional (M–theory) ancestor in the form of the Taub-NUT space, while an O6$^-$–plane in the form of the Atiyah-Hitchin space.

We uplifed the familiar enhançon solution (without an orientfold) into eleven dimensions, where it is represented by pure geometry and there are no dynamical objects (like the wrapped D6–branes in ten dimensions) we could interpret as

elementary building blocks of the solution. Still, we were able to argue that the repulson singularity in eleven dimensional supergravity on $K3$ must be resolved, in terms of the dual description of heterotic strings on T^3.

Using the fact that the large r approximation of the Atiyah-Hitchin metric is given by a negative mass Taub-NUT metric, we were able to combine together the eleven dimensional solutions, and returning back to ten dimensions, to obtain "orientifolded" enhançons in type IIA string theory. These results were reliable for large N, when the enhançon radius is sufficiently large, and deviations from the Atiyah-Hitchin metric are exponentially small.

Once having the supergravity solution, the rest of the analysis followed in an analogous manner to the discussions presented in chapter 2. The orientifol plane was responsible for the $1/N$ subleading corrections to the enhançon location and correspondingly to the one-loop moduli space metric. As a global feature the orientifold added an extra $\mathbb{Z}_2$ identification on the space-time geometry and correspondingly to the gauge theory moduli space.

Thus the enhançons can be classified into types A (for $SU(N)$), B (for $SO(2N+1)$), C (for $USp(2N)$), and D (for $SO(2N)$). There is no E type counterpart, since our solutions were valid in the regime of large N, but the maximal rank of exceptional groups is only eight.

Chapter 4

Oblate, Toroidal, and Other Shapes for the Enhançon

Results in physics acquired by studying spherical configurations may sometimes be a bit deceptive, because of happy coincidences due to the high amount of symmetry. In this chapter we will generalise the spherical enhançon considered in chapter 2, to a family of enhançons of different shapes. Instead of wrapping coincident D–branes on $K3$, we construct these shapes by wrapping D–brane distributions, obtained as extremal limits of rotating p–branes.

At the first step of the enterprize, before wrapping, we find to our surprise that the brane density of the corresponding D6–brane system is actually negative in a certain space-time region. There are also repulsive gravitational features associated with it. We consider what this might mean, and nevertheless proceed with wrapping, since distributions of branes of other p do behave normally.

We explore these configurations using techniques already familiar, and discover how the enhançon takes different shapes, as we may vary the parameters originally related to angular momentum of the non-extremal configuration. In all these situations the enhançon mechanism is able to rid the geometry of the unphysical repulson singularity, generated by wrapping branes on $K3$, but it does not correct the curious features of the D6–brane distribution. In the final section, we entertain the idea that varying the shapes of the enhançon might be viewed as a scattering of solitons in some dual picture.

4.1 D–Brane distributions

4.1.1 Extremal limit of rotating p–branes

It is possible to derive a metric for a continuous distribution of branes by taking extremal limits of rotating solutions. The limits remove the rotation and restore supersymmetry, and the parameters that corresponded to angular momentum remain in the geometry as parameters of the distribution (for D3–branes this was done first in refs. [166, 167]).

We can do this for D6–branes as follows. First take the rotating black six–brane solution[1]:

$$\begin{aligned} ds^2 &= \hat{f}_6^{-1/2}\Big(-K\, dt^2 + \sum_{i=1}^{6} dx_i^2\Big) + \hat{f}_6^{1/2}\Big(\bar{K}^{-1}\frac{\Delta}{\Xi}\, dr^2 + \Delta r^2\, d\theta^2 + \Xi r^2 \sin^2\theta\, d\phi^2\Big) \\ &\quad + \hat{f}_6^{-1/2}\frac{2m}{\Delta r}\Big(\ell^2 \sin^4\theta\, d\phi^2 - 2\cosh\delta\, \ell \sin^2\theta\, dt d\phi\Big)\,, \\ e^{2\Phi} &= \hat{f}_6^{-3/2}, \\ C_7 &= \frac{1}{\sinh\delta}\hat{f}_6^{-1}\Big(\cosh\delta\, dt - \ell \sin^2\theta\, d\phi\Big) \wedge dx_1 \wedge \ldots \wedge dx_6\,, \end{aligned} \tag{4.1.1}$$

where

$$\hat{f}_6 = 1 + \frac{2m\sinh^2\delta}{\Delta r}\,, \qquad K = 1 - \frac{2m}{\Delta r}\,, \qquad \bar{K} = 1 - \frac{2m}{\Xi r}\,, \tag{4.1.2}$$

and

$$\Delta = 1 + \frac{\ell^2}{r^2}\cos^2\theta\,, \qquad \Xi = 1 + \frac{\ell^2}{r^2}\,, \tag{4.1.3}$$

while r is a radial coordinate for three cartesian coordinates x_7, x_8, x_9 with $r^2 = x_7^2 + x_8^2 + x_9^2$ and we are using the standard spherical polar coordinates such that $x_9 = r\cos\theta$, and so on.

We can obtain the extremal limit by sending the non–extremality parameter $m \to 0$ and the boost parameter $\delta \to \infty$, while keeping $r_6 = 2m\sinh^2\delta$ fixed. In this limit the metric component, $g_{t\phi}$, indicating rotation, does not survive and the

[1] Solutions corresponding to rotating p–branes of type II supergravity were found in [166,168,169] by uplifting rotating black hole solutions of various types.

resulting solution is:

$$\begin{aligned} ds^2 &= f_6^{-1/2}\Big(-dt^2+\sum_{i=1}^{6} dx_i^2\Big)+f_6^{1/2}\Big(\frac{\Delta}{\Xi}\,dr^2+\Delta r^2\,d\theta^2+\Xi r^2\sin^2\theta\,d\phi^2\Big)\,, \\ e^{2\Phi} &= f_6^{-3/2}, \\ C_7 &= f_6^{-1}dt\wedge dx_1\wedge\ldots\wedge dx_6\,, \end{aligned} \tag{4.1.4}$$

where

$$f_6 = 1+\frac{r_6}{\Delta r} \qquad r_6=\frac{g_sN\alpha'^{1/2}}{2}\,. \tag{4.1.5}$$

A similar procedure can be applied for the other non-extremal rotating black brane solutions as well, giving different Dp–brane distributions.[2] We will consider the $p=4,5$ cases in section 4.4.

In the next section we wrap this configuration of D6–branes on K3. However, let us first examine the structure of this configuration, in order to understand better what new features are specifically brought about by the wrapping, and which are due to the distribution's geometry.

4.1.2 Density of branes

The parameter ℓ controls the departure from spherical geometry.[3] In the case $\ell=0$, the solution in equation (4.1.4) reduces to the usual spherically symmetric static D6–brane solution, where the singularity at $r=0$ is interpreted as the position where the branes reside. Now, as soon as $\ell\neq 0$, that singularity disappears except for on the equatorial plane $\theta=\pi/2$: The denominator in the harmonic function is now $r+(\ell^2/r)\cos^2\theta$, which only vanishes at $r=0$, $\theta=\pi/2$, so the source at $r=0$ has been modified. Let us try to understand how.

[2]The complete classification follows from the results presented in ref. [170].

[3]As ℓ was related to the angular momentum of the non–extremal rotating configurations we have assumed $\ell^2\geq 0$ here. But in fact, the extremal case (4.1.4) with $\ell^2\leq 0$ is also a solution, leading to prolate (instead of oblate) enhançon shapes after wrapping — the subject of section 4.6.

"Extended" coordinates

To get a better understanding of the source, let us perform the following transformation [168] to isotropic coordinates which we shall refer to as "extended":

$$\begin{aligned} y_1 &= \sqrt{r^2+\ell^2}\,\sin\theta\,\cos\phi\ , \\ y_2 &= \sqrt{r^2+\ell^2}\,\sin\theta\,\sin\phi\ , \\ y_3 &= r\,\cos\theta\ . \end{aligned} \tag{4.1.6}$$

We see that the origin $r=0$ is mapped to a disc, given by $y_1^2+y_2^2=\ell^2\sin^2\theta$, $y_3=0$. Going to $r=0$ along $\theta=0$ takes us to the centre of the disc at $y=0$, while an approach along $\theta=\pi/2$ takes us to the edge of the disc at $y_1^2+y_2^2=\ell^2$. Approaching under other angles takes us to the interior of the disc.

After this coordinate transformation the metric in equation (4.1.4) reduces to a standard brane form:

$$ds^2 = F_6^{-1/2}\Big(-dt^2+\sum_{i=1}^{6}dx_i^2\Big)+F_6^{1/2}\Big(dy_1^2+dy_2^2+dy_3^2\Big)\ , \tag{4.1.7}$$

where the harmonic function is given by

$$F_6 = 1+\frac{r_6\sqrt{\Lambda+\Sigma}}{\sqrt{2}\Sigma}\ , \tag{4.1.8}$$

with

$$\Sigma=\sqrt{\Lambda^2+4\ell^2y_3^2}\ , \qquad \Lambda=y^2-\ell^2\ , \qquad y=\sqrt{y_1^2+y_2^2+y_3^2}\ . \tag{4.1.9}$$

Brane densities

Now we see that the singularity we identified earlier is in fact a *ring* of radius ℓ. Is this where the branes are located? The harmonic function F_6 should have an integral representation given schematically by

$$F_6 = 1+\int\frac{\sigma(y')}{|y-y'|}dy'\ , \tag{4.1.10}$$

for some density function $\sigma(y)$ representing a continuous distribution of branes in the coordinate y.

How seriously we should take the physical meaning of this distribution is a matter of interest. First of all the notion of brane density is a simplification, since branes come in discrete amounts due to charge conservation. Under the assumption the number of branes is large, *e.g.* in various supergravity contexts, having a continuous distribution of branes should be a good and useful approximation. However, in the full string theory, we might wish to probe the structure of the solution at resolutions which might render the distribution meaningless.

Analogue of Gauss' law

It is possible to directly determine the distribution's dependence on y, using an analogue of Gauss' law. For six–branes, we have three transverse spatial dimensions, and so the problem of determining harmonic functions is in fact directly translated into a familiar electromagnetism problem.

Let us define $\rho = \sqrt{y_1^2 + y_2^2}$, $z = y_3$. It is sufficient to determine the harmonic function's behaviour along the z–axis as the density function and the angular dependence of F_6 follows directly from harmonic analysis. The analogue of Gauss' law in electrodynamics for a standard infinitesimal "pillbox" surface defined on the $z = 0$ plane is

$$(\vec{E}_+ - \vec{E}_-) \cdot \vec{n} = 4\pi\sigma \ , \tag{4.1.11}$$

where $\vec{n}$ is the unit normal vector of the surface directed from one side $(-)$ to the other side $(+)$ of the surface, and σ is the surface charge density. The electric field is $\vec{E} = -\vec{\nabla}\Phi$, while the role of the potential Φ is now played by the harmonic function. Taking the derivative,

$$\frac{\partial F_6}{\partial z} = \frac{z r_6}{\sqrt{2}\Sigma^3\sqrt{\Lambda+\Sigma}}\Big(\Sigma^2 - \Lambda\Sigma - 2\Lambda^2 - 2\ell^2(2\Lambda+\Sigma)\Big) \ , \tag{4.1.12}$$

we obtain

$$\sigma(\rho) = \frac{1}{4\pi}\left(\frac{\partial F_6}{\partial z}\Big|_{z\to 0^-} - \frac{\partial F_6}{\partial z}\Big|_{z\to 0^+}\right) = -\frac{r_6\ell}{2\pi(\ell^2-\rho^2)^{3/2}} \ , \tag{4.1.13}$$

where an expansion in small z was used to get this result. This density is negative, but happily (since it would be hard to see how to get a positive result for the D6–brane charge from this), it integrates to infinity over the disc, due to the boundary

contribution. We must therefore add an extra positive term to the boundary, so that the complete distribution is

$$\sigma(y) = -\frac{r_6 \ell}{2\pi(\ell^2-\rho^2)^{3/2}}\Theta(\ell-\rho)\delta(z) + \frac{r_6}{2\pi\sqrt{\ell^2-\rho^2}}\delta(\ell-\rho)\delta(z)\ . \tag{4.1.14}$$

It is worth checking that the normalisation of the configuration is indeed r_6 as expected

$$\begin{aligned}\int_0^\ell 2\pi\sigma(\rho)\rho d\rho &= \int_0^\ell \Big(-\frac{r_6\ell\rho}{(\ell^2-\rho^2)^{3/2}} + \frac{r_6\rho}{\sqrt{\ell^2-\rho^2}}\delta(\ell-\rho)\Big)d\rho \\ &= \left[-\frac{r_6\ell}{\sqrt{\ell^2-\rho^2}}\right]_{\rho=0}^{\rho=\ell} + \left.\frac{r_6\rho}{\sqrt{\ell^2-\rho^2}}\right|_{\rho=\ell} = r_6\ ,\end{aligned} \tag{4.1.15}$$

and that the brane distribution (4.1.14) correctly reproduces our harmonic function along the z–axis:

$$\begin{aligned}F_6 &= 1 + 2\pi\int_0^\ell \frac{\sigma(\rho)\rho d\rho}{\sqrt{z^2+\rho^2}} \\ &= 1 + \int_0^\ell \left(-\frac{r_6\ell\rho}{\sqrt{z^2+\rho^2}(\ell^2-\rho^2)^{3/2}} + \frac{r_6\rho}{\sqrt{z^2+\rho^2}\sqrt{\ell^2-\rho^2}}\delta(\ell-\rho)\right)d\rho \\ &= 1 + \left[-\frac{r_6\ell}{(\ell^2+z^2)}\frac{\sqrt{z^2+\rho^2}}{\sqrt{\ell^2-\rho^2}}\right]_{\rho=0}^{\rho=\ell} + \left.\frac{r_6\rho}{\sqrt{z^2+\rho^2}\sqrt{\ell^2-\rho^2}}\right|_{\rho=\ell} \qquad (4.1.16) \\ &= 1 + \frac{r_6 z}{\ell^2+z^2}\ . \qquad (4.1.17)\end{aligned}$$

4.1.3 Dp–brane disc distributions

This is very interesting, particularly when compared to the results, listed in (4.1.18), one can get by computing the analogous quantities for Dp–brane disc distributions for $p = 0, \cdots 5$. The results are easy to obtain[4] by noting first that along the z axis, the harmonic function's form in extended coordinates is exactly the same as in unextended coordinates:

$$f = 1 + \frac{r_p^{7-p}}{z^{7-p}\,(1+\ell^2/z^2)}\ .$$

[4]The case of disc distributions of D3–branes was known before, being dual to part of the Coulomb branch of the $\mathcal{N}=4$ $SU(N)$ gauge theory [166, 167]. The case of D5–brane distribution on a circle was first studied in [167].

This can be verified by simply examining the appropriate metrics, which can be derived by taking an extremal limit of the metrics listed in [169], as we did for equation (4.1.1) to get equation (4.1.4), keeping only one non–zero parameter $\ell_1 = \ell$. Given that the harmonic function should have an integral representation

$$f = 1 + \int \frac{\sigma(y')dy'}{|y - y'|^{7-p}} ,$$

it is easy to guess the densities in each case and check them by explicit integration. We list the densities here, and plot them in figure (4.1):

$$\begin{aligned}
\text{D0}: \quad \sigma(y) &= +\frac{5r_0^7}{2\pi\ell^5}\,(\ell^2-\rho^2)^{\frac{3}{2}}\,\Theta(\ell-\rho)\,\delta(z)\,, \\
\text{D1}: \quad \sigma(y) &= +\frac{4r_1^6}{2\pi\ell^4}\,(\ell^2-\rho^2)^{1}\,\Theta(\ell-\rho)\,\delta(z)\,, \\
\text{D2}: \quad \sigma(y) &= +\frac{3r_2^5}{2\pi\ell^3}\,(\ell^2-\rho^2)^{\frac{1}{2}}\,\Theta(\ell-\rho)\,\delta(z)\,, \\
\text{D3}: \quad \sigma(y) &= +\frac{2r_3^4}{2\pi\ell^2}\,(\ell^2-\rho^2)^{0}\,\Theta(\ell-\rho)\,\delta(z)\,, \\
\text{D4}: \quad \sigma(y) &= +\frac{r_4^3}{2\pi\ell}\,(\ell^2-\rho^2)^{-\frac{1}{2}}\,\Theta(\ell-\rho)\,\delta(z)\,, \\
\text{D5}: \quad \sigma(y) &= +\frac{r_5^2}{2\pi}\,(\ell^2-\rho^2)^{0}\delta(\ell-\rho)\,\delta(z)\,, \\
\text{D6}: \quad \sigma(y) &= -\frac{r_6\ell}{2\pi}(\ell^2-\rho^2)^{-\frac{3}{2}}\Theta(\ell-\rho)\delta(z) + \frac{r_6}{2\pi}(\ell^2-\rho^2)^{-\frac{1}{2}}\delta(\ell-\rho)\delta(z)\,.
\end{aligned} \tag{4.1.18}$$

(Now z in the above is shorthand for all of the directions transverse to the disc and, of course, to the brane's world–volume.) The pattern is worth noting. For a Dp–brane, as p becomes larger, the distribution increasingly spreads away from the centre. The D5–brane case is a limiting one, having all of the branes at the boundary forming a ring. The D6–brane case (not plotted) also has a δ–function on the boundary, but is accompanied by a negative contribution to $\sigma(y)$ in the interior.

4.1.4 The meaning of negative brane distributions

While there is a striking pattern here, we must pause to consider what the physical significance of the negative contribution to the distribution of branes might be.[5]

[5]In fact, this has occurred previously in a related context in [171], where appropriately cautious statements were made. The context was D3–brane distributions (in the decoupling limit), describ-

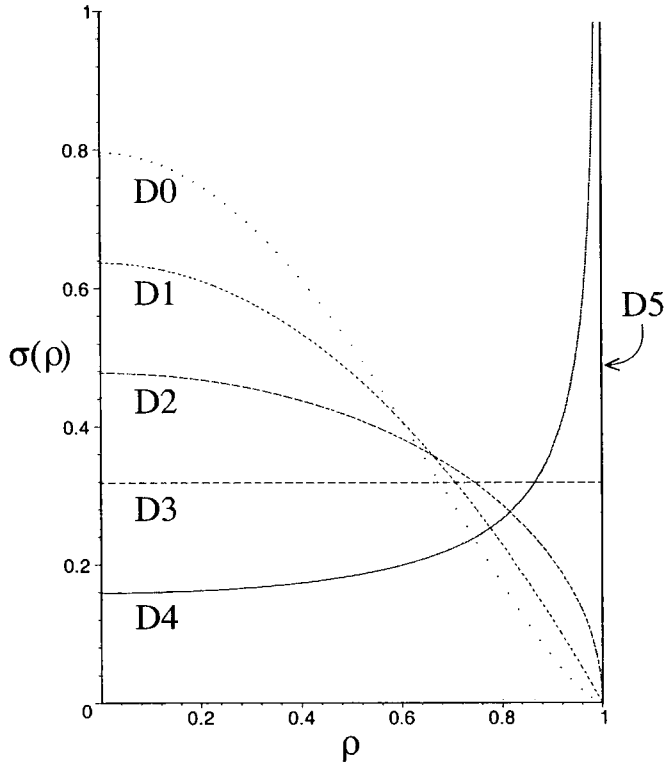

Figure 4.1: Disc density distributions of Dp–branes in a plane for $p = 0, \ldots, 5$, normalised to the same area. The case of D5–branes is a delta function on the edge, at $\rho = 1$. The pattern followed by these distributions is described in the text.

As we said previously, we must be careful about the meaning of the continuous distribution in general, since it is merely a supergravity approximation. However, the negative density (and hence tension and charge) is somewhat harder to accept, and may be another deficiency of the supergravity description, appealing to more stringy physics to resolve the problem.

This is of course reminiscent of the features which are resolved by the enhançon mechanism. But probing the configuration with a D6–brane is exactly similar to exercise we have already accomplished in section 1.5. A probe D6–brane will see no

ing part of the Coulomb branch of the dual $\mathcal{N} = 4$ $SU(N)$ gauge theory. There, switching on a vacuum expectation value of a perfectly physical operator in the gauge theory corresponded to a five dimensional ball distribution, which by a coincidence is described by the same function as we have listed above for the D6–brane disc.

potential for movement in this background, and the resulting moduli space metric is perfectly flat right down to $y = 0$. So it would seem that we can not argue that this distribution can not be constructed by bringing all of the constituent branes from infinity, *etc*, like we did for the wrapped D6–brane configuration.

Still, there is no compelling reason to think that the full string theory would leave the geometry as it currently is in the supergravity description. There may well be some other mechanism in operation, perhaps involving something analogous to the enhançon, which could able to fix or at least explain the meaning of this geometry.

4.1.5 Legendre polynomials

Later in section 4.5, we will also see that this sort of distribution corresponds to switching on apparently sensible vacuum expectation values for gauge theory operators. That discussion will be aided by noting that the harmonic function F_6 can be expanded in a series in the variable ℓ/y for $y > \ell$, or y/ℓ for $y < \ell$. It is delightful to see how these series arrange themselves in terms of Legendre polynomials:

$$F_6 = 1 + \frac{r_6}{y}\sum_{n=0}^{\infty}(-1)^n\left(\frac{\ell}{y}\right)^{2n} P_{2n}(\cos\,\hat{\theta})\,, \qquad y > \ell\,, \tag{4.1.19}$$

$$F_6 = 1 + \frac{r_6}{\ell}\sum_{n=0}^{\infty}(-1)^n\left(\frac{y}{\ell}\right)^{2n+1} P_{2n+1}(\cos\,\hat{\theta})\,, \qquad y < \ell\,, \tag{4.1.20}$$

where we have defined new polar coordinate angles with respect to the y_i's:

$$\begin{aligned}\hat{\theta} &= \cos^{-1}\left(\frac{y_3}{y}\right)\,,\\ \hat{\phi} &= \tan^{-1}\left(\frac{y_2}{y_1}\right) = \phi\,,\end{aligned} \tag{4.1.21}$$

and $P_n(x)$'s are the Legendre polynomials in the variable x, with the normalisation:

$$P_0(x) = 1\,; \quad P_1(x) = x\,; \quad P_2(x) = \frac{1}{2}(3x^2 - 1)\,; \quad \textit{etc.} \tag{4.1.22}$$

In hindsight, this is of course what we should expect from a direct expansion of equation (4.1.17), combined with harmonic analysis.

In the end let us remark that we can insert any harmonic potentials from electromagnetism (or higher dimensional generalisations) and get a supergravity solution

corresponding to a distribution of D–branes. This could in principle be wrapped on K3, as we do in the next section. However, since these are most commonly found as a series expansion of the form above, exact determination of the crucial enhançon and repulson loci (as we do later) will not in general be possible.

4.1.6 Particle probes of the geometry

It is instructive to probe the system with a point particle using the technology we are already familiar with from section 2.2. The purely radial motion on the equatorial plane or along the symmetry axis (*i.e.*assuming $\mathbf{u}^{\theta} = 0$, and $\mathbf{u}^{\phi} = 0$) of the test particle is described by

$$E = \frac{1}{2}\frac{\Delta}{\Xi}\left(\frac{dr}{d\tau}\right)^2 + V_{eff}(r) \ . \tag{4.1.23}$$

The effective potential that the particle probe feels is

$$V_{eff}(r) = -\frac{1}{2}\left(g_{tt} + 1\right) \ . \tag{4.1.24}$$

We plot V_{eff} for a particle approaching along the equator and also along the z–axis in figure 4.2. It is interesting to note that accompanying this negative brane region is a repulsive behaviour in the supergravity. A test particle located along the z–axis sees a potential which is repulsive inside a radius ℓ. The distance ℓ is the point where the repulsive force caused by the negative brane distribution on the disc is balanced by the attractive force due to positive branes sitting on the ring. Far away the attractive force of positive branes is stronger, since the overall charge of the configuration is positive. But as the test particle comes close to the centre of the disc, it starts to feel repulsion, because repelling sources are now significantly nearer to it than the attractive sources.

Let us stress, these repulsive features have nothing to do with the repulson singularity coming from wrapping, since we have not yet wrapped the configuration on $K3$. In the following discussions we will bear in mind that it is a feature which is inherited by the wrapped configuration from the unwrapped configuration. Later, in section 4.4, we shall see that there is no such behaviour for D5–brane distributions, and so we will treat this as an artifact of the D6–brane case in what follows, as it

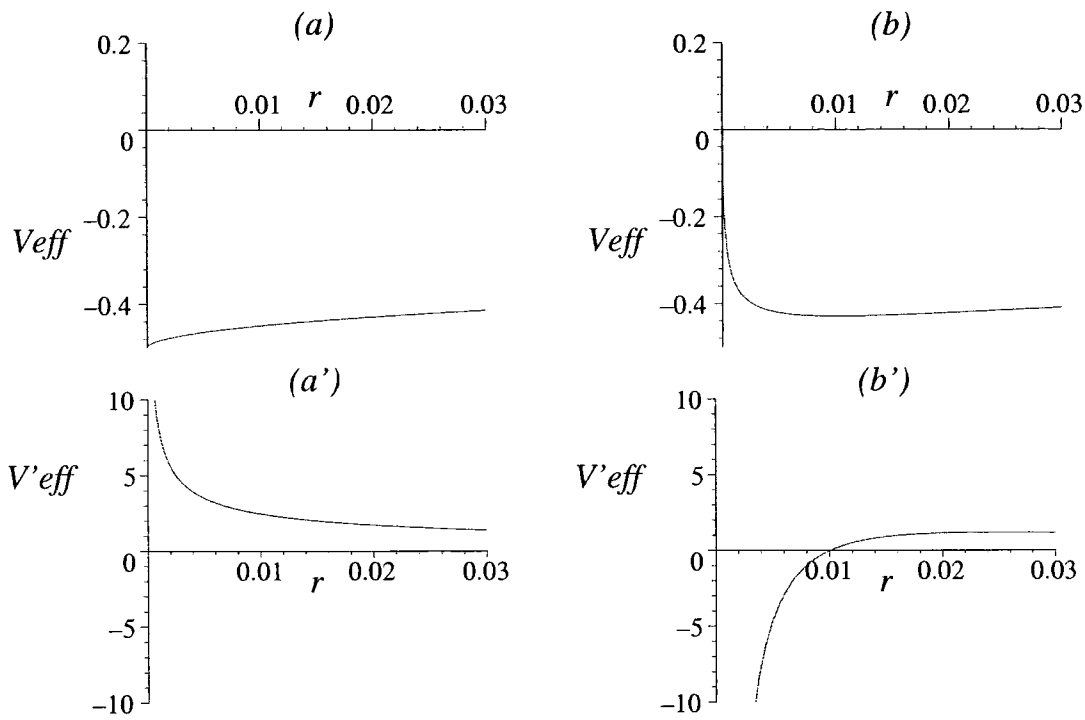

Figure 4.2: Gravitational features of the unwrapped D6–brane distribution as seen by a neutral test particle. The test particle effective potential (to) and its derivative (bottom) along the axis of symmetry ($\theta = 0$) corresponding to *(a)* $\ell = 0$, *(b)* $\ell > 0$. In the latter case the potential becomes repulsive at a distance ℓ from the origin. The effective potential for a particle moving on the equatorial plane ($\theta = \pi/2$) is always attractive, and is similar to case *(a)*.

will not affect our analysis of the excision of the repulson behaviour arising from wrapping.

4.2 Wrapping D6–brane distributions

We have learned enough about our configuration to return to our problem of wrapping the branes on K3. As we have seen before wrapping a D6–brane on K3 induces precisely one unit of negative D2 brane charge in the D6–brane world–volume, giving a configuration sketched in table 4.1. The naive supergravity solution (in string

	$\mathbb{R}^{5,1}$						K3			
	x_0	x_1	x_2	x_3	x_4	x_5	x_6	x_7	x_8	x_9
D6	–	–	–	*	*	*	–	–	–	–
D2	–	–	–	*	*	*	∼	∼	∼	∼

Table 4.1: A sketch of a D6–brane distribution wrapped on K3 and the induced negative D2–branes. The branes' world-volume directions are marked by "–", while "∼" indicates that the induced D2–branes are delocalised on K3. In the transverse directions the branes are not coincident, but form a distribution, symbolised by "*".

frame) can be written as follows:

$$\begin{aligned} ds^2 &= f_2^{-1/2} f_6^{-1/2}(-dt^2 + dx_1^2 + dx_2^2) + f_2^{1/2} f_6^{1/2} \left(\frac{\Delta}{\Xi} dr^2 + \Delta r^2 \, d\theta^2 + \Xi r^2 \sin^2\theta \, d\phi^2 \right) \\ &\quad + V^{1/2} f_2^{1/2} f_6^{-1/2} ds_{K3}^2 \,, \\ e^{2\Phi} &= f_2^{1/2} f_6^{-3/2} \,, \\ C^{(3)} &= f_2^{-1} dt \wedge dx_1 \wedge dx_2 \,, \\ C^{(7)} &= f_6^{-1} dt \wedge dx_1 \wedge dx_2 \wedge V ds_{K3} \,, \end{aligned} \tag{4.2.1}$$

with

$$f_2 = 1 - \frac{r_6 V_\star}{V \Delta r} \,, \quad f_6 = 1 + \frac{r_6}{\Delta r} \,, \tag{4.2.2}$$

ds_{K3}^2 is the metric of a unit volume K3 surface, while the functions Δ and Ξ are as defined previously in equation (4.1.3).

Despite being a solution to the supergravity equations of motion, the geometry for this configuration is not consistent. Again we observe naked singularities of repulson type appearing where the running K3 volume,

$$V(r,\theta) = V \frac{f_2}{f_6} \,, \tag{4.2.3}$$

shrinks to zero. Some algebra shows that this occurs at radii:

$$r_{\rm r} = \frac{r_6 V_\star}{2V} \left[1 \pm \left(1 - \frac{4V^2}{r_6^2 V_\star^2} \, \ell^2 \cos^2\theta \right)^{1/2} \right] . \tag{4.2.4}$$

When ℓ is zero, we have the spherically symmetric situation where the singularity appears on a sphere of radius $r_6 V_\star / V$. For non–zero, but sufficiently small ℓ the

singularity appears at two disconnected loci, one of them inside the other, and between these loci the metric (4.2.1) is imaginary. When ℓ reaches the critical value

$$\ell_{\rm r}^{\rm cr} = \frac{r_6 V_\star}{2V} \,, \tag{4.2.5}$$

these two surfaces meet and join into one single surface for $\ell > \ell_{\rm r}^{\rm cr}$.

4.2.1 Shapes of the enhançon

We expect stringy effects to have switched on long before a vanishing volume is reached, since when the volume gets to the value $V_\star$, there are extra massless states coming from wrapped D4– and anti–D4–branes, giving an enhanced $SU(2)$ in space-time. The radius at which this occurs is the enhançon radius, and it is easily computed to give:

$$r_{\rm e} = \frac{r_6 V_\star}{V - V_\star}\left[1 \pm \left(1 - \frac{(V-V_\star)^2}{r_6^2 V_\star^2}\ell^2 \cos^2\theta\right)^{1/2}\right] \,. \tag{4.2.6}$$

This is of course the same radius that gives a zero of the effective tension of a probe wrapped D6–brane, whose action we already know as equation (2.3.1),

$$S = -\int_{\mathcal{M}_3} d^3\xi\, e^{-\Phi}\left(\mu_6 V(r) - \mu_2\right)\left(-\det g_{ab}\right)^{1/2} + \mu_6 \int_{\mathcal{M}_3\times K3} C^{(7)} - \mu_2 \int_{\mathcal{M}_3} C^{(3)} \,. \tag{4.2.7}$$

Substituting in the background fields (4.2.1) and working through the familiar static gauge computation gives the effective lagrangian:

$$\mathcal{L} = \frac{\mu_6}{2g_s}(V f_2 - V_\star f_6)\left(\frac{\Delta}{\Xi}\,\dot{r}^2 + \Delta r^2\,\dot{\theta}^2 + \Xi\, r^2 \sin^2\theta\,\dot{\phi}^2\right) \,, \tag{4.2.8}$$

where we can read off the probe effective mass (tension) as

$$\tau_{\rm eff} = \frac{\mu_6}{g_s} f_6\left(V(r,\theta) - V_\star\right) \,. \tag{4.2.9}$$

Let us study the enhançon radius given in equation (4.2.6). For $\ell = 0$ we recover the spherically symmetric case with enhançon radius $2r_6 V_\star/(V - V_\star)$. For non–zero ℓ, two different situations can be observed, depending on whether ℓ is smaller or greater than the critical value:

$$\ell_{\rm e}^{\rm cr} = \frac{r_6 V_\star}{V - V_\star} \,. \tag{4.2.10}$$

When $\ell \leq \ell_e^{cr}$, there are two enhançon shells which divide our geometry into three distinct regions. The tension of a D6–brane probe drops to zero at the outer enhançon shell. Let us call the exterior region of positive tension region I. In between the outer and inner enhançon shells, the tension of our probe would be negative. We will call this region II. This is the region where we encountered the repulson singularities (4.2.4) and it will be excised shortly. Finally, the tension is again positive in region III, inside the inner enhançon shell. We can be sure that singularities are contained in the region II only, because the running K3 volume is a continuous function and $V_\star > 0$. The origin $r = 0$, appears to be problematic, since it solves both equation (4.2.4) and equation (4.2.6). In fact, if we approach $r = 0$ along the z–axis, we get $V(r,\theta) \to V$ while an approach along the equator shows that $V(r,\theta) \to -V_\star$, which is puzzling. This is partly resolved by going to the extended coordinates, where $r = 0$ opens up into a disc. Then we see that $V(r,\theta) \to -V_\star$ as we approach the edge of the disc, while $V(r,\theta) = V$ on the interior of the disc.

Notice what happens when $\ell = \ell_e^{cr}$. The inner and outer enhançon shells meet at two points on the z–axis. The tension of a brane probe moving along this axis drops to zero at the enhançon radius and becomes positive again.

For $\ell > \ell_e^{cr}$, the inner and outer enhançon shells have merged into a single connected shell with a toroidal shape. Our geometry is now divided into two distinct regions. The volume of K3 is less than $V_\star$ in the interior of the torus where the repulson singularities hide. Outside the torus the volume of K3 is greater than $V_\star$ and the geometry is acceptable. This configuration is really a torus since there is an infinitesimal "hole" in the middle. One can move along the z axis through the origin and nowhere does the running K3 volume reach the special value $V_\star$: it is possible to pass through without hitting the enhançon locus.

Actually, although there is no physical significance to the fact, it is worth noting that the repulson loci undergo a similar evolution from disconnected to connected (with the critical value ℓ_r^{cr} separating the two cases), with shapes of the same sort. Since $\ell_r^{cr} < \ell_e^{cr}$, the repulson always becomes connected before the enhançon locus does.

All this sounds rather complicated, but is quite beautiful to look at, in fact.

Figure 4.3 depicts the behaviour of K3 volume for different values of ℓ in a manner that helps to visualise both the enhançon and repulson loci present before the excision. The regions where the volume is greater than zero but less than $V_\star$ are shown by shades of dark grey (or blue if viewed/printed in colour). The light (or yellow) regions are volumes greater than $V_\star$, and so the boundary between these is the enhançon locus. The black region is for negative volumes, in other words, where the metric does not exist. The boundary between it and the grey (blue) is the repulson locus. (Figure 4.6 a few pages below offers a three dimensional view of the enhançon locus.)

In "extended" coordinates

One may wonder what happens to the enhançon if we transform the solution (4.2.1) into the "extended" coordinates given in equations (4.1.6). In these coordinates, essentially the same features arise. The singular region where the K3 volume shrinks to zero is surrounded by the enhançon shell(s). The same critical value of the parameter ℓ separates two families of enhançons as before. We re–plot the K3 volume in the extended coordinates in figure 4.4.

4.2.2 Particle probes of the geometry

Let us probe the system with a point particle, as we did previously for the purely spherical configuration in section 2.2, and in subsection 4.1.6 for the unwrapped case of D6–brane distribution. The analysis is the same, giving the effective potential (4.1.24), as before, but now we insert the metric components for the putative wrapped geometry.

The effective potential is singular (*i.e.*, exhibits infinite repulson) when g_{tt} is singular, and this happens at the repulson radius $r_{\rm r}$. The border between repulsive and attractive regions corresponds to the minimum of the potential, which occurs when

$$\frac{\partial}{\partial r}\,(f_2 f_6) = 0\ . \tag{4.2.11}$$

It is significant that the relation (4.2.11) is satisfied exactly at $r = r_{\rm e}$, *i.e.*on the enhançon shell.

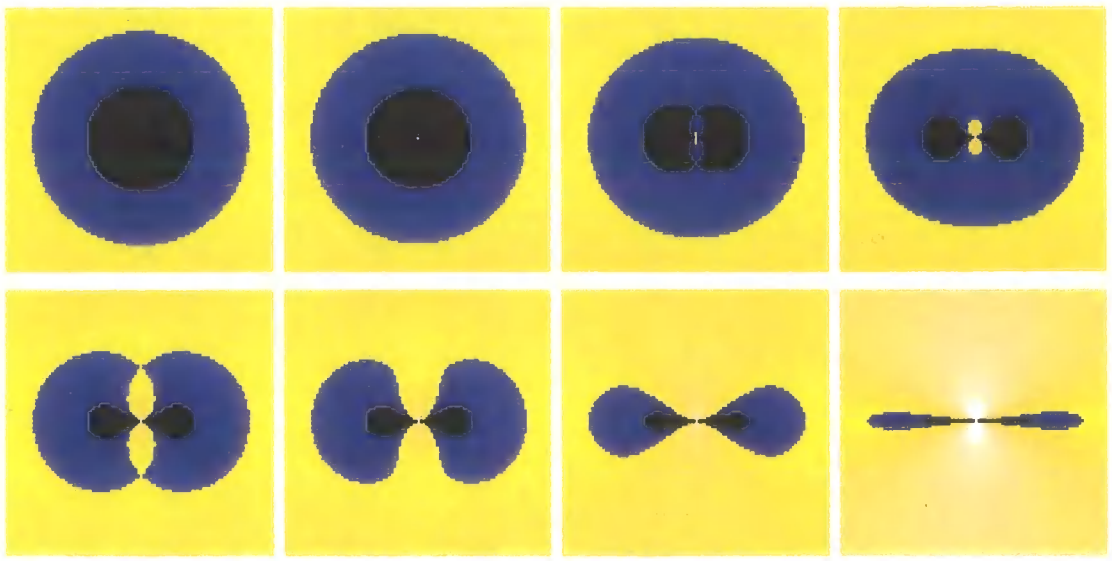

Figure 4.3: A vertical slice through the non–spherical wrapped D6–brane geometry before excision. The origin $r = 0$ is placed in the centre of the figure, while the symmetry axis, $\theta = 0$, corresponds to the vertical direction and $\theta = \pm\pi/2$ to the horizontal. The full three-dimensional view emerges when the plots are revolved around the vertical axis. The region where the K3 volume $V(r,\theta) < 0$ is black. The region where $0 \leq V(r,\theta) < V_\star$ is dark grey (blue). The repulson radius $r_{\rm r}$ is marked by the border between these two regions. The physically acceptable region $V(r,\theta) \geq V_\star$, where the tension of the probe brane is positive, is in the light shade (different shades between yellow ($V(r,\theta)$ is close to $V_\star$) and white ($V(r,\theta)$ is close to V)). The enhançon radius $r_{\rm e}$ is the border between the dark grey (blue) and the light regions. Spherical enhançon is given by $\ell = 0$. For increasing values of ℓ, two disconnected shells appear forming a double enhançon. Once $\ell_{\rm e}^{\rm cr}$ is exceeded, the two shells join forming a single enhançon. This pattern can be seen explicitly in the figure for the following values of ℓ : $\ell = 0$ (top, left), $\ell = \frac{1}{2}\ell_{\rm r}^{\rm cr}$, $\ell = \ell_{\rm r}^{\rm cr}$, $\ell = \ell_{\rm e}^{\rm cr} - \frac{1}{2}(\ell_{\rm e}^{\rm cr} - \ell_{\rm r}^{\rm cr})$ (top, right), $\ell = \ell_{\rm e}^{\rm cr}$ (bottom, left), $\ell = \frac{9}{8}\ell_{\rm e}^{\rm cr}$, $\ell = 2\ell_{\rm e}^{\rm cr}$, $\ell = 8\ell_{\rm e}^{\rm cr}$ (bottom, right). Other parameters r_6, V, and $V_\star$ have been fixed to some typical values.

On the equatorial plane this matches with the result of section 2.2, since the solution (4.2.1) at $\theta = \pi/2$ reduces to the spherically symmetric solution of $\ell = 0$. The test particle feels an attractive force as it approaches from infinity. Attraction would turn into repulsion at the enhançon radius, but at this point we will replace the geometry with a physical one.

For motion along the symmetry axis, the situation is more interesting, as it qualitatively depends on the value of the parameter ℓ (see figure 4.5). In the $\ell = 0$ case the physics is much like that described above for the equatorial motion: the

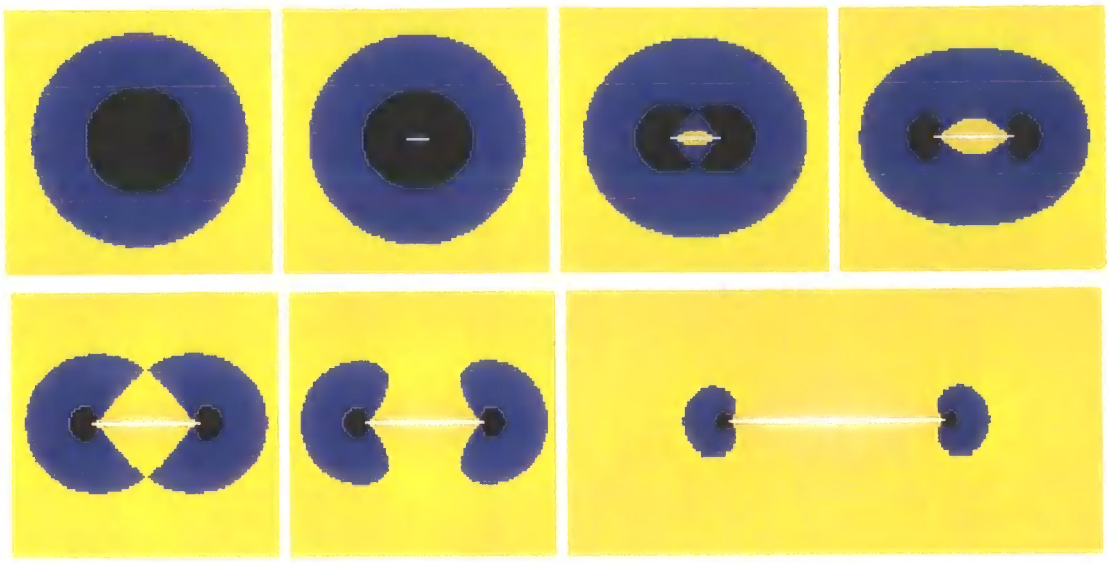

Figure 4.4: A slice through the untreated wrapped D6–brane geometry in "extended" coordinates. The colour coding is the same as in figure 4.3. The case $\ell = 0$ gives a spherical enhançon. For increasing values of ℓ, two disconnected enhançon shells appear forming coconut shape. Once $\ell_{\rm e}^{\rm cr}$ is exceeded, the two enhançon shells join to form a torus. This pattern can be seen for the following values of ℓ : $\ell = 0$ (top, left), $\ell = \frac{1}{2}\ell_{\rm r}^{\rm cr}$, $\ell = \ell_{\rm r}^{\rm cr}$, $\ell = \ell_{\rm e}^{\rm cr} - \frac{1}{2}(\ell_{\rm e}^{\rm cr} - \ell_{\rm r}^{\rm cr})$ (top, right), $\ell = \ell_{\rm e}^{\rm cr}$ (bottom, left), $\ell = \frac{9}{8}\ell_{\rm e}^{\rm cr}$, $\ell = 2\ell_{\rm e}^{\rm cr}$ (bottom, right).

potential becomes repulsive inside $r_{\rm e}$ and this repulsion is infinite at $r_{\rm r}$.

For ℓ small there are now two enhançon loci. The particle can come from infinity and reach the repulsive region just inside the outer enhançon. This is region II. Alternatively, it can start from the origin (*i.e.*, in region III, where the potential has the same value as at infinity), and be repelled towards the inner enhançon shell. This is the behaviour that we noticed before wrapping the distribution. It is *not* the repulson geometry which results from wrapping.

For a test particle moving from the origin outwards, the repulson region (resulting from wrapping) starts at the inner enhançon. Now, the repulsive force is directed towards the origin. This situation persists until $\ell = \ell_{\rm r}^{\rm cr}$.

When $\ell > \ell_{\rm r}^{\rm cr}$, a test particle moving along the symmetry axis will still feel a repulsive force, but not an infinite one. In principle, if it had enough energy, it could overcome the potential barrier between inner and outer enhançons and move from infinity to the origin, or *vice versa*. Still, because the tension of probe branes is still negative in this region, we consider it unphysical and will excise it.

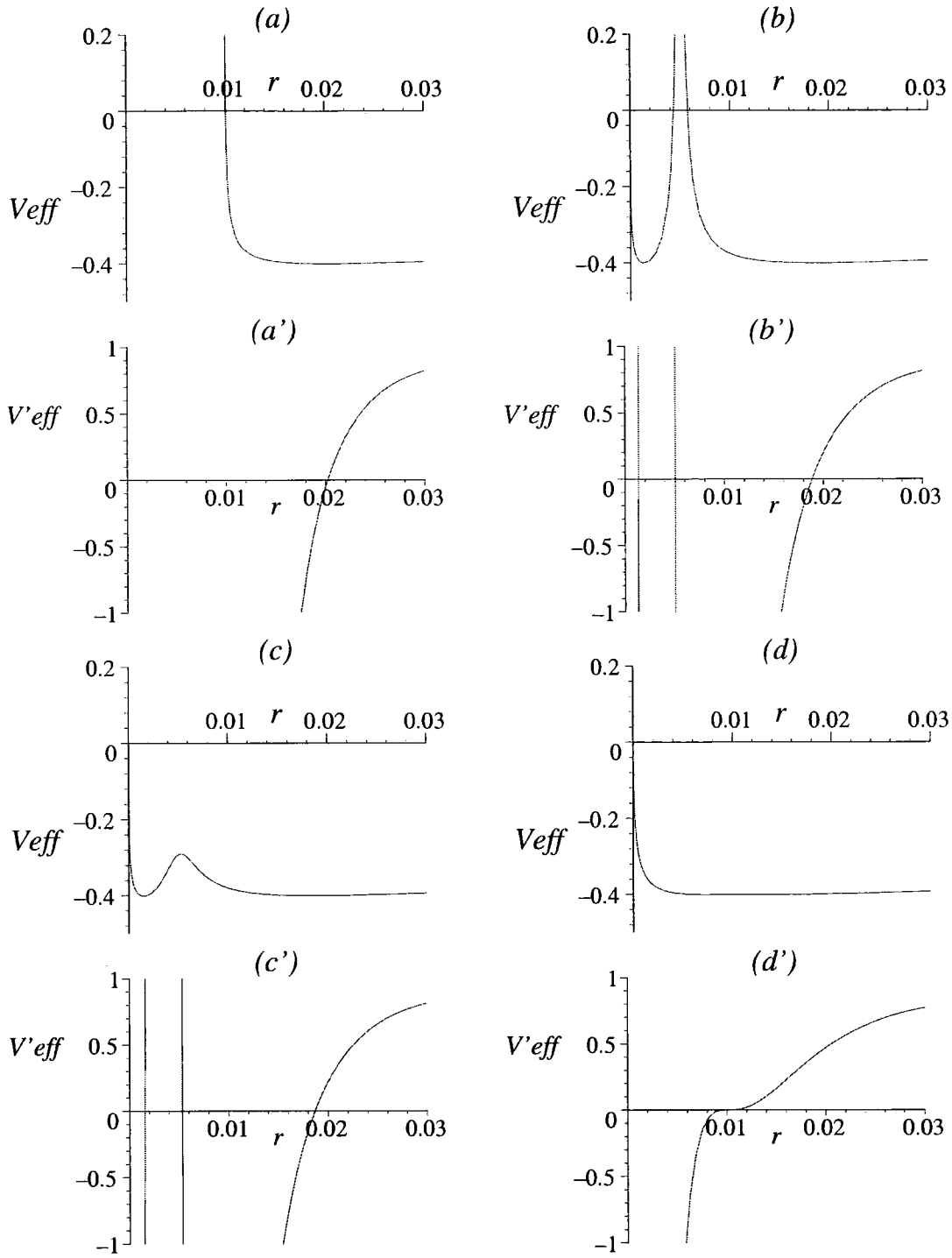

Figure 4.5: Gravitational features of the D6–brane distribution wrapped on K3 as seen by a neutral test particle. Test particle effective potential V_{eff} and its derivative V'_{eff} along the axis of symmetry ($\theta = 0$) corresponding to different values of parameter ℓ: *(a)* $\ell = 0$, *(b)* $\ell = \ell_{\rm r}^{\rm cr}$, *(c)* $\ell = \ell_{\rm r}^{\rm cr} + \frac{1}{16}(\ell_{\rm e}^{\rm cr} - \ell_{\rm r}^{\rm cr})$, *(d)* $\ell = \ell_{\rm e}^{\rm cr}$. For $\ell > \ell_{\rm e}^{\rm cr}$ the effective potential becomes increasingly similar to that of the unwrapped case in figure 4.2*(b)*. The effective potential is singular (exhibiting infinite repulson) at the singularity radius $r_{\rm r}$. A test particle moving on the equatorial plane ($\theta = \pi/2$) has potential *(a)* for all values of ℓ.

At $\ell = \ell_e^{cr}$ the inner and outer enhançon loci meet and the potential barrier vanishes. However, there is still a minimum of the potential, located at $r = \ell = r_e$. This minimum persists for $\ell > \ell_e^{cr}$, and is located at $r = \ell$, as in the unwrapped case. We stress again that this remaining repulsion has nothing to do with the wrapping, as it is the behaviour observed in the previous section for the unwrapped geometry.

4.3 Excision in supergravity

Ultimately, we must remove the parts of the geometry resulting from the wrapping which are unphysical. In order to do this, we must see what sorts of geometry we can replace the bad parts with, ascertaining whether it is consistent to do so. Consistency here will be measured at the level of supergravity, supported by intuition from the physics of the underlying string theory.

New stringy physics appears when the volume of the K3 gets to $V_\star$. A wrapped D6–brane probe becomes massless there and also delocalises. One cannot place wrapped D6–brane sources in the regions where the volume is less than $V_\star$ and so, as in previous cases, the geometry must be, to a good approximation, simply flat space. The junction between the flat space and the well–behaved geometry (across which the extrinsic curvature will jump, providing a stress tensor source) must be equivalent to a massless brane.

This is the logic we tested in section 2.5 for the spherically symmetric case. Here we have no spherical symmetry to make things simpler, but instead there are the nested shells that can intersect for some ranges of the parameters, making a toroidal shape. As we shall find out, despite this complication, the gravity junction technology allows us to analytically demonstrate that there is a variety of consistent excisions that we can perform.[6]

We must be careful about how we set up the problem. We need to compute the extrinsic curvature of the junction hypersurface Σ endowed with coordinates ξ^A and specified by an equation of the form $f(x^\mu(\xi^A)) = 0$. In the spherical case, this

[6]The introductory sections and examples presented in [173–175] were quite useful for learning about the computation for non–spherically symmetric geometries.

equation was just $f = r - R = 0$, for some constant R, and the general formula for extrinsic curvature (D.2) simplified considerably.

In the axially symmetric case, the equation specifying Σ is $f = r - R(\theta) = 0$, where R is now a function of θ. Since

$$\sigma = |\, G^{rr} + G^{\theta\theta}(\partial_\theta R)^2|^{-1/2} \ , \tag{4.3.1}$$

the unit normal vectors are

$$n^\pm_\gamma = \mp \frac{\delta^r_\gamma - \delta^\theta_\gamma \partial_\theta R}{\sqrt{|G^{rr} + G^{\theta\theta}(\partial_\theta R)^2|}} \ . \tag{4.3.2}$$

We can compute the extrinsic curvature:

$$\begin{aligned} K^\pm_{\alpha\beta} &= \frac{1}{2}\left(n^{r\pm}\partial_r + n^{\theta\pm}\partial_\theta\right) G_{\alpha\beta} \ , \\ K^\pm_{\theta\theta} &= -\, n^\pm_r \partial^2_\theta R + \frac{1}{2}(n^{r\pm}\partial_r G_{\theta\theta} - n^{\theta\pm}\partial_\theta G_{\theta\theta}) + \ \partial_\theta R(-n^{r\pm}\partial_\theta G_{rr} - n^{\theta\pm}\partial_r G_{\theta\theta}) \\ &\quad + \frac{(\partial_\theta R)^2}{2}(-n^{r\pm}\partial_r G_{rr} + n^{\theta\pm}\partial_\theta G_{rr}) \ , \end{aligned} \tag{4.3.3}$$

where $\alpha, \beta = t, x^1, ..., x^6, \phi$. This relation will be useful below when we calculate the stress–energy tensor along axially symmetric enhançon shells.

4.3.1 Toroidal enhançon

We will discuss the toroidal enhançon first (see figure 4.6). As observed before, the volume of K3 drops below $V_\star$ in the interior of the torus. In this region, the metric has the same form as given in equation (4.1.4), but we replace f_2 and f_6 with new harmonic functions, h_2 and h_6. The precise form of these functions will be determined by the consistency of the theory. After transforming the solution into Einstein frame by $G_{\mu\nu} = e^{-\Phi/2} g_{\mu\nu}$, we will use the axially symmetric extrinsic curvature (4.3.3) to determine the stress–energy tensor along the surface joining our two solutions.

There is a discontinuity in the extrinsic curvature across the junction defined by

$$\gamma_{AB} = K^+_{AB} + K^-_{AB} \ ,$$

and the stress–energy tensor supported at this junction is

$$S_{AB} = \frac{1}{\kappa^2}(\gamma_{AB} - G_{AB}\,\gamma^C_C) \ . \tag{4.3.4}$$

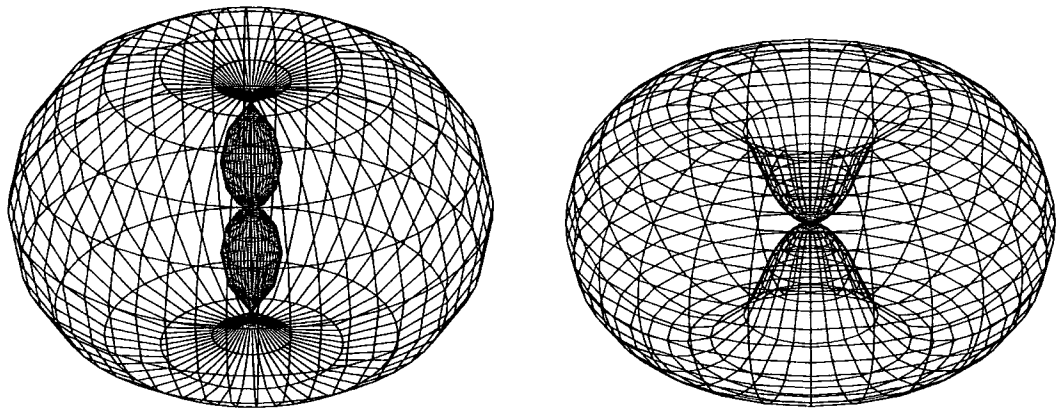

Figure 4.6: A three dimensional depiction of the connected enhançon locus, at $\ell = \ell_e^{cr}$ giving an example of the "double shell" shape (left), and $\ell > \ell_e^{cr}$ giving an example of the toroidal shape (right).

For our particular geometry, the stress–energy tensor can be computed to be:

$$\begin{aligned} S_{\mu\nu} &= \frac{\sigma}{2\kappa^2}(1+\partial_\theta R)\left(\frac{f_2'}{f_2}+\frac{f_6'}{f_6}-\frac{h_2'}{h_2}-\frac{h_6'}{h_6}\right) G_{\mu\nu}\ , \\ S_{ab} &= \frac{\sigma}{2\kappa^2}(1+\partial_\theta R)\left(\frac{f_6'}{f_6}-\frac{h_6'}{h_6}\right) G_{ab}\ , \\ S_{ij} &= 0\ , \end{aligned} \tag{4.3.5}$$

where σ has been defined in equation (4.3.1) and the prime denotes $\partial/\partial r$. The indices a and b run over the K3 directions (x^3, x^4, x^5, x^6), while parallel to the brane's unwrapped world–volume directions we have indices μ, ν which run over the (t, x^1, x^2). The transverse directions are labelled by indices (i, j).

As expected, the stress–energy tensor along the transverse directions vanishes, which is consistent with the BPS nature of the system's constituents. The tension of the discontinuity can be obtained from the components in the longitudinal directions. Recall from equation (4.2.11) that $(f_2 f_6)' = 0$ at the enhançon loci. For vanishing tension, then, looking at our result on the middle line of (4.3.5), we require that $(h_2 h_6)'$ vanishes at this radius as well. In addition to this constraint we should also demand $V(r,\theta) = V h_2/h_6 \geq V_\star$. If we wish to saturate the bound and assume h_2 and h_6 have a similar form to f_2 and f_6, the harmonic functions are in fact constant,

and a suitable solution is:

$$h_2 = 1 - \frac{(V - V_\star)}{2V} , \qquad h_6 = 1 + \frac{(V - V_\star)}{2V_\star} . \tag{4.3.6}$$

So we were able to successfully perform the task of cutting out the bad region contained within the toroidal enhançon and replacing it with flat space. It appears that we can have the resulting shell made of zero tension branes, as is in keeping with the intuition about the stringy fate of the constituent branes.

We must note that the "point" $r = 0$ is not entirely satisfactory. Indeed, we are justified in thinking of the entire geometry as that of a torus, since in the extended coordinates, this point is really a disc of radius ℓ. On the edge of this disc, as stated before, the asymptotic volume is ambiguous, but the value V seems to be the most physically consistent, as this is what it is in the disc's interior. There is no singularity on the disc's interior, and the volume is not at a special value. This means that there is no requirement to place physical branes there, and so the torus genuinely has a hole in the centre, and not just a single point.

We have ignored the fact that the form of the harmonic function in that region indicates that we might have a negative density of branes on the interior of the disc. We are free to ignore this, since there is no singularity there: the supergravity analysis tells us that we are free to place the zero tension distribution of branes over the whole toroidal surface instead. Of course, there is still the fact that there is repulsion along the symmetry axis as seen by a test particle moving in the geometry. Again, we stress that this behaviour has nothing to do with the wrapping: it is an artefact of the continuous brane distribution we started with. This would not occur for other branes, as we show in section 4.4.

4.3.2 Double and oblate enhançons

Now let us take the case $\ell < \ell_e^{cr}$, when the enhançon lies in two disconnected parts. In principle we have two choices what to do.

The first option is to simply cut out the entire region inside of the outer enhançon, and replace it by flat space. This gives a simple oblate enhançon shape. It is perfectly fine as a solution, and has the extra feature that it gives a case where wrapping

removes the entire disc located at $r = 0$. This means the enhançon mechanism would remove the negative tension branes which show up in the unwrapped distribution. In the event that the peculiarities associated to the ring at $r = 0$ turn out to be unacceptable, this is a satisfactory conservative choice. It is also the gentlest generalisation from the point of view of the dual moduli space of the gauge theory we shall discuss in section 4.5.

Alternatively we can also keep both the inner and the outer shell, and place flat space in between. This means that the ring is kept again, but then the same words that we used previously about the toroidal cases apply.[7]

Let us check the supergravity analysis if we opt for the second alternative. Recall the three regions defined on page 79. Region II represented the unphysical geometry where the tension of a brane probe becomes negative. It contains the repulson singularity. We can perform an incision as was done for the toroidal enhançon by defining h_2 and h_6 between the two enhançon shells as above in equation (4.3.6). The geometry of regions I and III is consistent and remains as it was in equation (4.1.4).

But we may also define the harmonic functions in the innermost region III to be

$$\tilde{f}_2 = 1 - \frac{r_6'}{r\Delta}\frac{V_\star}{V}\,, \qquad \tilde{f}_6 = 1 + \frac{r_6'}{r\Delta}\,, \tag{4.3.7}$$

where $r_6' \leq r_6$. Basically what this means is that some number $N' \leq N$ of wrapped D6–branes stay on the inner enhançon shell, while the rest reside on the outer enhançon shell. The former, being of total charge r_6', determine the geometry inside *via* the harmonic functions (4.3.7). Notice that the inner enhançon radius does also change because of this, it is still of the form (4.2.6), but now defined in terms of r_6'.

If we perform the excision, the stress–energy tensor for the outer shell is as in equation (4.3.5) where R is the outer enhançon radius. The inner shell has a stress

[7]There is an interesting possibility first raised by R. C Myers: Perhaps the interior region is an inverted copy of the exterior region. This would fit with the observation that at $r = 0$ the volume returns to the asymptotic value, V again. The inner enhançon would then be another copy of the outer one. It would also fit with the observation that there is a finite repulsion: it is in fact an attraction in this picture. While intriguing, the fact that we can connect to the $\ell > \ell^{\rm e}_{\rm cr}$ case may make this harder to justify. On the other hand, since ℓ is a parameter and not a physical quantity, it may be that we are free to explore this alternative.

energy tensor given by:

$$\begin{aligned} S_{\mu\nu} &= \frac{\sigma}{2\kappa^2}(1+\partial_\theta\tilde{R})\left(\frac{h_2'}{h_2}+\frac{h_6'}{h_6}-\frac{\tilde{f}_2'}{\tilde{f}_2}-\frac{\tilde{f}_6'}{\tilde{f}_6}\right) G_{\mu\nu}\ , \\ S_{ab} &= \frac{\sigma}{2\kappa^2}(1+\partial_\theta\tilde{R})\left(\frac{h_6'}{h_6}-\frac{\tilde{f}_6'}{\tilde{f}_6}\right) G_{ab}\ , \\ S_{ij} &= 0\ . \end{aligned} \tag{4.3.8}$$

where $\tilde{R}(\theta)$ is the inner enhançon radius set by r_6'. Again, the transverse stresses vanish and the tension vanishes at the inner enhançon shell. So, we see that we have constructed a geometry which is consistent with supergravity and excises the unphysical negative tension brane geometry resulting from wrapping.

How to make a double-shell

In the case of the double shell enhançon, one might wonder how such a geometry can be constructed. If we move in a wrapped D6–brane from infinity, it gets smeared around the outer enhançon shell. How to get the branes inside?

But remember, in section 2.7 we used n D2–D6 bound states to probe our geometry. As it turned out the presence of the bound D2–brane ensured that the volume of K3 did not drop below $V_\star$ and the bound state was able to pass through the outer enhançon shell and continue its journey down to the origin.

Once we get the bound state into the interior, region III, we can separate the D2–branes from the D6–branes since the K3 volume is greater than $V_\star$ there. The D6–branes have positive tension and hence are free to move about in the interior. If we attempt to move a D6–brane out of region III, the volume of K3 approaches $V_\star$ as the brane nears the inner enhançon shell. The D6–brane becomes tensionless at the inner enhançon and melts into the shell, as happens for brane approaching the outer shell from outside. Hence, D2-D6 bound states can be used to move D6–branes into the interior and to add D6 branes to the inner enhançon shell. It is easy to imagine building the double shell enhançon geometry in this fashion, starting with widely separated D2– and D6–branes, and then removing the D2–branes after the construction.

4.4 Wrapping other D–brane distributions

We focussed on D6–branes almost exclusively, but it should be clear that many of the characteristic features that we have seen, are also present for wrapping D4– and D5– branes. In fact, we ought to stress again here that the problematic feature of the negative brane density and its repulsive potential are not generic. (We have already seen that the disc brane distributions for all of the other branes have positive densities everywhere.)

The feature of having multiple solutions for the enhançon locus will occur also. In fact, it will give up to *three* solutions for the D4–brane's enhançon loci, but only one for the D5–brane. This is because the harmonic functions will be of the form:

$$f = 1 + \frac{r_p^{7-p}}{r^{7-p}\,(1 + (\ell^2/r^2)\cos^2\theta)} \ . \tag{4.4.1}$$

for $p = 4, 5$ and one non–zero parameter $\ell_1 = \ell$. The equation determining the enhançon loci is of the form of equating a ratio of two of these f's to a constant, $V_\star/V$ which gives a quadratic equation in the case of the D6–brane, as we have seen, but only a linear equation for D5–branes. The D4–brane case will give a cubic equation.

4.4.1 Unwrapped D5–brane distributions

Actually, it is worth looking briefly a bit more at the D5–brane case, keeping non–zero both of the parameters, ℓ_1, ℓ_2, that we can have with four transverse directions. Taking the extremal limit of the rotating black D5–brane solution[8] given in [169] we get for our unwrapped solution:

$$\begin{aligned} ds^2 &= f_5^{-1/2}\Big(-dt^2 + \sum_{i=1}^{5} dx_i^2\Big) \\ &\quad + f_5^{1/2}\Big(\frac{\Delta_{12}}{\Xi_1\Xi_2}dr^2 + \Delta_{12}r^2 d\theta^2 + \Xi_1 r^2\sin^2\phi_1 + \Xi_1 r^2\cos^2\phi_2\Big)\ , \\ e^{2\Phi} &= f_5^{-1}\ , \\ C^{(6)} &= f_5^{-1} dt\wedge dx_1\wedge\ldots\wedge dx_5\ , \end{aligned} \tag{4.4.2}$$

[8] Alternatively we could have used S-duality with rotating NS5–branes [172].

where

$$f_5 = 1 + \frac{r_5^2}{r^2 \Delta_{12}} \ , \tag{4.4.3}$$

and

$$\Delta_{12} = 1 + \frac{\ell_1^2}{r^2}\cos^2\theta + \frac{\ell_2^2}{r^2}\sin^2\theta \ , \qquad \Xi_1 = 1 + \frac{\ell_1^2}{r^2} \ , \qquad \Xi_2 = 1 + \frac{\ell_2^2}{r^2} \ . \tag{4.4.4}$$

The extended coordinates are given by:

$$\begin{aligned} y_1 &= \sqrt{r^2 + \ell_1^2}\sin\theta\cos\phi_1 \ , \qquad y_2 = \sqrt{r^2 + \ell_1^2}\sin\theta\sin\phi_1 \ , \\ y_3 &= \sqrt{r^2 + \ell_2^2}\cos\theta\cos\phi_2 \ , \qquad y_4 = \sqrt{r^2 + \ell_2^2}\cos\theta\sin\phi_2 \ . \end{aligned} \tag{4.4.5}$$

Considering the case $\ell_1 = \ell, \ell_2 = 0$ will give the ring density mentioned previously.

Let us consider particle probes of the geometry. Previously we associated repulsive gravitational features of the D6–brane distribution with a negative brane density on the disc. The D5–brane distribution did not have negative brane density, and indeed, does not show these repulsive features. In this case the transverse space–time has one more dimension, but it is also endowed with one additional Killing vector related to the ϕ_2 coordinate. Therefore an analysis similar to the one set forth in section 4.1.6 shows that test particle motion in $\theta = 0$ and $\theta = \pi/2$ directions is governed by the same effective potential as given in equation (4.1.24). In fact, the effective potential in the $\theta = 0$ direction does depend only on ℓ_1 and in the $\theta = \pi/2$ direction only on ℓ_2, while the form of dependence is identical. As figure 4.7 shows, the repulsive gravitational features are completely absent.

4.4.2 Wrapped D5–brane distributions

Wrapping the D5–brane configuration (4.4.2) on K3 yields (see also table 4.4.2)

$$\begin{aligned} ds^2 &= f_5^{-1/2} f_1^{-1/2}\big(-dt^2 + dx^2\big) + f_5^{-1/2} f_1^{1/2} V ds_{K3}^2 \\ &\quad + f_5^{1/2} f_1^{1/2}\Big(\frac{\Delta_{12}}{\Xi_1\Xi_2}dr^2 + \Delta_{12} r^2 d\theta^2 + \Xi_1 r^2\sin^2\phi_1 + \Xi_1 r^2\cos^2\phi_2\Big) \ , \\ e^{2\Phi} &= f_1 f_5^{-1} \ , \\ C^{(6)} &= f_5^{-1} dt \wedge dx \wedge V ds_{K3} \ , \\ C^{(2)} &= f_1^{-1} dt \ , \wedge dx \end{aligned} \tag{4.4.6}$$

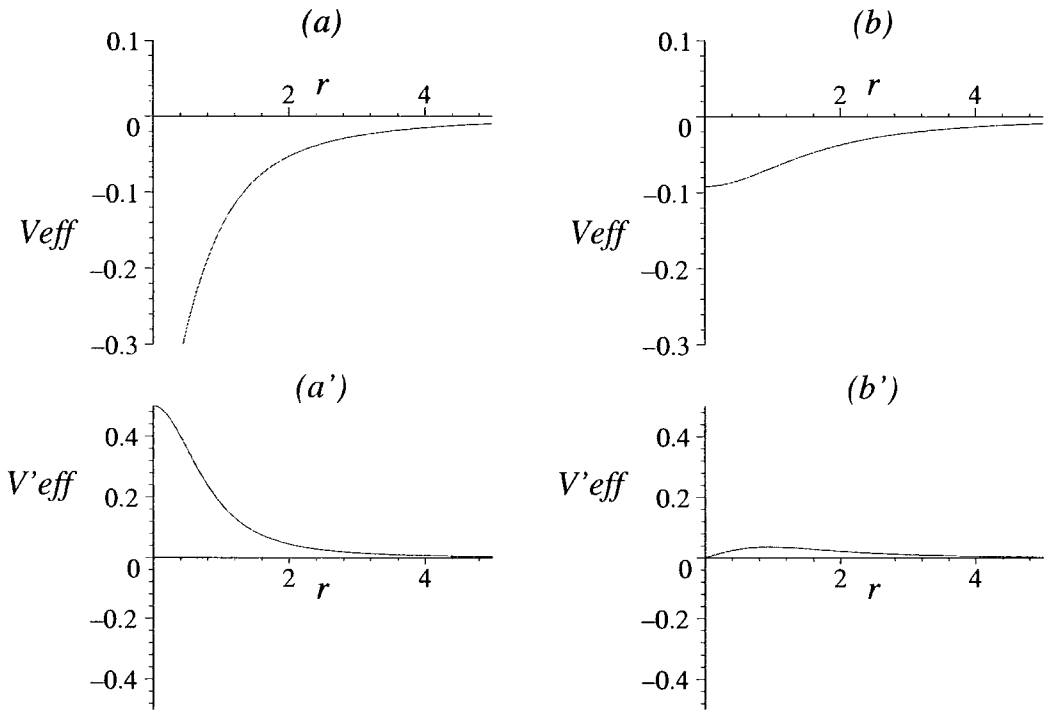

Figure 4.7: Gravitational features of the distributed D5–brane solution as seen by a neutral test particle. Test particle effective potential (top) and its derivative (bottom) along the $\theta = 0$ ($\theta = \pi/2$) direction corresponding to *(a)* $\ell_1 = 0$ ($\ell_2 = 0$), *(b)* $\ell_1 > 0$ ($\ell_2 > 0$). The potential is always attractive for a particle moving in from the infinity.

where

$$f_5 = 1 + \frac{r_5^2}{r^2\Delta_{12}}\,, \qquad f_1 = 1 - \frac{r_1^2}{r^2\Delta_{12}}\,, \qquad r_1^2 = \frac{V_\star}{V} r_5^2\,, \tag{4.4.7}$$

and Δ_{12}, Ξ_1, Ξ_2, *etc.*, defined as before. There is a repulson singularity at

$$r_{\rm r} = \sqrt{\frac{r_5^2 V_\star}{V}\Big(1 - \frac{V}{r_5^2 V_\star}(\ell_1^2\cos^2\theta + \ell_2^2\sin^2\theta)\Big)}\,,$$

where the running volume of K3 shrinks to zero. Interestingly, the singularity disappears completely when both parameters ℓ_1 and ℓ_2 exceed the critical value

$$\ell_{\rm r}^{\rm cr} = \sqrt{\frac{r_5^2 V_\star}{V}}\,.$$

The singularity is always surrounded by the enhançon shell at

$$r_{\rm e} = \sqrt{\frac{2r_5^2 V_\star}{V - V_\star}\Big(1 - \frac{V - V_\star}{2r_5^2 V_\star}(\ell_1^2\cos^2\theta + \ell_2^2\sin^2\theta)\Big)}\,.$$

Depending on the values of ℓ_1 and ℓ_2, this enhançon assumes various shapes, but is always connected. Again, it is interesting that when both parameters ℓ_1 and ℓ_2

	$\mathbb{R}^{5,1}$						K3			
	x_0	x_1	x_2	x_3	x_4	x_5	x_6	x_7	x_8	x_9
D5	–	–	*	*	*	*	–	–	–	–
D1	–	–	*	*	*	*	∼	∼	∼	∼

Table 4.2: A sketch of a D5–brane distribution wrapped on K3 and the induced negative D1–branes. The branes' world-volume directions are marked by "–", while "∼" indicates that the induced D1–branes are delocalised on K3. In the transverse directions the branes form a distribution, symbolised by "*".

exceed the critical value

$$\ell_{\rm e}^{\rm cr} = \sqrt{\frac{2r_5^2 V_\star}{V - V_\star}} \ ,$$

the enhançon disappears completely. See figure 4.8 for a series of snapshots. It is important to note that the following result is true

$$\frac{\partial}{\partial r}\Big(f_5 f_1\Big)\Big|_{r=r_{\rm e}} = 0 \ . \tag{4.4.8}$$

It is this that will ensure that the supergravity matching computation will go through in a similar manner as in the D6–brane distribution case of the previous section, and as in the spherical D5–brane case studied in [90].

Let us consider particle probes again, in order to check where the repulsive regions are. In contrast to the D6–brane case, we do not expect any repulsive features to arise which are not attributable to the wrapping. The presence of the repulson singularity is signalled by a singularity in the effective potential occurring at $r_{\rm r}$. This is surrounded by the enhançon shell, residing precisely at the minimum of the potential, *i.e.*, where the repulsive region starts. (See figure 4.9.) There is still some residual finite repulsion even after ℓ_1 (ℓ_2) exceeds $\ell_{\rm r}^{\rm cr}$ and the repulson singularity disappears (figure 4.9*(c)*). Beyond $\ell_1 > \ell_{\rm e}^{\rm cr}$ ($\ell_2 > \ell_{\rm r}^{\rm cr}$) the effective potential becomes completely attractive with a minimum at the origin $r = 0$.

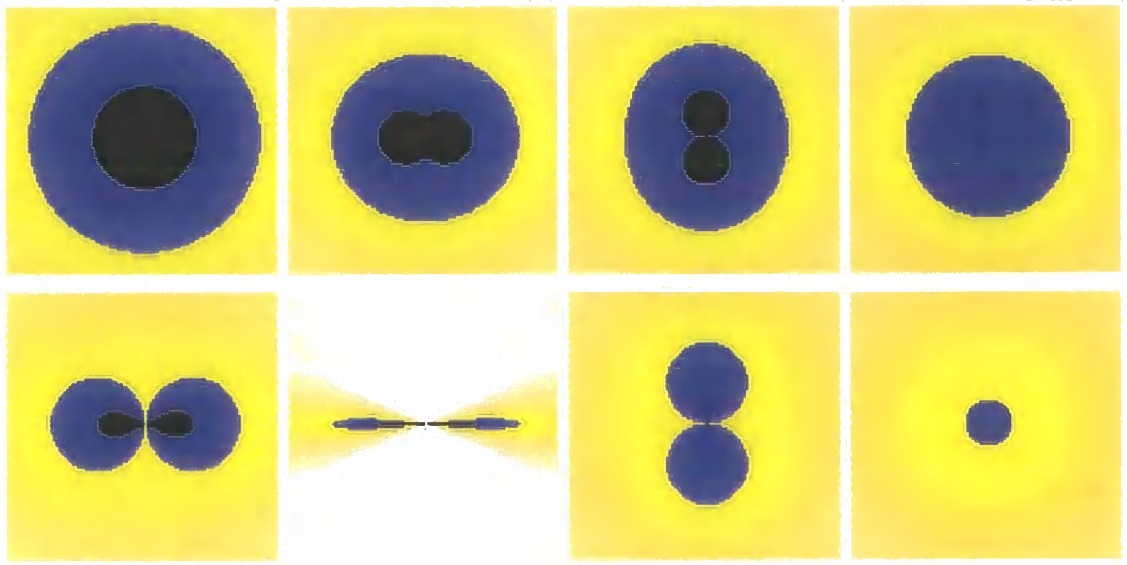

Figure 4.8: Some two–dimensional slices through the non–spherical wrapped D5–brane geometry before excision. $\theta = 0$ corresponds to the vertical direction and $\theta = \pm\pi/2$ to the horizontal. The configuration is symmetric in ϕ_1 and ϕ_2 (not shown on the figure). The colour coding is as in figure 4.3. The shapes vary for different values of the parameters ℓ_1 and ℓ_2: $\ell_1 = \ell_2 = 0$ (top, left), $\ell_1 = \frac{7}{8}\ell_r^{cr}$, $\ell_2 = 0$ (top, second), $\ell_1 = 0$, $\ell_2 = \ell_r^{cr}$ (top, third), $\ell_1 = \ell_2 = \ell_r^{cr}$ (top, right), $\ell_1 = \ell_e^{cr}$, $\ell_2 = 0$ (bottom, left) $\ell_1 = 8\ell_e^{cr}$, $\ell_2 = 0$ (bottom, second) $\ell_1 = \ell_r^{cr}$, $\ell_2 = \ell_e^{cr}$ (bottom, third) $\ell_1 = \ell_2 = \ell_e^{cr} - \frac{1}{16}(\ell_e^{cr} - \ell_r^{cr})$ (bottom, right).

4.5 Gauge theory results

As we should be accustomed to expect already, some of our results pertain to gauge theory. Wrapping the D6–branes on the K3 gives an $\mathcal{N} = 4$ $(2+1)$–dimensional gauge theory with the gauge coupling

$$g_{YM}^2 = (2\pi)^4 g_s \alpha'^{3/2} V^{-1} .$$

One of the results we extracted from the analysis of the spherical case is the piece of the gauge theory moduli space corresponding to the movement of a single wrapped probe, equation (2.6.12). In gauge theory, this is the metric derived from the kinetic terms in the low energy effective action for the field breaking $SU(N) \to SU(N-1) \times U(1)$. The probe computation yields the tree level and one–loop contribution to this result, and there are no perturbative corrections.

In the present case, we should be able to see new physics, since the parameter ℓ should have some meaning in the gauge theory. In fact, we expect that it should

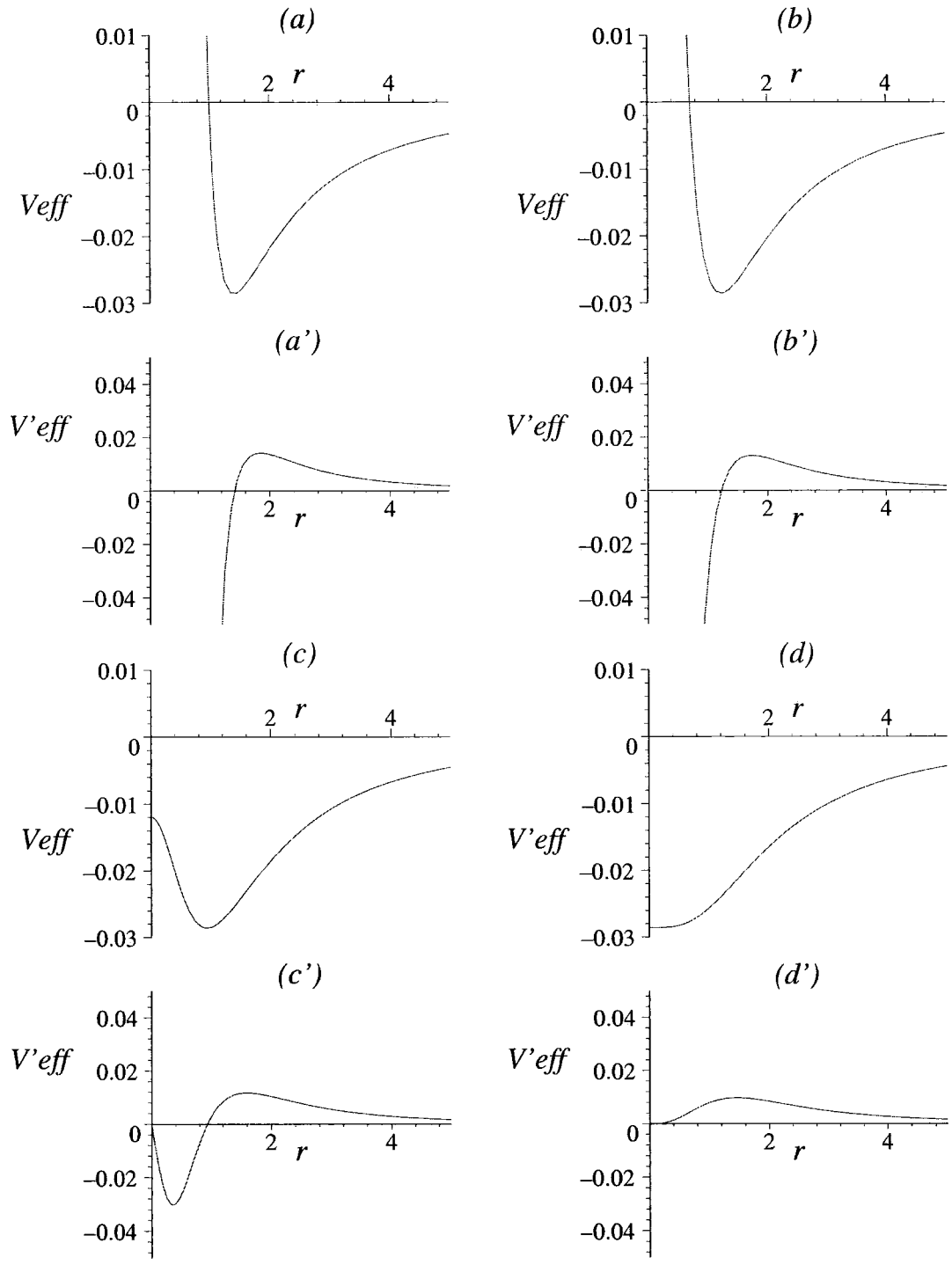

Figure 4.9: Gravitational features of the distributed D5–brane solution wrapped on K3 as seen by a neutral test particle. Test particle effective potential V_{eff} and its derivative V'_{eff} along the $\theta = 0$ ($\theta = \pi/2$) direction corresponding to *(a)* $\ell_1 = 0$ ($\ell_2 = 0$), *(b)* $\ell_1 = \ell_{\rm r}^{\rm cr}$ ($\ell_2 = \ell_{\rm r}^{\rm cr}$), *(c)* $\ell_1 = \ell_{\rm r}^{\rm cr} + \frac{1}{2}(\ell_{\rm e}^{\rm cr} - \ell_{\rm r}^{\rm cr})$, ($\ell_2 = \ell_{\rm r}^{\rm cr} + \frac{1}{2}(\ell_{\rm e}^{\rm cr} - \ell_{\rm r}^{\rm cr})$), *(d)* $\ell_1 = \ell_{\rm e}^{\rm cr}$ ($\ell_1 = \ell_{\rm e}^{\rm cr}$). Effective potential is singular (exhibiting infinite repulson) at $r_{\rm r}$ and has a minimum at $r_{\rm e}$.

be controlling the vacuum expectation value of an operator made by the symmetric product of the adjoint scalars, by analogy with the case in the AdS/CFT [50–52] context. Here, the R–symmetry is $SU(2) \simeq SO(3)$. The three adjoint scalars in the gauge multiplet, transforming as the **3**, can be combined by symmetric product. The R–charge of the resulting operator is computed in the usual way. For example, $\mathbf{3} \times \mathbf{3} = \mathbf{1} + \mathbf{5} + \mathbf{3}$, where the **5** is the symmetric traceless part. This is of course more familiar as the $j = 2$ case in the standard angular momentum notation where the irreducible representations of the R–symmetry group are written as $2j+1$ dimensional. We should see some sign of this show up here, and indeed we do.

4.5.1 Metric on the moduli Space

We probe the repaired geometry with a single wrapped D6–brane in order to extract the data of interest. After including the $U(1)$ world–volume gauge sector into the probe calculation and dualising the gauge field to get the extra periodic scalar (as in section 2.6), the kinetic term of the effective action in the non–flat regions becomes

$$T = h(r,\theta)\left(\frac{\Delta}{\Xi}\dot{r}^2 + \Delta r^2\dot{\theta}^2 + \Xi r^2\sin^2\theta\,\dot{\phi}^2\right) + h(r,\theta)^{-1}\left(\dot{s}/2 - \mu_2 C_\phi\dot{\phi}/2\right)^2 . \tag{4.5.1}$$

where $h(r,\theta)$ is defined by

$$h(r,\theta) = \frac{\mu_6}{2}\left(V f_2 - V_\star f_6\right) \tag{4.5.2}$$

and C_ϕ is the magnetic potential corresponding to the D6–brane charge

$$C_\phi = -r_6\,\frac{\Xi}{\Delta}\cos\theta\ . \tag{4.5.3}$$

To extract the gauge theory we work with variables

$$U = \frac{r}{\alpha'}\ , \quad a = \frac{\ell}{\alpha'}\ ,$$

and take the decoupling limit by taking $\alpha' \to 0$ while holding U, a, and g^2_{YM} fixed. The metric becomes:

$$ds^2 = h(U,\theta)\left(\frac{\Delta'}{\Xi'}dU^2 + \Delta' U^2\,d\theta^2 + \Xi' U^2\sin^2\theta\,d\phi^2\right) + h(U,\theta)^{-1}\left(d\sigma - \frac{N}{8\pi^2}A_\phi d\phi\right)^2 , \tag{4.5.4}$$

with

$$h(U,\theta) = \frac{1}{8\pi^2 g_{YM}^2}\left(1 - \frac{g_{YM}^2 N}{U\Delta'}\right) . \tag{4.5.5}$$

Here we have defined

$$\Delta' = 1 + \frac{a^2}{U^2}\cos^2\theta , \quad \Xi' = 1 + \frac{a^2}{U^2} , \tag{4.5.6}$$

and

$$\sigma = \frac{s\alpha'}{2} , \quad A_\phi = -\frac{1}{2}\frac{\Xi'}{\Delta'}\cos\theta . \tag{4.5.7}$$

This might not seem terribly inspiring, but recall that we can work in the "extended" coordinate system given by the obvious generalisation of equation (4.1.6):

$$\begin{aligned} W_1 &= \sqrt{U^2 + a^2}\,\sin\theta\,\cos\phi \\ W_2 &= \sqrt{U^2 + a^2}\,\sin\theta\,\sin\phi \\ W_3 &= U\,\cos\theta. \end{aligned} \tag{4.5.8}$$

In terms of these, our moduli space result is the standard Taub–NUT form

$$ds^2 = H(W,\hat{\theta})\,\left(d\vec{W}\cdot d\vec{W}\right) + H(W,\hat{\theta})^{-1}\left(d\sigma - \frac{N}{8\pi^2}A_\phi d\phi\right)^2 , \tag{4.5.9}$$

with

$$H(W,\hat{\theta}) = \frac{1}{8\pi^2 g_{YM}^2}\left(1 - \frac{g_{YM}^2 N\sqrt{\Lambda+\Sigma}}{\sqrt{2}\Sigma}\right) . \tag{4.5.10}$$

where

$$\Sigma = \sqrt{\Lambda^2 + 4a^2 W_3^2}, \qquad \Lambda = W^2 - a^2, \qquad W = \sqrt{W_1^2 + W_2^2 + W_3^2} . \tag{4.5.11}$$

The content is in the harmonic function, and we can expand it for large W using our earlier observations in equations (4.1.20):

$$H = \frac{1}{8\pi^2 g_{YM}^2}\left(1 - \frac{g_{YM}^2 N}{W}\sum_{n=0}^{\infty}(-1)^n\left(\frac{a}{W}\right)^{2n} P_{2n}(\cos\hat{\theta})\right) , \tag{4.5.12}$$

where we have defined new polar coordinate angles in an analogous manner to that shown in equation (4.1.21), and the $P_{2n}(x)$ are the Legendre polynomials in x, as before (see equation (4.1.22)).

The leading terms in this large W expansion should have an interpretation as the contribution of the operators which are switched on. The $n = 0$ result is that of the

spherical. The case $n = 1$ comes with the Legendre polynomial $P_2(\cos\hat{\theta})$, which has the R–charge of the **5**, the simplest operator one can make out the adjoint scalars. So the parameter ℓ, (*i.e.a*) controls the vacuum expectation value of this operator, with subleading contributions coming from the higher spherical harmonics.

Notice that this expansion is not sensitive to some of choices that we can make in doing the excision. In particular, while it works for any ℓ, it is for large y. So from the point of view of this expansion, all of the choices are equivalent to the excisions which give a single locus: For $\ell < \ell_{\rm e}^{\rm cr}$, this is the oblate enhançon with flat space inside, while for $\ell > \ell_{\rm e}^{\rm cr}$, it is the toroidal shape. The difference between the two is presumably non–perturbative in the operator expansion. It would be interesting to find gauge theory meaning for cases where we can choose to have a double shell.

4.6 Prolate enhançon

In the preceding discussion about oblate and toroidal enhançons we assumed the parameter ℓ^2 is positive, as ℓ was related to the angular momentum of the original rotating configuration, obviously a real quantity. But in the extremal solution ℓ enters in a squared form only. So let us now complement the analysis by considering the case of negative ℓ^2 which has no non-extremal rotating counterpart.

4.6.1 Unrapped prolate D6–brane distributions

The static (extremal) distribution of D6–branes is still be described by the solution (4.1.4)

$$\begin{aligned} ds^2 &= f_6^{-1/2}\Big(-dt^2 + \sum_{i=1}^{6} dx_i^2\Big) + f_6^{1/2}\Big(\frac{\Delta}{\Xi}\, dr^2 + \Delta r^2\, d\theta^2 + \Xi r^2 \sin^2\theta\, d\phi^2\Big)\,, \\ e^{2\Phi} &= f_6^{-3/2}, \\ C^{(7)} &= f_6^{-1} dt \wedge dx_1 \wedge \ldots \wedge dx_6\,, \end{aligned} \tag{4.6.1}$$

where

$$f_6 = 1 + \frac{r_6}{\Delta r}, \qquad \Delta = 1 + \frac{\ell^2}{r^2}\cos^2\theta\,, \qquad \Xi = 1 + \frac{\ell^2}{r^2}\,.$$

But now suppose $\ell^2 \leq 0$ and define $\tilde{\ell}^2 = -\ell^2$.

In this case the metric (4.6.1) has two singularities. One occurs where the harmonic function f_6 is zero, at

$$r_{s_6} = \frac{r_6}{2}\left(-1+\sqrt{1+\frac{4}{r_6^2}\,\tilde{\ell}^2\cos^2\theta}\right), \tag{4.6.2}$$

and another where f_6 is singular, at

$$r_s = \tilde{\ell}\,|\cos\theta|. \tag{4.6.3}$$

Between these radii f_6 is negative and the metric does not exist. This is also witnessed by the curvature invariants which blow up at r_{s_6} and r_s. (The situation may be contrasted with the oblate case which had only one singularity at $r = 0, \theta = \pi/2$.) The outer singularity at r_s is not naked, but surrounded by a spherical horizon at

$$r_h = \tilde{\ell}. \tag{4.6.4}$$

The effect of the horizon is that inside the inner singularity at r_{s_6} the metric components $g_{\theta\theta}$ and $g_{\phi\phi}$ have reversed their sign, but g_{rr} has the same sign as before. There is also an ambiguity of what happens at the origin, since the value of f_6 at $r = 0$ depends on the azimuthal angle of approach, if we approach along $\theta = \frac{\pi}{2}$, then $f_6 \to \infty$, otherwise $f_6 \to 0$.

"Contracted" coordinates

As we observed while studying the oblate configurations, there is another system of coordinates, which helps to give a better understanding of the distribution of branes in the solution. But instead of "extended" we may call these new coordinates

$$\begin{aligned} y_1 &= \sqrt{r^2-\tilde{\ell}^2}\,\sin\theta\,\cos\phi\,, \\ y_2 &= \sqrt{r^2-\tilde{\ell}^2}\,\sin\theta\,\sin\phi\,, \\ y_3 &= r\,\cos\theta \end{aligned} \tag{4.6.5}$$

"contracted", since they do not cover the whole of the previous space-time. Notice that the spherical horizon $r_h = \tilde{\ell}$ is mapped to a line $y_1 = y_2 = 0$, $y_3 = \pm\tilde{\ell}\,\cos\theta$, and everything that remained inside the horizon gets cut out from the new space-time.

Despite this the metric reduces to a standard brane form

$$ds^2 = F_6^{-1/2}\Big(- dt^2 + \sum_{i=1}^{6} dx_i^2\Big) + F_6^{1/2}\Big(dy_1^2 + dy_2^2 + dy_3^2\Big) \ , \tag{4.6.6}$$

where the harmonic function is given by

$$F_6 = 1 + \frac{r_6\sqrt{\Lambda + \Sigma}}{\sqrt{2}\Sigma} \ , \tag{4.6.7}$$

and

$$\Sigma = \sqrt{\Lambda^2 - 4\tilde{\ell}^2 y_3^2} \ , \qquad \Lambda = y^2 + \tilde{\ell}^2 \ , \qquad y = \sqrt{y_1^2 + y_2^2 + y_3^2} \ . \tag{4.6.8}$$

Brane density

The harmonic function F_6 has singularities at $y_1 = y_2 = 0$, $y_3 = \pm\tilde{\ell}$, suggesting a hint about where the branes are located in this configuration. Indeed, assumption that the branes are equally distributed at these two points,

$$\sigma(y) = \frac{r_6}{2}\delta(y_1)\delta(y_2)\delta(y_3 - \tilde{\ell}) + \frac{r_6}{2}\delta(y_1)\delta(y_2)\delta(y_3 + \tilde{\ell}) \ , \tag{4.6.9}$$

correctly reproduces the harmonic function F_6 along the y_3-axis

$$F_6(y_3) = 1 + \int \frac{\sigma(y')}{|y - y'|}\, dy' = 1 + \frac{r_6}{2}\left(\frac{1}{y_3 - \tilde{\ell}} + \frac{1}{y_3 + \tilde{\ell}}\right) = 1 + \frac{r_6 y_3}{y_3^2 + \tilde{\ell}^2}. \tag{4.6.10}$$

(And symmetry accompanied with harmonic analysis takes care that F_6 is correctly reproduced everywhere.) There is no horizon present in the "contracted" coordinates and probing with a massive test particle does not reveal any anomalous gravitationally repulsive regions.

4.6.2 Wrapped prolate D6–brane distributions

Wrapping this D6-brane configuration (4.1.4) on K3 yields the following metric (as we know already)

$$\begin{aligned} ds^2 \ = \ & f_2^{-1/2} f_6^{-1/2}(-dt^2 + dx_1^2 + dx_2^2) + f_2^{1/2} f_6^{1/2}\left(\frac{\Delta}{\Xi}\, dr^2 + \Delta r^2\, d\theta^2 + \Xi\, r^2 \sin^2\theta\, d\phi^2\right) \\ & + V^{1/2} f_2^{1/2} f_6^{-1/2} ds_{K3}^2 \end{aligned} \tag{4.6.11}$$

with

$$f_2 = 1 - \frac{r_6 V_\star}{V\Delta r} \ , \quad f_6 = 1 + \frac{r_6}{\Delta r} \ , \tag{4.6.12}$$

and all the definitions as stated before.

In the previous section we saw that the harmonic function f_6 vanished at r_{s_6} and became singular at r_s. The other harmonic function f_2 becomes singular at

$$r_s = \tilde{\ell}\,|\cos\theta| \tag{4.6.13}$$

and vanishes at

$$r_{s_2} = \frac{r_6 V_\star}{2\,V}\left(-1+\sqrt{1+\left(\frac{2\,V}{r_6 V_\star}\right)^2 \tilde{\ell}^2\cos^2\theta}\right). \tag{4.6.14}$$

The metric does not exist between r_{s_6} and r_{s_2}, since either f_6 or f_2 is negative in this region. (The would-be singular radius r_s lies in between of r_{s_6} and r_{s_2}, while $r_{s_6} \leq r_{s_2}$.) Examination of curvature invariants shows that at r_{s_6} and r_{s_2} we do have true curvature singularities. Notice here a basic difference from the oblate configuration — before we had two singularities due the behaviour of f_2, but now only one singularity comes about due to f_2, the other is caused by f_6.

Hoping that the enhançon mechanism can cure the presence of these singularities, let us probe the configuration with a single wrapped D6-brane, or equivalently, study the behaviour of the K3 volume

$$V(r) = V\frac{f_2}{f_6}\,. \tag{4.6.15}$$

At spatial infinity the volume $V(r)$ has a constant value V, and it starts to shrink as one moves in towards the origin. The volume reaches the special value $V_\star$ at

$$r_e = \frac{r_6 V_\star}{V-V_\star}\left(1+\sqrt{1+\left(\frac{V-V_\star}{r_6 V_\star}\right)^2 \tilde{\ell}^2\cos^2\theta}\right), \tag{4.6.16}$$

and vanishes completely at r_{s_2}, a point where the metric ceases to exist. We may still keep trace of the function $V(r)$ and see how it keeps decreasing until r_{s_6}, where it reaches a negative singularity. At this point a change in the sign occurs and so inside r_{s_6} the volume becomes suddenly positive again. It is infinite at r_{s_6} and drops continuously to V at the origin. Again there is an ambiguity at $r = 0$, since $V(r) \to -V_\star$ as one approaches along the equatorial plane $\theta = \frac{\pi}{2}$, but $V(r) \to V$ along other directions.

As in the unwrapped case there is also a horizon at $r_h = \tilde{\ell}$. This makes matters different from what we saw in the family of oblate configurations. First of all

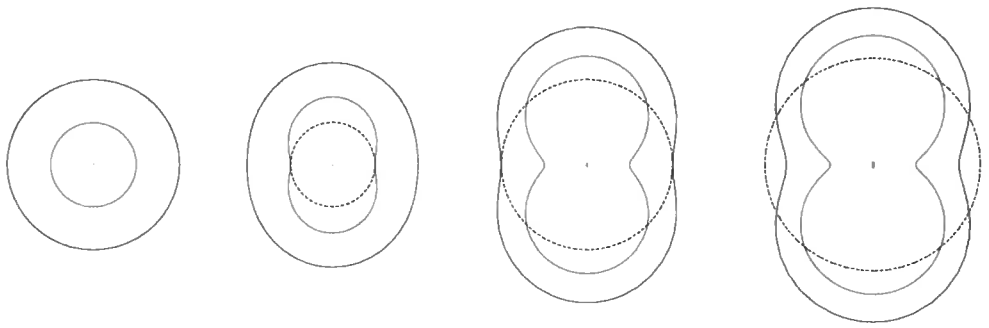

Figure 4.10: A series of slices through the untreated wrapped D6–brane geometry. The singularity (inner solid line, red) is surrounded by the enhançon shell (outer solid line, blue). There is also a horizon present (denoted by the dotted black line), see discussion in the body of the text. The case $\tilde{\ell} = 0$ gives a spherical enhançon, and as $\tilde{\ell}$ increases, the enhançon shell takes an increasingly prolate shape. This pattern can be seen for the following values of $\tilde{\ell}$: $\tilde{\ell} = 0$ (left), $\tilde{\ell} = 2\ \tilde{\ell}_{\rm r}^{\rm cr}$, $\tilde{\ell} = 2\ \tilde{\ell}_{\rm e}^{\rm cr}$, $\tilde{\ell} = 2.5\ \tilde{\ell}_{\rm e}^{\rm cr}$ (right).

$r_h \geq r_{s_6}$ with equality only at the polar points ($\theta = 0$). However, concerning the other singularity r_{s_2}, we seem to have a possibility that the horizon and singularity intersect. If

$$\tilde{\ell} < \frac{r_6 V_\star}{V} = 2\tilde{\ell}_r^{cr} \tag{4.6.17}$$

the singularity is completely naked (from outside). But if $\tilde{\ell}$ is greater than the value above, then the singularity gets partially covered by the horizon, although never fully, since along the axis $\theta = 0$ it is always true that $r_h < r_{s_2}$. Similarly, if

$$\tilde{\ell} < \frac{2r_6 V_\star}{V - V_\star} = 2\tilde{\ell}_e^{cr} \tag{4.6.18}$$

the horizon stays completely inside the enhançon shell, otherwise they will intersect along some θ. As both singularities are safely surrounded by the enhançon and we expect to replace this geometry with a new one, having a singularity intersecting with a horizon can be considered just a mathematical artefact. But how to understand the situation when part of the enhançon shell is covered by the horizon? Let us consider again the probe calculation. To obtain the effective lagrangian of the probe, equation (4.2.8), we assumed that the probe velocity

$$v^2 = \left(\frac{\Delta}{\Xi}\, \dot{r}^2 + \Delta r^2\, \dot{\theta}^2 + \Xi\, r^2 \sin^2\theta\, \dot{\phi}^2 \right) \tag{4.6.19}$$

was small. But at r_h the coefficient in front of $\dot{r}^2$ becomes singular, hence the assumption of slow motion can not hold any more. Therefore to study the enhançon shapes corresponding to the values of parameter $\tilde{\ell}$ beyond the critical value $2\tilde{\ell}_e^{cr}$ we can not rely on the probe results obtained in the slow motion approximation. The situation is summarized in figure 4.10.

In "contracted" coordinates

Fortunately this rather confusing picture gets clarified, when we transform the solution into "contracted" coordinates (4.6.5) where the metric simplifies to

$$\begin{aligned} ds^2 &= F_6^{-1/2}F_2^{-1/2}\Big(-dt^2+dx_1^2\Big)+F_6^{1/2}F_2^{1/2}\Big(dy_1^2+dy_2^2+dy_3^2\Big)+ \\ &\quad +V^{1/2}F_6^{-1/2}F_2^{1/2}ds_{K3}^2 \end{aligned} \tag{4.6.20}$$

with

$$F_2 = 1-\frac{r_6 V_\star\sqrt{\Lambda+\Sigma}}{\sqrt{2}V\Sigma}. \tag{4.6.21}$$

As noted before, everything up to and including the horizon at r_h gets cut out in these coordinates. The whole of the interior region with $V(r) > V$ and the inner singularity at r_{s_2} will not be present in the "contracted" coordinates. Only the outer singularity surrounded by the enhançon shell is mapped to the new space-time.

The critical values of the parameter $\tilde{\ell}$ also gain a specific meaning. First, when $\tilde{\ell}=0$ we have a spherical enhançon shell surrounding a spherical singularity, inside which the metric does not exist. As $\tilde{\ell}$ increases, the configuration turns into a more and more prolate shape. Further, at $\tilde{\ell}=2\tilde{\ell}_s^{cr}$ the singular region gets disconnected into two separate pieces, one above and the other below the $y_1=y_2=0$ plane. The same happens to the enhançon shell, which gets disconnected at $\tilde{\ell}=2\tilde{\ell}_e^{cr}$. (Notice that the breaking of the enhançon shell into two pieces corresponds to the enhançon intersecting with the horizon in the original coordinates.) As $\tilde{\ell}$ increases these shells keep moving apart, but will never disappear completely. See figure 4.11.

4.6.3 Discussion

Let us stop for a while and follow how the enhançon shape changes as the parameter ℓ^2 takes a whole range of values from negative to positive. A curious pattern emerges

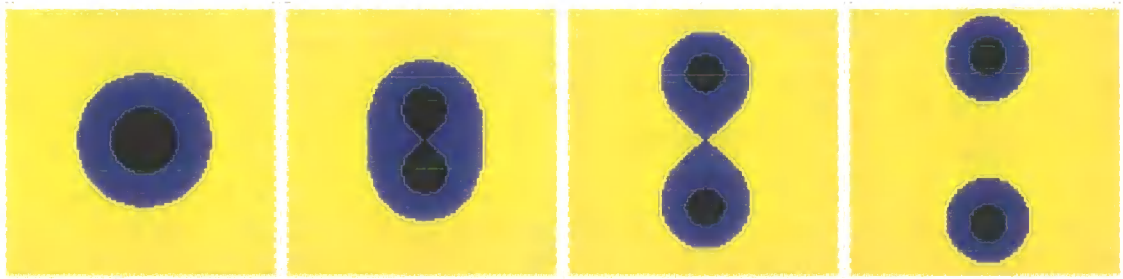

Figure 4.11: A slice through the untreated wrapped D6–brane geometry in "contracted" coordinates. The colour coding is the same as in our paper. The case $\tilde{\ell} = 0$ gives a spherical enhançon. As $\tilde{\ell}$ increases, the enhançon shell takes an increasingly prolate shape, until it gets disconnected into two pieces. This pattern can be seen for the following values of $\tilde{\ell}$: $\tilde{\ell} = 0$ (left), $\tilde{\ell} = 2\ \tilde{\ell}_{\rm r}^{\rm cr}$, $\tilde{\ell} = 2\ \tilde{\ell}_{\rm e}^{\rm cr}$, $\tilde{\ell} = 2.5\ \tilde{\ell}_{\rm e}^{\rm cr}$ (right).

when viewed in "contracted"-"extended" coordinates, *i.e.* by putting together figures 4.11 and 4.4. At ℓ^2 very large and negative we have two almost particle-like enhançon shells approaching each other along the z axis. Getting closer as ℓ^2 approaches zero from below they change their shape, touch each other and merge into a spherical configuration for $\ell = 0$. If we change ℓ^2 further into positive values the spherical shell turns into an oblate shape while at the same time there appears an increasing cavity at the centre. Soon this cavity breaks open turning the shell into a toroidal shape. At larger positive values of ℓ^2 the diameter of the torus increases thus effectively reducing the configuration into a ring on the $x - y$ plane.

If the parameter ℓ^2 could be given some dynamical meaning the situation would resemble a scattering process. Some parallels can be drawn with the scattering of two magnetic monopoles [176]. Two monopoles heading towards each other do merge as they get closer and then depart at an angle of 90° degrees. In our case the scattering objects merge, but will not separate from each other forming a ring (torus) instead. Still, the ring develops at 90° from the initial trajectories. Alternatively we might think of it as a collapsing ring that ejects two particles moving away in the opposite directions along the axis of symmetry.

This vague similarity with the behaviour of magnetic monopoles might not be just a random coincidence, if we remind ourselves all the parallels between monopole physics and the enhançon mechanism discussed *e.g.* in section 2.4. Perhaps a link can be found with some known (or unknown) aspect of magnetic monopoles and the

above described features of oblate/prolate enhançons.

4.7 Summary

We have seen in this chapter that the enhançon mechanism is not just a curiosity of spherical configurations, but it also operates successfully and is mathematically tractable in a wide class of axially symmetric situations.

The idea was to wrap distributions of D–branes (instead of a coincident configuration we used previously) on $K3$. We obtained these distributions as extremal limits of rotating p–brane solutions. Of course, since D–branes are BPS objects, we could take any distribution we may think of, but in a generic case there would be no nice and analytic supergravity solution available to describe the geometry.

We began by considering the corresponding D6–brane distribution, which in suitable coordinates looked like branes distributed on the edge of a disc with a puzzling negative contribution to brane density in the interior of the disc. Probing with test particles showed how they get repelled from regions very close to the disc interior, although there would be no obstacles for probing constituent D6–branes to move anywhere in the geometry. This feature is completely independent of the enhançon mechanism as it characterises an unwrapped configuration of D6–branes. Still, it may be yet another instance where the naive supergravity description must be considered inadequate, and it remains an interesting problem to understand how the full string theory could resolve the issue.

Noting that distributions of branes of other dimensionality are free of this problem (have a positive brane density everywhere in their location) we promised to be careful not to confuse the features of the unwrapped D6 system with those typical to the enhançon, and proceeded with wrapping the configuration on $K3$ (in section 4.2). Wrapping branes on $K3$ had an expected effect of an apparent repulson singularity surrounded by an enhançon where the brane tension vanishes. This allowed us to apply the same line of reasoning how the singularity should be resolved by the appearance of new massless degrees of freedom of enhanced gauge symmetry, *etc.*

The novel feature was that depending on the value of parameter ℓ (which was related to angular momentum of the non-extremal rotating configuration) the enhançon shell took different shapes. For ℓ small it was a "double-shell" where the problematic repulson region was surrounded both from outside and *inside* by a good geometry. For larger ℓ these two good regions joined, giving the enhançon a shape of a torus. There was still some repulsive behaviour left in the geometry which was clearly inherited from the odd features of the unwrapped configuration, showing the enhançon mechanism was only able to take care of the effects specifically arising from wrapping branes on $K3$.

In section 4.3 we generalised the supergravity excision computation to axially symmetric situations, finding for our satisfaction that these methods did give consistent results also in this case. Next in section 4.4 we considered wrapped D5– and D4–brane distributions leading again to various shapes for the enhançon, but now without the problematic heritage from the negative brane density like in the case of D6–branes. Then in section 4.5 we used our probe computation results to extract information about the moduli space of the corresponding world-volume gauge theory.

Lastly, in section 4.6 we extended our analysis to the cases when $\ell^2 < 0$, recovering a family of prolate enhançons for the D6 configuration. When viewed as a series of snapshots by varying the parameter ℓ^2 from large negative values to large positive values, the series reminds vaguely a typical scattering of solitons, which approach each other, merge at the core and then leave at an angle of 90° degrees to the initial trajectories (although the enhançons from an expanding ring instead).

Chapter 5

Rotation, Black holes, and the Enhançon

Having seen in the previous chapter how the enhançon can arise in different shapes, it is reasonable to ask whether a rotating enhançon is possible. In this chapter we will consider an example of a rotating enhançon configuration, constructed by wrapping a system of parallel D5– and D1–branes on $K3$ with a pp–wave propagating along the unwrapped spatial direction of the branes' world-volume. Although the geometry has a non-vanishing asymptotic angular momentum the enhançon shell itself is actually static as is revealed by the probe calculation and the analysis of junction matching conditions. This is related to the fact that we still have a BPS configuration blessed by the cancellation of forces.

When compactified further on S^1 the solution becomes a five dimensional black hole with finite horizon area. We will study some of the macroscopic properties of this black hole, paying special attention to its entropy which is proportional to the area of the horizon. Like in the static case [90] it seems at first the second law of thermodynamics can be violated in certain cases when sending in more D5–branes into the black hole could decrease the horizon area. But fortunately this is prevented from happening by the enhançon shell just outside of the horizon which stops these D5–branes from entering the black hole. In the end of the chapter we will comment on a similar apparent problem, related to a possibility of sending in branes with non-zero angular momentum.

5.1 Rotating enhançon

As we observed in the previous chapter, in the extremal BPS limit rotating D–brane solutions generally reduce to static distributions of branes. However, there still exists an extremal rotating solution featuring a D1–brane inside a D5–brane with a pp–wave running along the common part of the branes' world-volume [177]. The pp-wave, a planar fronted gravitational wave with parallel rays, is a special supersymmetric case of the Brinkmann wave [178]. It is a purely gravitational solution of the supergravity equations of motion and does not carry charge under the tensor fields. But it does carry momentum in its direction of propagation.

Compactifying this configuration on $T^4 \times S^1$ gives a rotating BMPV black hole in 5 dimensions [179]. Instead of T^4, we will wrap the system on a $K3$ manifold, which, as we know already, induces an extra amount of negative D1–brane charge on the unwrapped part of world-volume. To obtain a five dimensional black hole we need to compactify the remaining spatial direction of the branes' world-volume, *i.e.* make $x_1 \equiv z$ compact with period $2\pi R_z$. The presence of the pp–wave in this direction is necessary in order to give the resulting black hole a non-zero horizon area and therefore allow non-trivial macroscopic entropy.

There are four transverse dimensions where the branes can move. In particular this motion may include rotation in two independent directions, say ϕ_1 and ϕ_2. Rotation does not break an extra amount of supersymmetry and the configuration is still BPS. However, supersymmetry requirements demand that the linear combination of angular momenta in these directions should vanish [179, 180], and we take $J_{\phi_1} = -J_{\phi_2}$.

The configuration we have preserves 1/8 of the original supersymmetry (4 supercharges out of 32): 1/2 is broken by having D5–branes, another 1/2 by wrapping them on $K3$, but given the orientations of added D1–branes they do not break any further supersymmetry (as we noticed in section 2.7). A pp–wave in the z-direction with purely left- or right-moving momentum excited breaks 1/2 of supersymmetry, and we will keep only the right-moving part. A schematic diagram of our configuration appears in table 5.1.

	$\mathbb{R}^{5,1}$						K3			
	t	z	r	θ	ϕ_1	ϕ_2	x_6	x_7	x_8	x_9
D5	–	–	·	·	·	·	–	–	–	–
D1	–	–	·	·	·	·	∼	∼	∼	∼
pp	–	→	·	·	·	·	∼	∼	∼	∼

Table 5.1: A sketch of the D5–D1–pp configuration wrapped on K3. The world-volume directions are marked by "–" and transverse directions by "·", the symbol "∼" denotes that D1–branes are delocalised on K3, while "→" indicates the direction in which the wave is propagating.

The corresponding string frame IIB supergravity solution is

$$\begin{aligned} ds^2 &= H_5^{-1/2}H_1^{-1/2}\Big(-dt^2+k(dt-dz)^2+dz^2+\frac{J}{r^2}(\sin^2\theta\, d\phi_1-\cos^2\theta d\phi_2)(dz-dt)\Big) \\ &\quad +H_5^{-1/2}H_1^{1/2}V^{1/2}ds^2_{K3}+H_5^{1/2}H_1^{1/2}(dr^2+r^2\, d\Omega_3^2)\,, \end{aligned} \tag{5.1.1}$$

where

$$d\Omega_3^2 = d\theta^2+\sin^2\theta\, d\phi_1^2+\cos^2\theta\, d\phi_2^2 \tag{5.1.2}$$

is the metric on a transverse three sphere and ds^2_{K3} is the metric on a K3 manifold of unit volume. Like before, the $K3$ volume varies with the radial coordinate of the transverse space as $V(r) = VH_1/H_5$, reaching the asymptotic value V at spatial infinity. The dilaton and R-R potentials are defined as

$$\begin{aligned} e^{2\Phi} &= g_s^2\frac{H_1}{H_5}, \\ C^{(6)} &= g_s^{-1}H_5^{-1}\, dt\wedge dz\wedge ds_{K3}+\frac{J}{2r^2}H_5^{-1}(\sin^2\theta d\phi_1-\cos^2\theta d\phi_2)\wedge dz\wedge ds_{K3}, \\ C^{(2)} &= g_s^{-1}H_1^{-1}\, dt\wedge dz+\frac{J}{2r^2}H_1^{-1}(\sin^2\theta d\phi_1-\cos^2\theta d\phi_2)\wedge dz. \end{aligned} \tag{5.1.3}$$

The harmonic functions pertaining to D5–, D1–branes and the pp–wave are given as

$$H_5 = 1+\frac{r_5^2}{r^2}, \qquad H_1 = 1+\frac{r_1^2}{r^2}, \qquad k=\frac{r_P^2}{r^2}, \tag{5.1.4}$$

where the corresponding scales are set by

$$r_5^2 = g_s\ell_s^2Q_5\ , \quad r_1^2 = g_s\ell_s^2\frac{V_\star}{V}Q_1\ , \quad r_p^2 = g_s^2\ell_s^2\frac{V_\star}{V}\frac{\ell_s^2}{R_z^2}Q_p\ . \tag{5.1.5}$$

In this setup we have allowed the presence of extra positive charge D1–branes, not just the effective negative charge D1's that are induced by wrapping D5's on K3. (In

this sense our discussion is paralleled by section 2.7.) So defining N_5 and N_1 to be the numbers of (real, not effective) D5– and D1–branes, the charges in equation (5.1.5) are

$$Q_5 = N_5 \,, \qquad Q_1 = N_1 - N_5 \,, \tag{5.1.6}$$

the latter because each wrapped D5–brane induces minus one unit of D1–brane charge. Also Q_p is an integer parameterising the amount momentum we have in the compact direction z. Setting $J = 0$, rotation in transverse dimensions vanishes and we recover the static D5–D1–pp system studied in ref. [90].

In 5 dimensions this configuration describes a rotating black hole having a horizon of finite area at $r = 0$. We will consider some of the properties of this black hole later in sections 5.4 and 5.5. But first let us study the rotating enhançon from the ten dimensional point of view.

If the number of wrapped D5–branes is grater than the number of D1–branes, $N_5 > N_1$, then the overall D1–brane charge Q_1 is negative and, as we have seen a number of times before, the solution exhibits a naked repulson singularity accompanied by the $K3$ volume shrinking to zero. This unphysical behaviour is remedied by the enhançon mechanism — new degrees of freedom coming to play at the radius where the $K3$ volume $V(r)$ reaches its special value $V_\star = (2\pi\ell_s)^4$. It turns out the enhançon radius is the same as in the non-rotating case of ref. [90]

$$r_e^2 = g_s\ell_s^2 \frac{V_\star}{(V - V_\star)}(2N_5 - N_1), \tag{5.1.7}$$

where negative r_e^2 means that the enhançon lies inside the event horizon if $2N_5 < N_1$.

5.2 Probing the geometry

By now we are already experts in probing wrapped D–brane geometries with constituent D–branes and interpreting the results in the light of the enhançon mechanism. It feels like a routine exercise, but this time some extra challenge is provided by having a rotating background.

First, let us remind ourselves that rotating geometries exhibit the effect of frame dragging, *i.e.* observers are dragged to rotate with the background. The acceleration of a particle on a circular orbit with a constant angular velocity in an axially

symmetric stationary gravitational field can be be covariantly decomposed into three components corresponding to three forces: radial gravitational, Coriolis (linear in the angular velocity) and centrifugal (quadratic in the angular velocity) [181]. The latter two forces vanish identically if the angular velocity of the particle is zero as measured by a locally non-rotating observer [182], *i.e.* the particle rotates along with the background with angular velocity

$$\omega = -\frac{g_{t\phi}}{g_{\phi\phi}}. \tag{5.2.1}$$

Frame dragging becomes especially drastic inside the ergosphere where no observer can remain at rest (not rotating with respect to the asymptotics), this static limit is reached where g_{tt} changes its sign. In the case of non-extremal rotating branes the ergosphere may reach out of the horizon [169], but in our geometry the frame dragging effects are milder, as there is no ergosphere present.

The effective action for the composite brane probe is

$$\begin{aligned} S &= -\int_{\mathcal{M}_2} d^2\xi e^{-\Phi}(n_5\tau_5 V(r) + (n_1 - n_5)\tau_1)(-\det g_{ab})^{1/2} \\ &\quad + n_5\mu_5 \int_{\mathcal{M}_2\times K3} C^{(6)} + (n_1 - n_5)\mu_1 \int_{\mathcal{M}_2} C^{(2)}\,, \end{aligned} \tag{5.2.2}$$

where n_5 and n_1 denote the number of D5– and D1– branes we have assembled to make up the probe. Of course, it is still assumed $n_5 \ll N_5$.

In the static situations the terms from the WZ part of the effective action are cancelled by contributions from the DBI part, so that only the kinetic term remains. This happens due to the BPS condition — "electric" Coulomb repulsion is balanced by gravitational attraction. In the rotating case one would expect that frame dragging effects give some additional terms to the DBI (essentially gravity) part of the effective action. But as the RR potential in equation (5.1.3) is now endowed with additional "magnetic" components, the WZ action should also get an extra contribution. Since we have a rare occasion of a rotating BPS system, it is conceivable (or rather expected) that these additional terms in the DBI and WZ parts should again cancel with each other — the gravitational dragging must be neatly balanced by the "magnetic" force induced by rotating background.

Otherwise it was noticed in *e.g.* ref. [183], that in the non-extremal rotating D3–brane background the effective action of a probe D3–brane contained a term

proportional to the probe angular velocity, *e.g.* the gravitational drag and "magnetic" force did not cancel each other as the system was not BPS.

Cancellation does indeed occur when we choose a static gauge for the probe. Another possibility would be to adopt a "spinning" gauge, where the probe is set to rotate with the background by default and the kinetic term of the effective action should depend on deviations from this reference rotation (in addition to radial motion). In this gauge if the probe rotates along with the background with angular velocity (5.2.11) the dragging term in the DBI part will not arise, but there is term from the WZ part representing the "magnetic" force the probe is feeling. Alternatively, if the probe is set to rotate with an angular velocity exactly opposite to the background rotation, then the aforenamed WZ term will not arise, but there is an extra DBI dragging term present.

5.2.1 Static gauge

Let us try the static gauge computation first, defining the coordinates on the probe brane world-volume to be $\xi^0 = t, \xi^1 = z$, while $x^i = x^i(t)$, $x^i = (r, \theta, \phi_1, \phi_2)$. Pulling back the string frame metric to the probe world-volume and expanding the square root yields after some effort

$$\begin{aligned} S_{DBI} &= -\int_{\mathcal{M}_2} d^2\xi \Big\{ (n_5\tau_5 H_5^{-1} V + (n_1 - n_5)\tau_1 H_1^{-1}) \Big(1 + \frac{J}{2r^2}\big(\sin^2\theta\dot{\phi}_1 - \cos^2\theta\dot{\phi}_2\big)\Big) \\ &\quad -\frac{1}{2}(n_5\tau_5 H_1 V + (n_1 - n_5)\tau_1 H_5)(1+k)v^2 \Big\}, \end{aligned} \tag{5.2.3}$$

where we have assumed a slow motion of the probe in the expansion, *i.e.*

$$v^2 = \dot{r}^2 + r^2\left(\dot{\theta}^2 + \sin^2\theta\dot{\phi_1}^2 + \cos^2\theta\dot{\phi_2}^2\right) \tag{5.2.4}$$

being arbitrarily small. Similarly the WZ part of the effective action is

$$S_{WZ} = \int_{\mathcal{M}_2} d^2\xi \Big\{ (n_5\tau_5 H_5^{-1} V + (n_1 - n_5)\tau_1 H_1^{-1}) \Big(1 + \frac{J}{2r^2}\big(\sin^2\theta\dot{\phi}_1 - \cos^2\theta\dot{\phi}_2\big)\Big) \Big\}. \tag{5.2.5}$$

As we can see the usual potential terms of the DBI and WZ parts cancel because the radial gravitational attraction is exactly balanced by the "electric" Coulomb repulsion of R-R fields. But it happens also that the J terms linear in angular velocity

do cancel as well — the effects of gravitational frame dragging are neatly balanced by the "magnetic" force induced by rotation. Thus putting equations (5.2.3) and (5.2.5) together we find that only the kinetic term survives in the effective lagrangian

$$\mathcal{L} = \frac{1}{2}(n_5\tau_5 H_1 V + (n_1 - n_5)\tau_1 H_5)(1+k)v^2. \tag{5.2.6}$$

The prefactor of the kinetic energy gives the effective tension of the probe. This tension is positive as long as

$$r^2 > g_s\ell_s^2 V_\star \frac{(2N_5 - N_1)n_5 - N_5 n_1}{(V - V_\star)n_5 + V_\star n_1}\ , \tag{5.2.7}$$

As we will find out in section 5.3 the lower bound where the tension vanishes agrees perfectly with the supergravity junction computation.

The familiar enhançon discussion would follow from equation (5.2.7), but with a modification from having extra D1–branes in the game. (Remember section 2.7.) For a probe made up of D1–branes only, $n_5 = 0$ and the effective lagrangian reads

$$\mathcal{L} = \frac{1}{2}n_1\tau_1 H_5(1+k)v^2\ . \tag{5.2.8}$$

The tension remains positive everywhere and hence these probing D1–branes can make their way freely down to $r = 0$ without being forced to stop at the enhançon shell. Moreover, if we consider the case $n_5 = n_1$, or more precisely using not just a collection of equal number of D5– and D1–branes, but a bound state of them, then

$$\mathcal{L} = \frac{1}{2}n_5\tau_5 H_1 V(1+k)v^2\ . \tag{5.2.9}$$

Again the tension of such a probe is positive. This means D5–branes can penetrate beyond the enhançon radius and move to the origin, even though the volume of $K3$ is below $V_\star$ in this region. We will keep this fact in mind as it will have implications for the black hole discussion later on.

5.2.2 "Spinning" gauge

Alternatively we may try to use a "spinning" gauge by defining

$$\xi^0 = t + \frac{1}{\omega_1}\phi_1 + \frac{1}{\omega_2}\phi_2, \qquad \xi^1 = z, \tag{5.2.10}$$

where

$$\omega_1 = -\frac{g_{t\phi 1}}{g_{\phi_1\phi_1}}, \qquad \omega_2 = -\frac{g_{t\phi 2}}{g_{\phi_2\phi_2}}, \tag{5.2.11}$$

can be interpreted as reference background velocities. What this choice of world-volume coordinates essentially means is that we have set the probe to rotate with the background angular velocities ω_1 and ω_2, while $\dot{\phi}_2$ and $\dot{\phi}_2$ are understood as deviations from these reference velocities. As a result the J terms in the DBI part of the probe effective action do cancel and the result is similar to the static case

$$\begin{aligned} S_{DBI} &= -\int_{\mathcal{M}_2} d^2\xi \Big\{ (n_5\tau_5 H_5^{-1} V + (n_1 - n_5)\tau_1 H_1^{-1}) \\ &\quad -\frac{1}{2}(n_5\tau_5 H_1 V + (n_1 - n_5)\tau_1 H_5)(1+k)v^2 \Big\}. \end{aligned} \tag{5.2.12}$$

But at the same time in the WZ part the J term is present:

$$S_{WZ} = \int_{\mathcal{M}_2} d^2\xi \Big\{ (n_5\tau_5 H_5^{-1} V + (n_1 - n_5)\tau_1 H_1^{-1}) \Big(1 + \frac{J}{2r^2} \big(\sin^2\theta(\dot{\phi}_1 + \omega_1) - \cos^2\theta(\dot{\phi}_2 + \omega_2) \big) \Big) \Big\}, \tag{5.2.13}$$

and the final effective lagrangian is

$$\begin{aligned} \mathcal{L} &= \frac{1}{2}(n_5\tau_5 H_1 V + (n_1 - n_5)\tau_1 H_5)(1+k)v^2 \\ &\quad + \frac{J}{2r^2}(n_5\tau_5 H_5^{-1} V + (n_1 - n_5)\tau_1 H_1^{-1}) \Big(\sin^2\theta(\dot{\phi}_1 + \omega_1) - \cos^2\theta(\dot{\phi}_2 + \omega_2) \Big) . \end{aligned} \tag{5.2.14}$$

Here the potential terms describing radial gravitational and R-R forces cancel as usual, but the J term will vanish only if $\dot{\phi}_i + \omega_i$. But the latter condition actually means there is no force if the probe is static from the point of view of a distant observer. In fact, had we changed signs in equation (5.2.11) the result would have been exactly the opposite with a similar J term coming from the DBI part and none from the WZ part. So the physical picture is quite clear — gravity wants to drag the probe in one way, while the "magnetic" field in the opposite way. If we set the probe to rotate as gravity wants it (by choosing the "spinning" gauge), then the probe feels a "magnetic" potential. If we set the particle to rotate in the opposite direction (by choosing the "spinning" gauge with appropriate minus signs), the "magnetic" potential does vanish, but now the gravitational drag potential will

arise instead. For a non-rotating probe these two forces exactly cancel, as they should since we know the configuration is BPS.

Finally we should notice that the coefficient of the kinetic term in the effective lagrangian (5.2.14), giving the effective tension of the probe, is still the same as in the static gauge result (5.2.6). So considering the "spinning" gauge did not tell as anything really new, it perhaps only helped to clarify matters concerning the effects of a rotating background.

5.3 Excision

The enhançon mechanism instructs us to cut out the unphysical region and replace it with a modified and better behaving space, gluing these two geometries together at some radius $r = r_i$. The procedure goes through pretty much along the same lines as in the static case of sections 2.5 and 2.7.

A certain number δN_5 of D5–branes and δN_1 of D1–branes are stuck on the shell at r_i, while $N_5' = N_5 - \delta N_5$ of D5–branes and $N_1' = N_1 - \delta N_1$ can move in to the interior. The solution describing the interior region has the same form as equation (5.1.1) above, only the harmonic functions H_1, H_5 are now substituted by

$$h_1 = 1 + \frac{r_1^2 - \tilde{r}_1^2}{r_i^2} + \frac{\tilde{r}_1^2}{r^2}, \qquad h_5 = 1 + \frac{r_5^2 - \tilde{r}_5^2}{r_i^2} + \frac{\tilde{r}_5^2}{r^2}, \tag{5.3.1}$$

with the scales

$$\tilde{r}_1^2 = g_s \ell_s^2 \frac{V_\star}{V} Q_1' \,, \qquad \tilde{r}_5^2 = g_s \ell_s^2 Q_5', \tag{5.3.2}$$

being proportional to the number of branes inside, *i.e.* $Q_5' = N_5'$, $Q_1' = N_1' - N_5'$, and of course $Q_1' \geq 0$ to avoid the singularity.

It is easy to see that the metric of the corrected solution is continuous at r_i. The discontinuity in the extrinsic curvature on the junction surface at r_i has an interpretation as the surface stress-energy tensor of this thin shell. After some effort we find that the stress-energy tensor of the gluing surface to be of the same form as

in the static case, but now with additional (t, ϕ_i) and (z, ϕ_i) terms

$$S_{\mu\nu} = \frac{1}{2\kappa^2\sqrt{G_{rr}}}\left(\frac{H_1'}{H_1}+\frac{H_5'}{H_5}-\frac{h_1'}{h_1}-\frac{h_5'}{h_5}\right)G_{\mu\nu}, \tag{5.3.3a}$$

$$S_{\mu\phi_i} = \frac{1}{2\kappa^2\sqrt{G_{rr}}}\left(\frac{H_1'}{H_1}+\frac{H_5'}{H_5}-\frac{h_1'}{h_1}-\frac{h_5'}{h_5}\right)G_{\mu\phi_i}, \tag{5.3.3b}$$

$$S_{ij} = 0, \tag{5.3.3c}$$

$$S_{ab} = \frac{1}{2\kappa^2\sqrt{G_{rr}}}\left(\frac{H_5'}{H_5}-\frac{h_5'}{h_5}\right)G_{ab}, \tag{5.3.3d}$$

where indices μ, ν denote the t and z directions, a, b denote the $K3$ directions, i, j denote the angular directions along the junction three-sphere. The Einstein frame metric G_{MN}, natural in this computation, is related to the string frame metric g_{MN} in equation (5.1.1) by $G_{MN} = e^{-\Phi/2}g_{MN}$.

The tension along the angular directions vanishes, since despite rotation we still have a BPS system that does not need some force between the branes to support the shell at arbitrary radius. In the $K3$ directions the tension depends only on the harmonic functions of the D5–branes as only they wrap these directions. Finally in the t and z directions as well as $t-\phi_i$ and $z-\phi_i$ directions the surface stress-energy is proportional to a tension

$$T_{\text{eff}} = \frac{1}{2\kappa^2\sqrt{G_{rr}}}\left(\frac{H_1'}{H_1}+\frac{H_5'}{H_5}-\frac{h_1'}{h_1}-\frac{h_5'}{h_5}\right) \tag{5.3.4}$$

These results are consistent with what one would expect from the fact that the shell is built of D5– and D1–brane sources.

If there are no D1–branes on the shell ($\delta N_1 = 0$), the tension (5.3.4) vanishes precisely at the enhançon radius (5.1.7). Alternatively if some D1–branes stay on the shell, the tension is positive down to

$$\tilde{r}_e^2 = g_s\ell_s^2 V_\star \frac{(2N_5 - N_1)\delta N_5 - N_5\delta N_1}{(V - V_\star)\delta N_5 + V_\star\delta N_1}, \tag{5.3.5}$$

in the latter case $\tilde{r}_e^2 < r_e^2$. Notice that this lower bound where the tension vanishes agrees perfectly with the probe computation results (5.2.7) if one substitutes $n_1 \to \delta N_1$, $n_5 \to \delta N_5$. It is satisfying that the consistency conditions derived here and the probe results of the previous section are in perfect agreement with each other.

We must notice that as we replace the geometry inside of the enhançon radius with a repaired geometry given by the harmonic functions (5.3.1) the running $K3$

volume in the interior is now

$$V(r) = \frac{h_1}{h_5} V_\star \ , \tag{5.3.6}$$

and in particular at the horizon

$$V(r=0) = \frac{\tilde{r}_1^2}{\tilde{r}_1^2} V_\star = \frac{N_1' - N_5'}{N_5'} \ . \tag{5.3.7}$$

The volume at the enhançon radius is still $V_\star$, but now we have a possibility that inside, *i.e.* for $r < \tilde{r}_e^2$, it can actually grow larger. Therefore means the D5–branes can actually pass the enhançon radius and move in as their tension does not become negative in the process. This is subject to the condition $N_1' > 2N_5'$, apparent also from equation (5.3.7), which shows $V(r=0) > V_\star$ if the condition holds. In fact, in the limit $N_1' = 2N_5'$ the $K3$ volume is $V(r) = V_\star$ uniformly everywhere in interior up to the enhançon radius.

5.3.1 Rotation of the space-time

So far the story has gone exactly along the same lines as in the static $J = 0$ case, studied in [90]. Does rotation show up anywhere in the consistency arguments? Yes, it does. The $S_{\mu\phi_i}$ components of the surface stress-energy tensor depend on $G_{\mu\phi_i}$ and hence on J. But at the enhançon radius these components of stress-energy do vanish nevertheless, indicating that the surface is not rotating if placed at the enhançon radius $\tilde{r}_e^2$. This conclusion gets further support from the fact that for a static gauge probe the effects of rotation do exactly cancel. We can build the enhançon by moving in non-rotating branes, and thus it is not a big wonder that the resulting shell should not rotate either.

But then another question arises: if the enhançon shell manages to stay static, what makes the geometry to rotate at all? This problem might need a deeper investigation, but a hint about a possible answer can be found in the physics of rotating supersymmetric black holes in five dimensions [184]. Namely the horizon of such a black hole can be shown to have a vanishing angular velocity although the corresponding geometry is characterised by finite angular momentum. As it turned out in this case the angular momentum is stored in the Maxwell field. (And for another surprise, a negative fraction of the total angular momentum is actually

stored behind the horizon. Hence the fact that the horizon is static was interpreted as a cancellation of opposite dragging effects.)

We will see in the next section that the black hole we get by compactifying our brane configuration on $K3 \times S^1$ does also have a non-rotating horizon with finite area.

5.4 Constructing a black hole

5.4.1 Black holes in string theory

One of the most fruitful applications of D–brane technology in string theory has been the study of black holes, which allows a microscopic description of the black hole entropy [185]. The idea behind this procedure is simple. One first constructs a D–brane configuration with appropriate conserved charges. The configuration then needs to be compactified on some compact manifold to yield a point like source in lower dimensions that behaves like a black hole with non-zero horizon area. The microscopic picture of entropy follows from the degeneracy of D–brane arrangements which give rise to the black hole. Having a BPS configuration we may trust this counting of microstates at weak coupling to hold also for strong coupling, where the black hole should form in the limit. Indeed, this microscopic derivation can be found to be in agreement with the macroscopic Bekenstein-Hawking formula of black hole entropy [186]

$$S = \frac{\mathcal{A}}{4G_N^{(D)}} \ , \tag{5.4.1}$$

where $\mathcal{A}$ is the area of the black hole and $G_N^{(D)}$ is Newton's constant in D dimensions.

The microscopic formulation of a static five dimensional black hole of type IIB string theory in terms of the D1–D5–pp brane system was first given in ref. [185], and generalised for the rotating case in refs. [179, 187]. (See *e.g.* ref. [188] for an extensive review and refs. [189, 190] for a detailed introduction to the subject.)

However, we will not discuss the microscopic description of black holes in any greater detail here, but content ourselves with some interesting macroscopic phenomena arising when the brane configuration is wrapped on K3, as investigated in

ref. [90]. At first instance there seems to be a possibility to violate the celebrated second law of thermodynamics, but we will see how the enhançon mechanism keeps guard of good physics and helps to avoid a decrease in the black hole entropy.

5.4.2 Five dimensional black hole from dimensional reduction

First we need to perform a dimensional reduction of our solution (5.1.1) integrating out all dependence on the compact $K3 \times S^1$. The procedure for $K3$ is in general more complicated than the usual Kaluza-Klein reduction on a torus, but the components of the lower dimensional metric are the same as the corresponding components of the higher dimensional metric. The five dimensional dilaton is given by

$$e^{-2\Phi^{(5)}} = e^{-2\Phi^{(10)}} \sqrt{\det\, g_{ab}^{(K3\times S^1)}} = H_1^{-1/4} H_5^{-1/4} (1+k)^{1/2} \,, \tag{5.4.2}$$

and we will use it to find the five dimensional Einstein frame metric $G^{(5)}_{\mu\nu}$ (related to the string frame metric by $G^{(5)}_{\mu\nu} = e^{-\frac{4}{3}\Phi^{(5)}} g^{(5)}_{\mu\nu}$) to be

$$\begin{aligned} ds^2_{(5)} &= -H_1^{-2/3} H_5^{-2/3} (1+k)^{-2/3} \left(dt + \frac{J}{2r^2} (\sin^2\theta d\phi_1 - \cos^2\theta d\phi_2) \right)^2 \\ &\quad + H_1^{1/3} H_5^{1/3} (1+k)^{1/3} \left(dr^2 + r^2 d\Omega_2^2 \right). \end{aligned} \tag{5.4.3}$$

The geometry (5.4.3) above describes a black hole with a horizon at $r = 0$. As mentioned before, although the geometry has non-vanishing asymptotic angular momentum, the angular velocity of the horizon is actually zero:

$$\omega_i = -\frac{G_{t\phi_i}}{G_{\phi_i\phi_i}}\bigg|_{r=0} = 0.$$

The area $\mathcal{A}$ of the horizon can be computed as follows:

$$\begin{aligned} \mathcal{A} &= \lim_{r\to 0} \int_0^{\frac{\pi}{2}} \int_0^{2\pi} \int_0^{2\pi} \sqrt{G_{\theta\theta} G_{\phi_1\phi_1} G_{\phi_2\phi_2} - G_{\theta\theta} G_{\phi_1\phi_2} G_{\phi_2\phi_1}}\, d\theta d\phi_1 d\phi_2 \\ &= \lim_{r\to 0} 2\pi^2 \sqrt{r^6 H_1 H_5 (1+k) - \frac{J^2}{4}} \\ &= 2\pi^2 \sqrt{r_1^2 r_5^2 r_P^2 - \frac{J^2}{4}} \,. \end{aligned} \tag{5.4.4}$$

5.4.3 Bound on the angular momentum

Expecting the area of the black hole to be a real (not imaginary) quantity, sets a bound on the angular momentum

$$J^2 \leq 4\, r_1^2 r_5^2 r_P^2 \,. \tag{5.4.5}$$

In an "over-rotating" situation, for angular momenta above this bound, the system starts to entertain unphysical behaviour: closed time-like curves develop above the horizon and causality is violated [177,191]. This poses a hard problem. For example one is entitled to worry whether it is possible to pass from the under-rotating to the over-rotating case, increasing the angular momentum of space-time and expending only a finite amount of energy. The authors of ref. [191] gave a simple thermodynamical argument presenting some evidence that the passage from the under to over-rotating space-time is forbidden, although the matter has not been conclusively proven. One can also find some consolation in the fact that it is only a problem from the point of view of five dimensional physics, in ten dimensions these anomalous features are not present [177].

Let us emphasize the problematic effects described above are not specific to wrapping branes on $K3$, the same bound would arise if we wrap on T^4. In the light of this it is hard to see what the enhançon mechanism alone could do to resolve this puzzle, since the problem itself is more general. In our following discussion we hope to be on safe side and assume that our branes are far from the over-rotating case, *i.e.* the bound (5.4.5) is not violated.

There is one more subtlety, however, related specifically to wrapping branes on $K3$. We should remember the bound (5.4.5) applies not just to the original geometry (that remains valid outside of the enhançon), but also to the internal geometry when we have performed excision. In the latter case r_1^2 and r_5^2 in the area formula (5.4.4) and in the corresponding bound on angular momentum are replaced by $\tilde{r}_1^2$ and $\tilde{r}_5^2$, while J is the same.[1] For example we would run into a problem when r_1^2 and r_5^2 are big enough to satisfy the bound, but $\tilde{r}_1^2$ and $\tilde{r}_5^2$ are two small and fail. Or, in other

[1] It is hard to see how we could glue together two geometries with different J, since the metric must be continuous over the junction surface.

words, we can not build our internal geometry with neither $N_1' - N_5'$ nor N_5' being arbitrarily small, since this would lead to causality violations above the horizon. The only exception seems to be when $N_1' = N_5' = 0$, *i.e.* there are no branes inside, just a flat space without any black hole.

Consider a situation when there are only a large number N_5 of D5–branes present, forming an enhançon shell, and no D1–branes around. Following the logic behind the enhançon mechanism we are instructed to cut out the internal geometry and replace it with a flat space. Now let us bring in some smaller number N_1 of D1–branes with momentum. We may move these D1–branes straight in, so that the metric inside ceases to be flat and a black hole forms. If J is not zero this black hole would have an imaginary area and should therefore be prohibited somehow. It does not matter how many D1–branes are in there, until $N_5' = 0$ the black hole area would be imaginary. We need to supply the internal region with sufficient number of D5–branes to satisfy the bound (5.4.5). A similar problem would arise if we decide to send in only the D5–D1 bound states, because this implies $\tilde{r}_1^2 = 0$, and yet again the black hole area would be imaginary.

This is a puzzling situation since it is hard to see what would prevent us from sending in only the D5–D1 bound states or only D1–branes without D5–branes. We will learn now a bit more about how the enhançon affects a black hole, and come briefly back to this issue towards the end of this chapter — to find that *once* an acceptable ("under-rotating") black hole has been formed, the enhançon mechanism actually protects it from turning into "over-rotating" species, despite what combinations of constituent branes we might try to send in.

5.4.4 Enhançon around the horizon

In the following let us assume J has some almost negligible value, since we would like to understand better what does the enhançon do when build the black hole by (adiabatically) bringing in the constituent branes. First, say, we have only some large number N_5 of the D5–branes present. They have stay smeared around the enhançon shell at some finite radius, since without D1–branes there is no way how they could move inside. The geometry of the internal region is simply flat and there

is no black hole.

Now let us supply the configuration with some number N_1 of additional D1–branes. As we discussed in section 5.2, they find no obstacle for passing the enhançon shell and moving further in. Once the D1–branes have found their way in, the geometry inside ceases to be flat and the volume of $K3$, given by equation (5.3.6), will also grow above $V_\star$ in the internal region. Correspondingly, this allows for some N_5' of D5–branes to feel free and move to the interior, until $N_1' > 2N_5'$. (We assume all the D1–branes in the game will eventually move to the origin $r = 0$, thus using the notation defined in the beginning of this chapter: $N_1' = N_1$, $\delta N_1 = 0$.)

Furthermore, the black hole can take even more of the D5–branes. This is because a D5–brane can form a bound state with a D1–brane, and as we observed in section 5.2, such a pair is also allowed to pass beyond the enhançon, even when the $K3$ volume is below $V_\star$ in the region. We may ask the incoming D1–branes to bind with D5–branes at the enhançon shell and bring them in. Thus the maximal number of D5–branes that can in principle enter the black hole is $N_5' = N_1$.

Last, but not least, to form a black hole with non-vanishing area, we should not forget to send in some momentum Q_p. Otherwise, as the momentum will not play a major role in our story, let us assume it is carried in to the black hole by the first few D1–branes.

The situation can be summarized as follows:

- If $N_1 = 0$ all the D5–branes have to stay on the enhançon shell, there is just a flat space inside, and hence no black hole.

- If $N_1 < N_5$ there is a black hole at $r = 0$. A certain number $N_5' = N_1$ of D5–branes can can move inside along with D1–branes, while the rest will stay at the enhançon shell at $r_e^2 > 0$.

- If $N_5 \leq N_1 < 2N_5$ all the D5–branes can enter the black hole, although we still have an enhançon at $r_e^2 > 0$ above the horizon, but not necessarily any D5–branes staying on it. If the D5–branes are inside the volume of $K3$ in the region is below $V_\star$.

- If $2N_5 \leq N_1$ then $r_e^2 \leq 0$ and all the branes can stay happily at the horizon, since $V(r) \geq V_\star$ above.

Notice that in the two latter cases the original geometry (5.1.1) is valid down to the horizon at $r = 0$. In the first two cases we need to perform excision and replace the interior geometry by a new one, and the black hole area, equation (5.4.4), will depend only on the number of D5–branes that have moved in.

5.5 The black hole entropy and the second law

Now it's time to look at the macroscopic entropy of our five dimensional black hole. Inserting the area (5.4.4) into the Bekenstein-Hawking formula (5.4.1) gives

$$\begin{aligned} S &= \frac{2\pi^2}{4G_N^{(5)}}\sqrt{r_1^2 r_5^2 r_P^2 - \frac{J^2}{4}} \\ &= 2\pi\sqrt{(N_1 - N_5)N_5 Q_P - \frac{J^2\pi^2}{16G_N^{(5)2}}} \end{aligned} \tag{5.5.1}$$

where $G_N^{(5)} = G_N^{(10)}/2\pi R_z V$ is the five dimensional Newton's constant. It is important to understand where exactly are the novelties due to wrapping our branes on $K3$ instead of T^4. Obviously these are hiding in the first term under the square root above. Had we wrapped our branes on T^4 the first term would have simply read $N_1 N_5 Q_P$, but now this term is modified by the extra contribution of negative D1–brane charge induced by wrapping D5–branes on $K3$.

5.5.1 Entropy and the enhançon

Let us fix the values of N_1, Q_P, and J, and consider how the area (entropy) of the black hole depends on the number N_5 of D5–branes in the configuration. We may note that the area actually vanishes for the values

$$N_5^{\pm} = \frac{N_1}{2}\left(1 \pm \sqrt{1 - \frac{\pi^2}{4G_N^{(5)2}}\frac{J^2}{N_1^2 Q_P}}\right), \tag{5.5.2}$$

and is positive for $N_5^- < N_5 < N_5^+$. In fact, this condition is nothing else than restatement of the bound on J we discussed previously. For $N_5 < N_5^-$ and for

$N_5 > N_5^+$ the bound (5.4.5) is not satisfied. In the static case when $J = 0$ obviously $N_5^- = 0$ and $N_5^+ = N_1$. Next, we should also note the entropy is maximized if $N_5 = N_1/2$, a value that lies exactly between N_5^- and N_5^+.

Consider what is happening. We may start with some number N_1 of D1–branes and N_5^- of D5–branes forming the black hole. Sending slowly in more D5–branes would increase the black hole area and hence its entropy, which is in agreement with the second law of thermodynamics. However, there is a turning point at $N_5 = N_1/2$, and adding more than $N_1/2$ of D5–branes to the black hole should actually make its area decrease. At first sight this is alarming, since it seems we have found a way to violate the second law by *adiabatic* motion of branes. But fortunately this is not the case. Remember, there is an enhançon above the horizon. As we have discussed before, the D5–branes are allowed to enter the black hole only until $N_5 = N_1/2$, which is precisely the bound necessary to protect the entropy from decreasing. In other words, if $N_5 > N_1/2$ the incoming D5–brane gets stopped at the enhançon radius outside of the horizon and it can not move in to breach the second law of thermodynamics.

Of course, the D5–branes have still permission to enter the black hole as bound states with D1–branes. But in this case it is in accordance with the second law, because N_1 is not constant, contrary to the assumptions of the previous argument. In fact, sending in a bound state of D5–D1–branes would increase the entropy, as is apparent from equation (5.5.1), where N_5 increases while $N_1 - N_5$ remains unchanged.

To make the situation clear, let us consider sending in a collection of n_5 D5–branes and n_1 D1–branes in addition to larger numbers N_5 and N_1 of D5– and D1–branes already present at the black hole. The square of the entropy is proportional to

$$S^2 \sim (N_1 + n_1 - N_5 - n_5)(N_5 + n_5)Q_P - \frac{J^2\pi^2}{16G_N^{(5)2}} \,. \tag{5.5.3}$$

Assuming $n_5, n_1 \ll N_5, N_1$, an infinitesimal shift in the entropy (squared) is given by

$$\delta S^2 \sim (N_5 n_1 - (2N_5 - N_1)n_5)Q_P \,. \tag{5.5.4}$$

For certain values of the quantities involved, it seems δS^2 has a possibility of being

negative, therefore suggesting ways how the entropy could decrease. But remarkably the expression (5.5.4) also appears in the numerator of equation (5.2.7) which describes the tension of the probe and sets the corresponding enhançon radius. There is also an important sign difference between (5.5.4) and (5.2.7), which solves the problem we are facing. Namely, if $\delta S^2 < 0$ then $\tilde{r}_e^2 > 0$, *i.e.* when the probe is potentially threatening to decrease the entropy, it is actually stopped at the enhançon radius $\tilde{r}_e^2$ above the horizon, and the second law of thermodynamics is not violated. Alternatively for $\delta S^2 > 0$ the enhançon radius is behind the horizon, $\tilde{r}_e^2 < 0$, and the probe is allowed to enter the black hole, only to make the entropy increase. Therefore we have seen how the enhançon mechanism plays a crucial role in ensuring the physics obeys the second law of thermodynamics.

This apparent problem with the black hole entropy and its resolution were first described in the study of the corresponding static configuration [90]. In the rotating case we can observe in addition that the enhançon mechanism does also its valuable service in preventing an "under-rotating" black hole from turning into a problematic "over-rotating" type. What we have essentially shown in the preceding argument, the enahnçon does not allow the combination of $\tilde{r}_1^2\tilde{r}_5^2r_P^2$ to decrease as we send in various combinations of constituent (static) branes. This is sufficient to ensure that once we have an internal geometry obeying the bound (5.4.5), the bound will not be violated later on.

5.5.2 Entropy and angular momentum

So far in our discussion we have assumed the parameter J is constant, *i.e.* moving in the branes from infinity did not produce a change in J. But what if J can change? The infinitesimal shift in the black hole entropy, equation (5.5.4), would bring an additional contribution from the change of angular momentum, say δJ^2, with a minus sign. This suggests we may reduce the black hole entropy by increasing J. For example we might try to send in some branes with sufficiently high δJ associated with them, so that the additional charges these branes contribute do not outweigh the contribution added to the term containing J, *i.e.* if

$$\delta J^2 > 4\delta(r_1^2r_5^2r_P^2) \tag{5.5.5}$$

the entropy would decrease as a result. Hence there must be a bound between the brane charge and angular momentum that can enter the black hole. The bound above, although structurally similar to (5.4.5), characterises a problem that is independent of the puzzle about having an "over-rotating" geometry and the corresponding causality violations we discussed in section 5.4.3. Even for otherwise well-behaved "under-rotating" geometry it might be possible to add some δJ, making the area of the black hole shrink and thus violating the second law.

In the framework of classical general relativity one finds that for a particle to enter the horizon of the black hole there is a limit on infalling mass for a given charge and angular momentum.[2] In other words a particle that could possibly cause a violation of the second law of thermodynamics can not move along a trajectory that crosses the black hole horizon.

We may hope to distill a similar bound from the dynamics of probing branes. Yet the probe calculations we performed in section 5.2 showed the probe is insensitive towards the background angular momentum and prefers not to rotate itself. This is not a surprise, since the logic behind the calculation was essentially to connect together a series of BPS "no force" situations assuming a slow motion of the probe. We may try to give a probe some angular momentum, but this would make the analysis qualitatively different as the motion is not near-BPS any more. Thus in contrast with the previous discussion of adding charges, it is not clear whether adding angular momentum with constituent branes actually implies a new violation of the second law for rotating black holes, since we do not know if the probes are adding angular momentum in an adiabatic way. So, there might not be a violation.

Again, we must stress the problem of increasing J in a manner that could possibly violate the second law of thermodynamics is not specific to the enhançon configuration when the branes are wrapped on $K3$. It would also occur for a similar configuration wrapped on T^4. Therefore the mechanism or a line of reasoning fixing this problem should probably not depend on the features of the enhançon alone, although having the enhançon may add an extra twist to the argument.

[2]See for example the end of chapter 33 of ref. [137] and references therein.

5.6 Summary

In this chapter we studied a configuration of D5– and D1– branes with a pp–wave giving rise to a rotating enhançon when wrapped on a $K3$ surface. However, it turned out the enhançon radius did not depend on the amount of angular momentum J present and was equal to that of a static solution.

Next in section 5.2 we probed the geometry with constituent slowly moving branes and observed how not just the forces describing the radial gravitational attraction and the "electric" Coulomb repulsion did cancel (as we already know from static situations), but also how another pair of potentials, linear in angular velocity, describing the effects of gravitational frame dragging and the "magnetic" force induced by rotation, did exactly cancel as well. The latter is a beautiful feature of a rotating BPS system.

As instructed by the logic of the enhançon mechanism, we performed an excision in section 5.3 to replace the problematic interior geometry with a well-behaved one, showing this procedure is consistent from the supergravity point of view. We also learned that the enhançon shell itself is not rotating, a result which is in accordance with the probe analysis, as we should be able to build the geometry by bringing in non-rotating branes. In the light of this there was a need for a brief comment on how to understand the rotation of the geometry, subsection 5.3.1.

In section 5.4 we compactified our brane configuration on $K3 \times S^1$ to get a rotating black hole in five dimensions. We computed the black hole area and derived an upper bound on the angular momentum beyond which naked closed time-like curves occur and causality is violated. Further on we investigated how the presence of an enhançon above the black hole horizon interferes with attempts to send more branes into the black hole.

The preceding discussion was useful for considering black hole entropy in section 5.5. We showed how the enhançon mechanism operates to protect the second law of thermodynamics. As related result we also found the enhançon mechanism does manage to guard causality — once we have a black hole that obeys the bound between the angular momentum and the charges of its constituting branes, we can not make the black hole to violate this bound by sending in more constituent branes

in various quantities.

There were two problems we encountered in the black hole discussions which we could not solve. The first was how to rule out "over-rotating" geometries, where the bound between the angular momentum and the charges of branes at the black hole is violated. The second was how to rule out a possibility of increasing the angular momentum in a way that leads to decreasing black hole area and thus violates the second law of thermodynamics. Both these problems are more general and not specifically related to wrapping branes on $K3$ and the enhançon mechanism. Therefore it is reasonable to expect the enhançon mechanism alone would not be able to deal with them. We need some other arguments of a more wider scope to succeed.

Conclusion

Theories of classical gravity commonly admit solutions afflicted by space-time singularities. It is an important question how, or indeed whether, quantum corrections to the classical picture are able to resolve these singularities. String theory, which offers a consistent quantum formulation of gravity, knows several nice cases how singularities arising in the classical description are resolved by new quantum degrees of freedom entering the game. The enhançon mechanism is one such example, where a naked space-time singularity is resolved by stringy physics.

Our study of the enhançon relied heavily on the remarkable properties of D–branes, which relate space-time geometry with a gauge field theory on their world-volume. To construct the enhançon we wrapped various configurations of D–branes on a $K3$ manifold (although there are many dual realisations), witnessing an unphysical singularity arising in the supergravity picture. However, application of a brane probe calculation and supergravity junction conditions as principal tools, suggests a more healthy vision of the situation. In a region surrounding the putative singularity the classical supergravity fields get endowed with enhanced gauge symmetry making the geometry smooth inside.

After discussing in detail the prototypical example of the spherical enhançon pertaining to $SU(N)$ gauge theory (chapter 2), we proceeded to generalise the setup in three ways: including orientifolds to have configurations pertaining to $SO(2N+1)$, $USp(2N)$ and $SO(2N)$ gauge theories (chapter 3), using D–brane distributions to find many non-spherical shapes of the enhançon (chapter 4), and considering a rotating enhançon configuration (chapter 5). In each of these cases we confirmed the key mathematical techniques are fully applicable and tractable, while the enhançon mechanism is up to its job, *i.e.* it removes the singularity which appears in the

supergravity description.

However, when confronted with problematic circumstances being there due to some other reasons, the enhançon was able to correct only the unphysical features coming from wrapping branes on $K3$, but not to resolve all the issues completely. Examples of this kind where the puzzle of negative brane densities in chapter 4 and the possibilities related to "over-rotating" geometries in chapter 5. It is reasonable to believe these two issues could essentially be occasions analogous to the enhançon, where the pure supergravity description turns out to be inadequate, but some (yet unknown) stringy mechanism handles the situation. While concentrating on the enhançon, we mapped out these independent issues as well as we could, as they are also appealing problems themselves.

Appendix A

Supergravity Equations of Motion

We are interested in various Dp–brane configurations solving the following ten dimensional type II (truncated) supergravity action (in Einstein frame)

$$S = \frac{1}{2\kappa^2}\int d^{10}x\sqrt{-G^{(e)}}\left(R - \frac{1}{2}\partial_\mu\Phi\partial^\mu\Phi - \frac{1}{2}\sum_I \frac{e^{a_I\Phi}}{n_I!}G_{\mu_1\cdots\mu_{n_I}}G^{\mu_1\cdots\mu_{n_I}}\right) , \quad \text{(A.1)}$$

where $G^{(e)}$ is the determinant of the Einstein frame metric $G^{(e)}_{\mu\nu}$ related to the string frame metric $g^{(s)}_{\mu\nu}$ by $G^{(e)}_{\mu\nu} = e^{-\Phi/2}g^{(s)}_{\mu\nu}$. The various (real or effective) Dp–branes in the configuration couple to $C^{(p+1)}$ R-R potentials of field strength $G_{\mu_1\cdots\mu_{p+2}}$. The coefficient $a_I = \frac{3-p}{2}$, while the gravitational coupling is defined as before in (1.3.8). Varying the action (A.1) produces the following set of equations of motion:[1]

$$\begin{aligned}
R^\mu{}_\nu &= \frac{1}{2}\partial^\mu\phi\partial_\mu\phi + \frac{1}{2}\sum_I \frac{e^{a_I\phi}}{n_I!}\left(n_I G^{\mu\alpha_1\cdots\alpha_{n_I-1}}G_{\nu\alpha_1\cdots\alpha_{n_I-1}} - \frac{n_I-1}{8}\,\delta^\mu{}_\nu G_{\mu_1\cdots\mu_{n_I}}G^{\mu_1\cdots\mu_{n_I}}\right) ,\\
0 &= \partial_\mu\left(\sqrt{-G^{(e)}}e^{a_I\phi}\,G^{\mu\alpha_1\cdots\alpha_{n_I-1}}\right) ,\\
\Box\phi &= \frac{1}{2}\sum_I \frac{a_I\,e^{a_I\phi}}{n_I!}G_{\mu_1\cdots\mu_{n_I}}G^{\mu_1\cdots\mu_{n_I}} . \qquad \text{(A.2)}
\end{aligned}$$

The solutions (2.1.4), (4.1.4), (4.4.2), and (5.1.1), appropriately transformed into Einstein frame, were explicitly checked to satisfy the equations of motion above by using the Tensor package of MAPLE® computer algebra software.

[1] See *e.g.* refs [111, 112].

Appendix B

Some Facts about the K3 Manifold

K3 is a four dimensional Ricci-flat simply connected compact Kähler manifold with holonomy group $SU(2)$. There are no non-trivial 1-cycles on $K3$ (unlike on tori), but instead one 0-cycle, 22 2-cycles (19 of them self-dual, 3 anti-self-dual), and one 4-cycle.

Although no explicit metric for K3 is known, its various properties can still be determined. Its Euler characteristic $\chi(K3)$ may be found for example by using the fact that K3 has $T^4/\mathbb{Z}_N$, $N \in \{2,3,4,6\}$ orbifolds as a geometrical limits [192,193]. The answer is 24. This reveals something about the K3 curvature, since the Euler characteristic can be written (in two ways)

$$\begin{aligned}
\chi(K3) &= \frac{1}{32\pi^2}\int_{K3}\sqrt{g}\left(R_{abcd}R^{abcd} - 4R_{ab}R^{ab} + R^2\right) \\
&= \frac{1}{32\pi^2}\int_{K3}\sqrt{g}\epsilon_{abcd}R^{ab}R^{cd} \\
&= -\frac{1}{16\pi^2}\int_{K3}\mathrm{Tr}\, R\wedge R \qquad \text{(B.1)} \\
&= 24\,. \qquad \text{(B.2)}
\end{aligned}$$

In particular it determines the Pontryagin class

$$p_1 = -\frac{1}{8\pi^2}\mathrm{Tr}R\wedge R \;= 48\,, \qquad \text{(B.3)}$$

a quantity we need in the computation (2.1.1).

Type IIA strings on $K3$

Compactification of type IIA superstrings on K3 breaks half of the supersymmetry and gives the following massless fields. First coming by direct dimensional reduction there are the 6 dimensional metric $g_{\mu\nu}$ and the B-field $B_{\mu\nu}$ from the NS-NS sector, together with the 1-form $C^{(1)}$ and the 3-form $C^{(3)}$ fields from the R-R sector. In addition we get 22 1-forms from integrating the 10 dimensional R-R 3-form on various $K3$ 2-cycles. Actually in 6 dimensions the 3-form is dual to the 1-form, so all together we have 24 1-form fields in the massless spectrum. (Alternatively we could have taken 5-form which in ten dimensions is dual to the three 3-form, and integrated it over the 4-cycle of $K3$, the result would again give a 1-form in six dimensions.) In addition we get 81 scalars: 58 moduli parametrising the K3 metric (corresponding to independent deformations of Kähler structure and complex structure), 22 moduli from integrating the B-field over 22 2-cycles, and finally the dilaton.

Enhanced gauge symmetry

Type II string theory on K3 is S-dual to heterotic strings on T^4 [27,28]. At certain points in the moduli space of the heterotic theory the $U(1)^{24}$ gauge symmetry gets enhanced [194]. To realise this for type IIA on $K3$ we have two possibilities [195]:

- Enhanced gauge symmetries correspond to the orbifold singularities of the $K3$ surface. These singularities have an A-D-E classification just like the enhanced gauge symmetries [28,196]. Actually an orbifold singularity is not a sufficient condition for an enhanced gauge symmetry, one also has to tune the B-field to a right value [198]. The basic physical mechanism behind this case is that there are nearly massless solitons where appropriate 2-branes wrap around the vanishing 2-cycles [36,197].

- Alternatively enhanced gauge symmetry my arise when the $K3$ surface is very small and is given just the right (possibly smooth) shape [195]. The enhançon mechanism is an example of this case.

Appendix C

Magnetic Monopoles in SU(2) Gauge Theory

The model

We consider a gauge field $\mathbf{W} = W_\mu^a \mathbf{T}_a$ and Higgs field $\mathbf{H} = H^a \mathbf{T}_a$, both in the adjoint representation of $SU(2)$, $\mathbf{T}_a$ representing the generators of the gauge group. The model is given by the lagrangian density

$$\mathcal{L} = -\frac{1}{4} F_{\mu\nu}^a F^{a\ \mu\nu} - \frac{1}{2} D^\mu H^a D_\mu H^a - V(H) \tag{C.1}$$

where

$$F_{\mu\nu}^a = \partial_\mu A_\nu^a - \partial_\nu A_\mu^a + ie\epsilon^{abc} A_\mu^b A_\nu^c \tag{C.2}$$

$$D_\mu H^a = \partial_\mu H^a + ie\epsilon^{abc} A_\mu^b H^c \tag{C.3}$$

and the Higgs potential

$$V(H) = \frac{\lambda}{4} \left(H^a H^a - v^2 \right)^2 . \tag{C.4}$$

It is also useful to define $SU(2)$ electric and magnetic vectors

$$F_{0i}^a = -E_i^a , \qquad F_{ij}^a = \epsilon_{ijk} B_k^a \tag{C.5}$$

so that the energy density can be written

$$\mathcal{E} = \frac{1}{2} \left(E_i^a E_i^a + B_i^a B_i^a \right) + \frac{1}{2} D^0 H^a D_0 H^a + \frac{1}{2} D^i H^a D_i H^a + \frac{\lambda}{4} \left(H^a H^a - v^2 \right)^2 . \tag{C.6}$$

The full vacuum is given by a configuration with a vanishing gauge field and a constant Higgs field lying in the minimum of its potential (C.4). We may also define the "Higgs vacuum" where only the last three terms in (C.6) are zero.

For finite energy solutions it is necessary that the spatial integral $E = \int d^3x\ \mathcal{E}$ exists, hence the fields must approach their vacuum configuration asymptotically.

"Higgsing"

When the Higgs field resides in the minimum of its potential (C.4), the original $SU(2)$ gauge symmetry is broken to $U(1)$. To explore the resulting perturbative spectrum of the model, we have take the lagrangian (C.1) and expand the Higgs around its minimum

$$H^a = v^a + h^a, \qquad v^a v^a = v^2, \tag{C.7}$$

where $\mathbf{v} = v^a \mathbf{T}_a$ is a vector in $SU(2)$ space (it can point to different directions at different points in space-time, but has always the same magnitude v), and h^a are small oscillations (they depend on the space-time coordinates as well).

It is useful to distinguish between the Higgs oscillations parallel to $\mathbf{v}$ (in the $SU(2)$ sense)

$$h = \frac{1}{v}\ v^a H^a \tag{C.8}$$

and the ones that are orthogonal. Substituting the expansion (C.7) into Higgs potential (C.4) we find that the "parallel" component (C.8) retains mass, while the "orthogonal" ones get no mass term.

Further on, the "parallel" component of the gauge field

$$A_\mu = \frac{1}{v}\ v^a A^a_\mu \tag{C.9}$$

can be identified with a photon, as it remains massless and exhibits unbroken $U(1)$ gauge invariance, while the "orthogonal" gauge field components become massive. We may call the latter $W^\pm_\mu$, because they couple to the photon.

It also turns out that the "parallel" component of Higgs (C.8) is not charged under the unbroken $U(1)$, while the "orthogonal" components are. Actually, we should think of the "orthogonal" Higgs components as being absorbed into $W^\pm_\mu$,

since they are not physical and can be gauged away if we adopt a suitable gauge (of $SU(2)$). To summarise here is the perturbative spectrum after "higgsing":

Field	Mass	Electric charge
A_μ	0	0
h	$m_h = v\sqrt{2\lambda}$	0
$W_\mu^\pm$	$m_W = ve$	$q = \pm e$

Table C.1: Perturbative spectrum after "higgsing".

't Hooft-Polyakov ansatz

In the Higgs vacuum $H^a = v^a$, the "parallel" (photon) component of the gauge field strength turns out to be

$$\begin{aligned} F_{\mu\nu} &= \frac{1}{v}\, v^a F^a_{\mu\nu} \\ &= \partial_\mu A_\nu - \partial_\nu A_\mu - \frac{1}{ev^3}\, \epsilon_{abc} v^a \partial_\mu v^b \partial_\nu v^c, \end{aligned} \tag{C.10}$$

which reduces to the usual Maxwell field strength if $v^a = const$, i.e. $\mathbf{v}$ points to the same $SU(2)$ direction everywhere. On the other hand, even when A_μ is zero (in the full vacuum for example), the field strength (C.10) may still be upheld by the Higgs field staying in its vacuum.

This explains how a monopole can be a finite energy solution, but still have non-zero magnetic flux at spatial infinity giving magnetic charge

$$\begin{aligned} g &= \int_{S^2_\infty} B_i dS^i = \frac{1}{ev^3} \int_{S^2_\infty} \epsilon_{ijk}\epsilon_{abc} v^a \partial_j v^b \partial_k v^c \; dS_i \\ &= \frac{4\pi N}{e}, \end{aligned} \tag{C.11}$$

where N is an integer (the winding number of the Higgs field configuration).

To construct such finite energy magnetically charged solutions we will rely on a

simplifying ansatz due to 't Hooft and Polyakov [199,200]

$$\begin{aligned} H^a &= \frac{x^a}{er^2}F(ver) \\ A_i^a &= -\epsilon^a{}_{ij}\frac{x^j}{er^2}(1-K(ver)) \\ A_0^a &= 0, \end{aligned} \tag{C.12}$$

notice the mixing of $SU(2)$ and space-time indices, $r=\sqrt{x^i x^i}$ is the radial coordinate in space-time. This ansatz will yield a finite energy configuration provided the following boundary conditions are satisfied

$$\begin{aligned} &K(ver)\to 1, \qquad F(ver)\to 0, \qquad && r\to 0; \\ &K(ver)\to 0, \qquad \frac{F(ver)}{ver}\to 1, \qquad && r\to\infty. \end{aligned} \tag{C.13}$$

It remains to substitute this ansatz into the equations of motion and solve for the functions $F(ver)$ and $K(ver)$. This is not so easy, but explicit solutions of this kind are available in a certain limit known as BPS.

Going BPS

Bogomol'nyi pointed out a clever trick how to derive a bound for the energy (mass) of configurations with non-zero magnetic charge [201]

$$\begin{aligned} E_M &= \frac{1}{2}\int d^3x\,(\ldots + B_i^a B_i^a + D^i H^a D_i H^a + \ldots) \\ &= \frac{1}{2}\int d^3x\,(\ldots + (B_i^a - D_i H^a)^2 + 2B_i^a D_i H^a + \ldots) \\ &= \frac{1}{2}\int d^3x\,(\ldots + (B_i^a - D_i H^a)^2 + \ldots) + \int_{S^2_\infty} B_i^a H^a dS^i \\ &= \frac{1}{2}\int d^3x\,(\ldots + (B_i^a - D_i H^a)^2 + \ldots) + \frac{4\pi v}{e} \end{aligned} \tag{C.14}$$

where we used Bianchi identity ($D_i B_i^a = 0$), integration by parts and finally the result (C.11) together with an assumption that the configuration will approach Higgs vacuum asymptotically. All terms in the first integral are quadratic, hence we have found a nice bound for the energy

$$E_M \geq \frac{4\pi v}{e}. \tag{C.15}$$

If we consider a static configuration with vanishing electric field, the Bogomol'nyi bound (C.15) above is saturated provided

$$\begin{aligned} V(H) &= 0, \\ B_i^a &= D_i H^a, \end{aligned} \tag{C.16}$$

the latter known as the Bogomol'nyi equations.

Symmetry breaking from $SU(2)$ to $U(1)$ with vanishing potential (C.16) will still make sense in limit proposed by Prasad and Sommerfield [202]. We let $\lambda \to 0$, but demand that $H^a H^a = v^2$ still holds at spatial infinity. From table (C) it also becomes clear that the Higgs field is massless in this limit.

Now it is possible to write down an explicit solution [202]

$$H^a = \frac{x^a}{er^2}\left(ver\coth(ver) - 1\right) \tag{C.17}$$

$$A_i^a = -\epsilon^a{}_{ij}\frac{x^j}{er^2}\left(1 - \frac{ver}{\sinh(ver)}\right). \tag{C.18}$$

Outside the monopole there is just a radial $U(1)$ magnetic field, while the Higgs is sitting in the minimum of its potential. Inside the monopole core Higgs vanishes, $W^{\pm}$ are excited, but the solution is not singular.

To conclude the story, this is the full BPS spectrum of the theory:

Field	Mass	Electric charge	Magnetic charge
A_μ	0	0	0
h	0	0	0
$W_\mu^{\pm}$	$m_W = ve$	$q = \pm e$	0
$M^{\pm}$	$m_M = \frac{4\pi v}{e}$	0	$g = \pm\frac{4\pi}{e}$

Table C.2: The full BPS spectrum.

Appendix D

Extrinsic Curvature

Consider a space-time M with coordinates x^μ and a metric $G_{\mu\nu}$. A general hypersurface Σ within M deserves its own coordinates ξ^A, and so it is specified by an equation of the form $f(x^\mu(\xi^A)) = 0$. A unit vector normal to this hypersurface is

$$n_\mu^\pm = \mp\sigma \frac{\partial f}{\partial x^\mu} , \quad \text{where } \sigma = \left| G^{\mu\nu} \frac{\partial f}{\partial x^\mu} \frac{\partial f}{\partial x^\nu} \right|^{-1/2} . \tag{D.1}$$

The extrinsic curvature of the surface is given by the pullback of the covariant derivative of the normal vector:

$$K_{AB} = \frac{\partial x^\mu}{\partial \xi^A} \frac{\partial x^\nu}{\partial \xi^B} \nabla_\mu n_\nu = -n_\mu \left(\frac{\partial^2 x^\mu}{\partial \xi^A \partial \xi^B} + \Gamma^\mu_{\nu\rho} \frac{\partial x^\nu}{\partial \xi^A} \frac{\partial x^\rho}{\partial \xi^B} \right) \tag{D.2}$$

and it is a tensor in the space-time Σ.

In special symmetric cases the formulas simplify considerably. Extrinsic curvature for a spherical shell is given in equation (2.5.4) and for an axially symmetric shell in (4.3.3).

Bibliography

[1] L. Järv and C. V. Johnson, *Orientifolds, M-theory, and the ABCD's of the enhançon*, Phys. Rev. D **62** (2000) 126010 [arXiv:hep-th/0002244].

[2] L. M. Dyson, L. Järv and C. V. Johnson, *Oblate, toroidal, and other shapes for the enhançon*, JHEP **0205** (2002) 019 [arXiv:hep-th/0112132].

[3] L. M. Dyson, L. Järv and C. V. Johnson, to appear.

[4] C. D. Hoyle, U. Schmidt, B. R. Heckel, E. G. Adelberger, J. H. Gundlach, D. J. Kapner and H. E. Swanson, *Sub-millimeter tests of the gravitational inverse-square law: A search for 'large' extra dimensions*, Phys. Rev. Lett. **86** (2001) 1418 [arXiv:hep-ph/0011014].

G. L. Smith, C. D. Hoyle, J. H. Gundlach, E. G. Adelberger, B. R. Heckel and H. E. Swanson, *Short Range Tests Of The Equivalence Principle*, Phys. Rev. D **61** (2000) 022001.

[5] J. R. Friedman, V. Patel, W. Chen, S. K. Tolpygo, J. E. Lukens, *Quantum superposition of distinct macroscopic states*, Nature **406**, (2000) 43 [arXiv:cond-mat/0004293].

[6] K. Hagiwara *et al.* [Particle Data Group Collaboration], *Review Of Particle Physics*, Phys. Rev. D **66** (2002) 010001 [URL: http://pdg.lbl.gov].

[7] R. Penrose, *Wavefunction Collapse as a Real Gravitational Effect*, in "Mathematical Physics 2000" edited by A. S. Fokas et. al., Imperial College Press, 2000.

[8] G. 't Hooft and M. J. Veltman, *One Loop Divergencies In The Theory Of Gravitation*, Annales Poincare Phys. Theor. A **20** (1974) 69.

[9] M. H. Goroff and A. Sagnotti, *The Ultraviolet Behavior Of Einstein Gravity*, Nucl. Phys. B **266** (1986) 709.

[10] A. E. van de Ven, *Two loop quantum gravity*, Nucl. Phys. B **378** (1992) 309.

[11] Z. Bern, L. J. Dixon, D. C. Dunbar, M. Perelstein and J. S. Rozowsky, *On the relationship between Yang-Mills theory and gravity and its implication for ultraviolet divergences*, Nucl. Phys. B **530** (1998) 401 [arXiv:hep-th/9802162].

[12] R. Penrose, *Gravitational Collapse and Space-Time Singularities*, Phys. Rev. Lett. **14** (1965) 57.

[13] S. W. Hawking, *The Occurrence of Singularities in Cosmology. III. Causality and Singularities*, Proc. Roy. Soc. Lond. A **300** (1967) 182.

[14] S. W. Hawking and R. Penrose, *The Singularities Of Gravitational Collapse And Cosmology*, Proc. Roy. Soc. Lond. A **314** (1970) 529.

[15] V. Mukhanov and R. H. Brandenberger, *A Nonsingular universe*, Phys. Rev. Lett. **68** (1992) 1969.

R. H. Brandenberger, V. Mukhanov and A. Sornborger, *A Cosmological theory without singularities*, Phys. Rev. D **48** (1993) 1629 [arXiv:gr-qc/9303001].

[16] G. W. Gibbons, G. T. Horowitz and P. K. Townsend, *Higher dimensional resolution of dilatonic black hole singularities*, Class. Quant. Grav. **12** (1995) 297 [arXiv:hep-th/9410073].

[17] G. T. Horowitz and R. C. Myers, *The value of singularities*, Gen. Rel. Grav. **27** (1995) 915 [arXiv:gr-qc/9503062].

[18] M. B. Green, J. H. Schwarz and E. Witten, "Superstring Theory" Vols. I and II (Cambridge Monographs On Mathematical Physics), Cambridge University Press, 1987.

[19] J. Polchinski, "String Theory" Vols. I and II (Cambridge Monographs On Mathematical Physics), Cambridge University Press, 1998.

[20] K. Ezawa, *Nonperturbative solutions for canonical quantum gravity: An overview*, Phys. Rept. **286** (1997) 271 [arXiv:gr-qc/9601050].

[21] C. Rovelli, *Loop quantum gravity*, Living Rev. Rel. **1** (1998) 1 [arXiv:gr-qc/9710008].

[22] A. Ashtekar, *Quantum geometry and gravity: Recent advances*, arXiv:gr-qc/0112038.

[23] J. C. Baez (Editor), "Knots and Quantum Gravity" (Oxford Lecture Series in Mathematics and Its Applications, No 1), Clarendon Press, 1994.

[24] G. T. Horowitz, *Quantum gravity at the turn of the millennium*, arXiv:gr-qc/0011089.

[25] S. Carlip, *Quantum gravity: A progress report*, Rept. Prog. Phys. **64** (2001) 885 [arXiv:gr-qc/0108040].

[26] G. Amelino-Camelia, *Quantum-gravity phenomenology: Status and prospects*, Mod. Phys. Lett. A **17** (2002) 899 [arXiv:gr-qc/0204051].

[27] C. M. Hull and P. K. Townsend, *Unity of superstring dualities*, Nucl. Phys. B **438** (1995) 109 [arXiv:hep-th/9410167].

[28] E. Witten, *String theory dynamics in various dimensions*, Nucl. Phys. B **443** (1995) 85 [arXiv:hep-th/9503124].

[29] P. K. Townsend, *The eleven-dimensional supermembrane revisited*, Phys. Lett. B **350** (1995) 184 [arXiv:hep-th/9501068].

[30] J. Polchinski, *Dirichlet-Branes and Ramond-Ramond Charges*, Phys. Rev. Lett. **75** (1995) 4724 [arXiv:hep-th/9510017].

[31] M. Natsuume, *The singularity problem in string theory*, arXiv:gr-qc/0108059.

[32] L. J. Dixon, J. A. Harvey, C. Vafa and E. Witten, *Strings On Orbifolds*, Nucl. Phys. B **261** (1985) 678.

[33] P. S. Aspinwall, B. R. Greene and D. R. Morrison, *Multiple mirror manifolds and topology change in string theory*, Phys. Lett. B **303** (1993) 249 [arXiv:hep-th/9301043].

P. S. Aspinwall, B. R. Greene and D. R. Morrison, *Calabi-Yau moduli space, mirror manifolds and spacetime topology change in string theory*, Nucl. Phys. B **416** (1994) 414 [arXiv:hep-th/9309097].

[34] E. Witten, *Phases of $N = 2$ theories in two dimensions*, Nucl. Phys. B **403** (1993) 159 [arXiv:hep-th/9301042].

[35] B. R. Greene, D. R. Morrison and A. Strominger, *Black hole condensation and the unification of string vacua*, Nucl. Phys. B **451** (1995) 109 [arXiv:hep-th/9504145].

[36] A. Strominger, *Massless black holes and conifolds in string theory*, Nucl. Phys. B **451** (1995) 96 [arXiv:hep-th/9504090].

[37] R. H. Brandenberger and C. Vafa, *Superstrings In The Early Universe*, Nucl. Phys. B **316** (1989) 391.

[38] M. Gasperini and G. Veneziano, *Pre - big bang in string cosmology*, Astropart. Phys. **1** (1993) 317 [arXiv:hep-th/9211021].

[39] R. Brustein and R. Madden, *Graceful exit and energy conditions in string cosmology*, Phys. Lett. B **410** (1997) 110 [arXiv:hep-th/9702043].

[40] N. Seiberg, *From big crunch to big bang - is it possible?*, arXiv:hep-th/0201039.

[41] J. Khoury, B. A. Ovrut, N. Seiberg, P. J. Steinhardt and N. Turok, *From big crunch to big bang*, Phys. Rev. D **65** (2002) 086007 [arXiv:hep-th/0108187].

[42] V. Balasubramanian, S. F. Hassan, E. Keski-Vakkuri and A. Naqvi, *A space-time orbifold: A toy model for a cosmological singularity*, arXiv:hep-th/0202187.

[43] N. A. Nekrasov, *Milne universe, tachyons, and quantum group*, arXiv:hep-th/0203112.

[44] L. Cornalba and M. S. Costa, *A New Cosmological Scenario in String Theory*, arXiv:hep-th/0203031.

[45] H. Liu, G. Moore and N. Seiberg, *Strings in time-dependent orbifolds*, arXiv:hep-th/0206182.

[46] S. Elitzur, A. Giveon, D. Kutasov and E. Rabinovici, *From big bang to big crunch and beyond*, JHEP **0206** (2002) 017 [arXiv:hep-th/0204189].

[47] L. Cornalba, M. S. Costa and C. Kounnas, *A resolution of the cosmological singularity with orientifolds*, arXiv:hep-th/0204261.

[48] B. Craps, D. Kutasov and G. Rajesh, *String propagation in the presence of cosmological singularities*, JHEP **0206** (2002) 053 [arXiv:hep-th/0205101].

[49] S. Kachru and L. McAllister, *Bouncing brane cosmologies from warped string compactifications*, arXiv:hep-th/0205209.

[50] J. M. Maldacena, *The large N limit of superconformal field theories and supergravity*, Adv. Theor. Math. Phys. **2** (1998) 231 [Int. J. Theor. Phys. **38** (1999) 1113] [arXiv:hep-th/9711200].

[51] S. S. Gubser, I. R. Klebanov and A. M. Polyakov, *Gauge theory correlators from non-critical string theory*, Phys. Lett. B **428** (1998) 105 [arXiv:hep-th/9802109].

[52] E. Witten, *Anti-de Sitter space and holography*, Adv. Theor. Math. Phys. **2** (1998) 253 [arXiv:hep-th/9802150].

[53] O. Aharony, S. S. Gubser, J. M. Maldacena, H. Ooguri and Y. Oz, *Large N field theories, string theory and gravity*, Phys. Rept. **323** (2000) 183 [arXiv:hep-th/9905111].

[54] S. S. Gubser, *Curvature singularities: The good, the bad, and the naked*, Adv. Theor. Math. Phys. **4** (2002) 679 [arXiv:hep-th/0002160].

[55] J. Polchinski and M. J. Strassler, *The string dual of a confining four-dimensional gauge theory*, arXiv:hep-th/0003136.

[56] I. Bena, *The M-theory dual of a 3 dimensional theory with reduced supersymmetry*, Phys. Rev. D **62** (2000) 126006 [arXiv:hep-th/0004142].

[57] O. Aharony and A. Rajaraman, *String theory duals for mass-deformed SO(N) and USp(2N) N = 4 SYM theories*, Phys. Rev. D **62** (2000) 106002 [arXiv:hep-th/0004151].

[58] I. Bena and A. Nudelman, *Warping and vacua of (S)YM(2+1)*, Phys. Rev. D **62** (2000) 086008 [arXiv:hep-th/0005163].

[59] I. Bena and A. Nudelman, *Exotic polarizations of D2 branes and oblique vacua of (S)YM(2+1)*, Phys. Rev. D **62** (2000) 126007 [arXiv:hep-th/0006102].

[60] M. Cvetič, H. Lu and C. N. Pope, *Brane resolution through transgression*, Nucl. Phys. B **600** (2001) 103 [arXiv:hep-th/0011023].

[61] R. C. Myers, *Dielectric-branes*, JHEP **9912** (1999) 022 [arXiv:hep-th/9910053].

[62] I. R. Klebanov and A. A. Tseytlin, *Gravity duals of supersymmetric SU(N) x SU(N+M) gauge theories*, Nucl. Phys. B **578** (2000) 123 [arXiv:hep-th/0002159].

[63] I. R. Klebanov and M. J. Strassler, *Supergravity and a confining gauge theory: Duality cascades and chiSB-resolution of naked singularities*, JHEP **0008** (2000) 052 [arXiv:hep-th/0007191].

[64] K. Pilch and N. P. Warner, *N = 2 supersymmetric RG flows and the IIB dilaton*, Nucl. Phys. B **594** (2001) 209 [arXiv:hep-th/0004063].

[65] A. Brandhuber and K. Sfetsos, *An N = 2 gauge theory and its supergravity dual*, Phys. Lett. B **488** (2000) 373 [arXiv:hep-th/0004148].

[66] A. Buchel, A. W. Peet and J. Polchinski, *Gauge dual and noncommutative extension of an $N = 2$ supergravity solution*, Phys. Rev. D **63** (2001) 044009 [arXiv:hep-th/0008076].

[67] N. Evans, C. V. Johnson and M. Petrini, *The enhancon and $N = 2$ gauge theory/gravity RG flows*, JHEP **0010** (2000) 022 [arXiv:hep-th/0008081].

[68] I. R. Klebanov and N. A. Nekrasov, *Gravity duals of fractional branes and logarithmic RG flow*, Nucl. Phys. B **574** (2000) 263 [arXiv:hep-th/9911096].

[69] M. Graña and J. Polchinski, *Gauge / gravity duals with holomorphic dilaton*, Phys. Rev. D **65** (2002) 126005 [arXiv:hep-th/0106014].

[70] M. Bertolini, P. Di Vecchia, M. Frau, A. Lerda, R. Marotta and I. Pesando, *Fractional D-branes and their gauge duals*, JHEP **0102** (2001) 014 [arXiv:hep-th/0011077].

[71] J. Polchinski, *$N = 2$ gauge-gravity duals*, Int. J. Mod. Phys. A **16** (2001) 707 [arXiv:hep-th/0011193].

[72] O. Aharony, *A note on the holographic interpretation of string theory backgrounds with varying flux*, JHEP **0103** (2001) 012 [arXiv:hep-th/0101013].

[73] M. Petrini, R. Russo and A. Zaffaroni, *$N = 2$ gauge theories and systems with fractional branes*, Nucl. Phys. B **608** (2001) 145 [arXiv:hep-th/0104026].

[74] M. Billo, L. Gallot and A. Liccardo, *Classical geometry and gauge duals for fractional branes on ALE orbifolds*, Nucl. Phys. B **614** (2001) 254 [arXiv:hep-th/0105258].

[75] M. Bertolini, P. Di Vecchia, M. Frau, A. Lerda and R. Marotta, *$N = 2$ gauge theories on systems of fractional D3/D7 branes*, Nucl. Phys. B **621** (2002) 157 [arXiv:hep-th/0107057].

[76] A. Fayyazuddin and D. J. Smith, *Warped AdS near-horizon geometry of completely localized intersections of M5-branes*, JHEP **0010** (2000) 023 [arXiv:hep-th/0006060].

B. Brinne, A. Fayyazuddin, S. Mukhopadhyay and D. J. Smith, *Supergravity M5-branes wrapped on Riemann surfaces and their QFT duals*, JHEP **0012** (2000) 013 [arXiv:hep-th/0009047].

[77] J. P. Gauntlett, N. Kim, D. Martelli and D. Waldram, *Wrapped fivebranes and $N = 2$ super Yang-Mills theory*, Phys. Rev. D **64** (2001) 106008 [arXiv:hep-th/0106117].

[78] F. Bigazzi, A. L. Cotrone and A. Zaffaroni, *$N = 2$ gauge theories from wrapped five-branes*, Phys. Lett. B **519** (2001) 269 [arXiv:hep-th/0106160].

[79] C. V. Johnson, A. W. Peet and J. Polchinski, *Gauge theory and the excision of repulson singularities*, Phys. Rev. D **61** (2000) 086001 [arXiv:hep-th/9911161].

[80] K. Behrndt, *About a class of exact string backgrounds*, Nucl. Phys. B **455** (1995) 188 [arXiv:hep-th/9506106].

[81] R. Kallosh and A. D. Linde, *Exact supersymmetric massive and massless white holes*, Phys. Rev. D **52** (1995) 7137 [arXiv:hep-th/9507022].

[82] M. Cvetič and D. Youm, *Singular BPS saturated states and enhanced symmetries of four-dimensional N=4 supersymmetric string vacua*, Phys. Lett. B **359** (1995) 87 [arXiv:hep-th/9507160].

[83] C. V. Johnson, R. C. Myers, A. W. Peet and S. F. Ross, *The enhançon and the consistency of excision*, Phys. Rev. D **64** (2001) 106001 [arXiv:hep-th/0105077].

[84] K. Maeda, T. Torii, M. Narita and S. Yahikozawa, *The stability of the shell of D2-D6 branes in a $N = 2$ supergravity solution*, Phys. Rev. D **65** (2002) 024030 [hep-th/0107060].

[85] A. Dimitriadis and S. F. Ross, *Stability of the non-extremal enhancon solution. I: Perturbation equations*, arXiv:hep-th/0207183.

[86] C. V. Johnson, *Enhançons, fuzzy spheres and multi-monopoles*, Phys. Rev. D **63** (2001) 065004 [hep-th/0004068].

[87] C. V. Johnson, *The enhançon, multimonopoles and fuzzy geometry*, Int. J. Mod. Phys. A **16** (2001) 990 [hep-th/0011008].

[88] M. Wijnholt and S. Zhukov, *Inside an enhancon: Monopoles and dual Yang-Mills theory*, [hep-th/0110109].

[89] D. Astefanesei and R. C. Myers, *A new wrinkle on the enhancon*, JHEP **0202** (2002) 043 [arXiv:hep-th/0112133].

[90] C. V. Johnson and R. C. Myers, *The enhançon, black holes, and the second law*, Phys. Rev. D **64** (2001) 106002 [arXiv:hep-th/0105159].

[91] N. R. Constable, *The entropy of 4D black holes and the enhançon*, Phys. Rev. D **64** (2001) 104004 [arXiv:hep-th/0106038].

[92] A. Karch, D. Lüst and D. J. Smith, *Equivalence of geometric engineering and Hanany-Witten via fractional branes*, Nucl. Phys. B **533** (1998) 348 [arXiv:hep-th/9803232].

[93] K. Dasgupta and S. Mukhi, *Brane constructions, fractional branes and anti-de Sitter domain walls*, JHEP **9907** (1999) 008 [arXiv:hep-th/9904131].

[94] M. Frau, A. Liccardo and R. Musto, *The geometry of fractional branes*, Nucl. Phys. B **602** (2001) 39 [arXiv:hep-th/0012035].

[95] P. Bain, *Fractional D3-branes in diverse backgrounds*, arXiv:hep-th/0112145.

[96] P. Merlatti, *About the enhançon mechanism*, arXiv:hep-th/0112107.

[97] M. Natsuume, *The heterotic enhançon*, Phys. Rev. D **65** (2002) 086002 [arXiv:hep-th/0111044].

[98] R. Kallosh, T. Mohaupt and M. Shmakova, *Excision of singularities by stringy domain walls*, J. Math. Phys. **42** (2001) 3071 [arXiv:hep-th/0010271].

[99] P. Berglund, T. Hubsch and D. Minic, *Probing naked singularities in non-supersymmetric string vacua*, JHEP **0102** (2001) 010 [arXiv:hep-th/0012042].

[100] P. Berglund, T. Hubsch and D. Minic, *On relativistic brane probes in singular spacetimes*, JHEP **0101** (2001) 041 [arXiv:hep-th/0012180].

[101] C. V. Johnson, "D–Branes" (Cambridge Monographs On Mathematical Physics), Cambridge University Press, 2002.

[102] M. Gutperle and A. Strominger, *Spacelike branes*, JHEP **0204** (2002) 018 [arXiv:hep-th/0202210].

[103] C. M. Chen, D. V. Gal'tsov and M. Gutperle, *S-brane solutions in supergravity theories*, Phys. Rev. D **66** (2002) 024043 [arXiv:hep-th/0204071].

[104] M. Kruczenski, R. C. Myers and A. W. Peet, *Supergravity S-branes*, JHEP **0205** (2002) 039 [arXiv:hep-th/0204144].

[105] A. Sen, *Stable non-BPS states in string theory*, JHEP **9806** (1998) 007 [arXiv:hep-th/9803194].

A. Sen, *Stable non-BPS bound states of BPS D-branes*, JHEP **9808** (1998) 010 [arXiv:hep-th/9805019].

A. Sen, *Tachyon condensation on the brane antibrane system*, JHEP **9808**, 012 (1998) [arXiv:hep-th/9805170].

O. Bergman and M. R. Gaberdiel, *Stable non-BPS D-particles*, Phys. Lett. B **441** (1998) 133 [arXiv:hep-th/9806155].

[106] A. Sen, *Non-BPS states and branes in string theory*, arXiv:hep-th/9904207.

[107] M. R. Gaberdiel, *Lectures on non-BPS Dirichlet branes*, Class. Quant. Grav. **17** (2000) 3483 [arXiv:hep-th/0005029].

[108] E. Cremmer, I. V. Lavrinenko, H. Lu, C. N. Pope, K. S. Stelle and T. A. Tran, *Euclidean-signature supergravities, dualities and instantons*, Nucl. Phys. B **534** (1998) 40 [arXiv:hep-th/9803259].

[109] C. M. Hull, *Timelike T-duality, de Sitter space, large N gauge theories and topological field theory*, JHEP **9807** (1998) 021 [arXiv:hep-th/9806146].

[110] G. T. Horowitz and A. Strominger, *Black Strings And P-Branes*, Nucl. Phys. B **360** (1991) 197.

[111] M. J. Duff, R. R. Khuri and J. X. Lu, *String solitons*, Phys. Rept. **259** (1995) 213 [arXiv:hep-th/9412184].

[112] K. S. Stelle, *BPS branes in supergravity*, arXiv:hep-th/9803116.

[113] R. G. Leigh, *Dirac-Born-Infeld Action From Dirichlet Sigma Model*, Mod. Phys. Lett. A **4** (1989) 2767.

[114] M. R. Douglas, *Branes within branes*, arXiv:hep-th/9512077.

[115] M. Li, *Boundary States of D-Branes and Dy-Strings*, Nucl. Phys. B **460** (1996) 351 [arXiv:hep-th/9510161].

[116] M. Bershadsky, C. Vafa and V. Sadov, *D-Branes and Topological Field Theories*, Nucl. Phys. B **463** (1996) 420 [arXiv:hep-th/9511222].

[117] M. B. Green, J. A. Harvey and G. W. Moore, *I-brane inflow and anomalous couplings on D-branes*, Class. Quant. Grav. **14** (1997) 47 [arXiv:hep-th/9605033].

[118] K. Dasgupta, D. P. Jatkar and S. Mukhi, *Gravitational couplings and Z(2) orientifolds*, Nucl. Phys. B **523** (1998) 465 [arXiv:hep-th/9707224].

[119] C. P. Bachas, P. Bain and M. B. Green, *Curvature terms in D-brane actions and their M-theory origin*, JHEP **9905** (1999) 011 [arXiv:hep-th/9903210].

[120] A. A. Tseytlin, *On non-abelian generalisation of the Born-Infeld action in string theory*, Nucl. Phys. B **501** (1997) 41 [arXiv:hep-th/9701125].

[121] R. C. Myers, *Nonabelian D-branes and noncommutative geometry*, Int. J. Mod. Phys. A **16** (2001) 956 [arXiv:hep-th/0106178].

[122] M. R. Douglas and C. M. Hull, *D-branes and the noncommutative torus*, JHEP **9802** (1998) 008 [arXiv:hep-th/9711165].

[123] N. Seiberg and E. Witten, *String theory and noncommutative geometry*, JHEP **9909** (1999) 032 [arXiv:hep-th/9908142].

[124] S. H. Shenker, *Another Length Scale in String Theory?*, arXiv:hep-th/9509132.

[125] M. R. Douglas, *Gauge Fields and D-branes*, J. Geom. Phys. **28** (1998) 255 [arXiv:hep-th/9604198].

[126] M. R. Douglas, D. Kabat, P. Pouliot and S. H. Shenker, *D-branes and short distances in string theory*, Nucl. Phys. B **485** (1997) 85 [arXiv:hep-th/9608024].

[127] C. V. Johnson, N. Kaloper, R. R. Khuri and R. C. Myers, *Is string theory a theory of strings?*, Phys. Lett. B **368** (1996) 71 [arXiv:hep-th/9509070].

[128] R. d. Sorkin, *Kaluza-Klein Monopole*, Phys. Rev. Lett. **51** (1983) 87.

[129] D. J. Gross and M. J. Perry, *Magnetic Monopoles In Kaluza-Klein Theories*, Nucl. Phys. B **226** (1983) 29.

[130] R. R. Khuri, *A Multimonopole solution in string theory*, Phys. Lett. B **294** (1992) 325 [arXiv:hep-th/9205051].

[131] R. R. Khuri, *A Heterotic multimonopole solution*, Nucl. Phys. B **387** (1992) 315 [arXiv:hep-th/9205081].

[132] J. P. Gauntlett, J. A. Harvey and J. T. Liu, *Magnetic monopoles in string theory*, Nucl. Phys. B **409** (1993) 363 [arXiv:hep-th/9211056].

[133] M. Krogh, *S-duality and tensionless 5-branes in compactified heterotic string theory*, JHEP **9912** (1999) 018 [arXiv:hep-th/9911084].

[134] A. Hanany and E. Witten, *Type IIB superstrings, BPS monopoles, and three-dimensional gauge dynamics*, Nucl. Phys. B **492** (1997) 152 [arXiv:hep-th/9611230].

[135] G. Darmois, "Memorial de Sciences Mathematiques," Fascicule XXV, *Les equations de la gravitation einsteinienne*, Chapitre V (1927).

[136] W. Israel, *Singular Hypersurfaces And Thin Shells In General Relativity*, Nuovo Cim. B **44S10** (1966) 1 [Erratum-ibid. B **48** (1967 NUCIA,B44,1.1966) 463].

[137] C. W. Misner, K. S. Thorne and J. A. Wheeler, "Gravitation" San Francisco: Freeman, 1973.

[138] C. Lanczos, *Flächenhafte Verteilung der Materie in der Einsteinschen Gravitationstheorie*, Ann. Phys. (Leipzig) **74** (1924) 518.

[139] L. Alvarez-Gaume and D. Z. Freedman, *Geometrical Structure And Ultraviolet Finiteness In The Supersymmetric Sigma Model*, Commun. Math. Phys. **80** (1981) 443.

[140] N. J. Hitchin, A. Karlhede, U. Lindstrom and M. Rocek, *Hyperkahler Metrics And Supersymmetry*, Commun. Math. Phys. **108** (1987) 535.

[141] P. K. Townsend, *D-branes from M-branes*, Phys. Lett. B **373** (1996) 68 [arXiv:hep-th/9512062].

[142] C. Schmidhuber, *D-brane actions*, Nucl. Phys. B **467** (1996) 146 [arXiv:hep-th/9601003].

[143] N. Seiberg and E. Witten, *Gauge dynamics and compactification to three dimensions*, in "Saclay 1996, The mathematical beauty of physics," 333-366 [arXiv:hep-th/9607163].

[144] G. Chalmers and A. Hanany, *Three dimensional gauge theories and monopoles*, Nucl. Phys. B **489** (1997) 223 [arXiv:hep-th/9608105].

[145] E. J. Weinberg, *Parameter Counting For Multi - Monopole Solutions*, Phys. Rev. D **20** (1979) 936.

[146] W. Nahm, *Interacting Monopoles*, Phys. Lett. B **85** (1979) 373.

[147] N. S. Manton, *A Remark On The Scattering Of Bps Monopoles*, Phys. Lett. B **110** (1982) 54.

[148] M. F. Atiyah and N. J. Hitchin, *Low-Energy Scattering Of Nonabelian Monopoles*, Phys. Lett. A **107** (1985) 21.

M. F. Atiyah and N. J. Hitchin, *Low-Energy Scattering Of Nonabelian Magnetic Monopoles*, Phil. Trans. Roy. Soc. Lond. A **315** (1985) 459.

[149] S. W. Hawking, *Gravitational Instantons*, Phys. Lett. A **60** (1977) 81.

[150] G. W. Gibbons and N. S. Manton, *Classical And Quantum Dynamics Of Bps Monopoles*, Nucl. Phys. B **274** (1986) 183.

[151] N. Dorey, V. V. Khoze, M. P. Mattis, D. Tong and S. Vandoren, *Instantons, three-dimensional gauge theory, and the Atiyah-Hitchin manifold*, Nucl. Phys. B **502** (1997) 59 [arXiv:hep-th/9703228].

[152] B. Craps and F. Roose, *Anomalous D-brane and orientifold couplings from the boundary state*, Phys. Lett. B **445** (1998) 150 [arXiv:hep-th/9808074].

B. Craps and F. Roose, *(Non-)anomalous D-brane and O-plane couplings: The normal bundle*, Phys. Lett. B **450** (1999) 358 [arXiv:hep-th/9812149].

[153] J. F. Morales, C. A. Scrucca and M. Serone, *Anomalous couplings for D-branes and O-planes*, Nucl. Phys. B **552** (1999) 291 [arXiv:hep-th/9812071].

[154] B. J. Stefanski, *Gravitational couplings of D-branes and O-planes*, Nucl. Phys. B **548** (1999) 275 [arXiv:hep-th/9812088].

[155] C. A. Scrucca and M. Serone, *Anomalies and inflow on D-branes and O-planes*, Nucl. Phys. B **556** (1999) 197 [arXiv:hep-th/9903145].

[156] S. Mukhi and N. V. Suryanarayana, *Gravitational couplings, orientifolds and M-planes*, JHEP **9909** (1999) 017 [arXiv:hep-th/9907215].

[157] J. H. Schwarz, *Lectures on superstring and M theory dualities*, Nucl. Phys. Proc. Suppl. **55B** (1997) 1 [arXiv:hep-th/9607201].

[158] C. Vafa and E. Witten, *A One loop test of string duality*, Nucl. Phys. B **447** (1995) 261 [arXiv:hep-th/9505053].

[159] M. J. Duff, J. T. Liu and R. Minasian, *Eleven-dimensional origin of string / string duality: A one-loop test*, Nucl. Phys. B **452** (1995) 261 [arXiv:hep-th/9506126].

[160] E. Witten, *Small Instantons in String Theory*, Nucl. Phys. B **460** (1996) 541 [arXiv:hep-th/9511030].

[161] E. G. Gimon and J. Polchinski, *Consistency Conditions for Orientifolds and D-Manifolds*, Phys. Rev. D **54** (1996) 1667 [arXiv:hep-th/9601038].

[162] A. Sen, *Dynamics of multiple Kaluza-Klein monopoles in M and string theory*, Adv. Theor. Math. Phys. **1** (1998) 115 [arXiv:hep-th/9707042].

[163] E. Witten, *Heterotic string conformal field theory and A-D-E singularities*, JHEP **0002** (2000) 025 [arXiv:hep-th/9909229].

[164] A. Sen, *A note on enhanced gauge symmetries in M- and string theory*, JHEP **9709** (1997) 001 [arXiv:hep-th/9707123].

[165] A. Sen, *Strong coupling dynamics of branes from M-theory*, JHEP **9710** (1997) 002 [arXiv:hep-th/9708002].

[166] P. Kraus, F. Larsen and S. P. Trivedi, *The Coulomb branch of gauge theory from rotating branes*, JHEP **9903** (1999) 003 [arXiv:hep-th/9811120].

[167] K. Sfetsos, *Branes for Higgs phases and exact conformal field theories*, JHEP **9901** (1999) 015 [arXiv:hep-th/9811167].

[168] J. G. Russo, *New compactifications of supergravities and large N QCD*, Nucl. Phys. B **543** (1999) 183 [arXiv:hep-th/9808117].

[169] T. Harmark and N. A. Obers, *Thermodynamics of spinning branes and their dual field theories*, JHEP **0001** (2000) 008 [arXiv:hep-th/9910036].

[170] I. Bakas and K. Sfetsos, *Gravitational domain walls and p-brane distributions*, Fortsch. Phys. **49** (2001) 419 [arXiv:hep-th/0012125].

[171] D. Z. Freedman, S. S. Gubser, K. Pilch and N. P. Warner, *Continuous distributions of D3-branes and gauged supergravity*, JHEP **0007** (2000) 038 [arXiv:hep-th/9906194].

[172] K. Sfetsos, *Rotating NS5-brane solution and its exact string theoretical description*, Fortsch. Phys. **48** (2000) 199 [arXiv:hep-th/9903201].

[173] P. Musgrave and K. Lake, *Junctions and thin shells in general relativity using computer algebra I: The Darmois-Israel Formalism*, Class. Quant. Grav. **13** (1996) 1885 [arXiv:gr-qc/9510052].

[174] S. P. Drake and R. Turolla, *The Application of the Newman-Janis Algorithm in Obtaining Interior Solutions of the Kerr Metric*, Class. Quant. Grav. **14** (1997) 1883 [arXiv:gr-qc/9703084].

[175] R. Mansouri and M. Khorrami, *Equivalence of Darmois-Israel and Distributional-Methods for Thin Shells in General Relativity*, J. Math. Phys. **37** (1996) 5672 [arXiv:gr-qc/9608029].

[176] M. F. Atiyah and N. J. Hitchin, "The Geometry And Dynamics Of Magnetic Monopoles" (M.B. Porter Lectures), Princeton University Press, 1988.

[177] C. A. Herdeiro, *Special properties of five dimensional BPS rotating black holes*, Nucl. Phys. B **582** (2000) 363 [arXiv:hep-th/0003063].

[178] H. W. Brinkmann, *Einstein spaces which are mapped conformally to each other*, Math. Ann. **95** (1925) 119.

[179] J. C. Breckenridge, R. C. Myers, A. W. Peet and C. Vafa, *D-branes and spinning black holes*, Phys. Lett. B **391** (1997) 93 [arXiv:hep-th/9602065].

[180] A. A. Tseytlin, *Extreme dyonic black holes in string theory*, Mod. Phys. Lett. A **11** (1996) 689 [arXiv:hep-th/9601177].

[181] A. R. Prasanna, *Inertial frame dragging and Mach's principle in general relativity*, Class. Quant. Grav. **14** (1997) 227 [arXiv:gr-qc/9607046].

[182] J. M. Bardeen, W. H. Press and S. A. Teukolsky, *Rotating black holes: locally nonrotating frames, energy extraction, and scalar synchroton radiation*, Astrophys. J. **178** (1972) 347.

[183] R. G. Cai, *Dynamics and thermodynamics of a probe brane in the multicenter and rotating D3-brane background*, JHEP **9909** (1999) 027 [arXiv:hep-th/9909077].

[184] J. P. Gauntlett, R. C. Myers and P. K. Townsend, *Black holes of $D = 5$ supergravity*, Class. Quant. Grav. **16** (1999) 1 [arXiv:hep-th/9810204].

[185] A. Strominger and C. Vafa, *Microscopic Origin of the Bekenstein-Hawking Entropy*, Phys. Lett. B **379** (1996) 99 [arXiv:hep-th/9601029].

[186] J. D. Bekenstein, *Black Holes And Entropy*, Phys. Rev. D **7** (1973) 2333.

S. W. Hawking, *Particle Creation By Black Holes*, Commun. Math. Phys. **43** (1975) 199.

[187] J. C. Breckenridge, D. A. Lowe, R. C. Myers, A. W. Peet, A. Strominger and C. Vafa, *Macroscopic and Microscopic Entropy of Near-Extremal Spinning Black Holes*, Phys. Lett. B **381** (1996) 423 [arXiv:hep-th/9603078].

[188] J. R. David, G. Mandal and S. R. Wadia, *Microscopic formulation of black holes in string theory*, arXiv:hep-th/0203048.

[189] A. W. Peet, *TASI lectures on black holes in string theory*, arXiv:hep-th/0008241.

[190] T. Mohaupt, *Black holes in supergravity and string theory*, Class. Quant. Grav. **17** (2000) 3429 [arXiv:hep-th/0004098].

[191] G. W. Gibbons and C. A. Herdeiro, *Supersymmetric rotating black holes and causality violation*, Class. Quant. Grav. **16** (1999) 3619 [arXiv:hep-th/9906098].

[192] T. Eguchi, P. B. Gilkey and A. J. Hanson, *Gravitation, Gauge Theories And Differential Geometry*, Phys. Rept. **66** (1980) 213.

[193] M. A. Walton, *The Heterotic String On The Simplest Calabi-Yau Manifold And Its Orbifold Limits*, Phys. Rev. D **37** (1988) 377.

[194] K. S. Narain, *New Heterotic String Theories In Uncompactified Dimensions ¡ 10*, Phys. Lett. B **169** (1986) 41.

[195] P. S. Aspinwall, *K3 surfaces and string duality*, arXiv:hep-th/9611137.

[196] L. Bonora, C. Reina and A. Zampa, *Enhanced gauge symmetries on elliptic K3*, Phys. Lett. B **452** (1999) 244 [arXiv:hep-th/9807057].

[197] M. Bershadsky, C. Vafa and V. Sadov, *D-Strings on D-Manifolds*, Nucl. Phys. B **463** (1996) 398 [arXiv:hep-th/9510225].

[198] P. S. Aspinwall, *Enhanced gauge symmetries and K3 surfaces*, Phys. Lett. B **357** (1995) 329 [arXiv:hep-th/9507012].

[199] G. 't Hooft, *Magnetic Monopoles In Unified Gauge Theories*, Nucl. Phys. B **79** (1974) 276.

[200] A. M. Polyakov, *Particle Spectrum In Quantum Field Theory*, JETP Lett. **20** (1974) 194 [Pisma Zh. Eksp. Teor. Fiz. **20** (1974) 430].

[201] E. B. Bogomolny, *Stability Of Classical Solutions*, Sov. J. Nucl. Phys. **24** (1976) 449 [Yad. Fiz. **24** (1976) 861].

[202] M. K. Prasad and C. M. Sommerfield, *An Exact Classical Solution For The 'T Hooft Monopole And The Julia-Zee Dyon*, Phys. Rev. Lett. **35** (1975) 760.